Development and Application of A Compact Long Wavelength Fluorescence Detection System

By

SI JUNG HU

BSc., MSc., MIES, MIEEE

A Doctoral Thesis Submitted in partial fulfilment of the requirements for the award of

DOCTOR OF PHILOSOPHY

Of

Loughborough University

1999

Supervisors:

Professor James N Miller
Department of Chemistry, Loughborough University, Loughborough, Leicestershire, LE11 3TU

Drs. Martin T French & Derek A Palmer
Kalibrant Limited, 2 Oakwood Drive, Loughborough Park, Loughborough, Leicestershire, LE11 3NH

To

My wife Minhua and lovely daughter Yida, both

of whom are such an important part of my life

ACKNOWLEDGEMENTS

The author wishes to thank the following organisation and individuals for help in completing this research:

Kalibrant Limited — New Technology Development for Biochemistry and Biochemical Analysis

They not only financed all my research activities and expenditure, but also provided 'excellent' conditions in my research period at this department.

Professor James N Miller — Head of Analytical Section, Department of Chemistry, Loughborough University

He was my supervisor and gave me good guidance and support with the organisation and activities of this project. His advice and comments encouraged me to achieve 'big step' progress in the laboratory.

Dr Martin T French — Scientific Director, Kalibrant Limited

He was genuinely helpful in organisation, suggestion and practical test through this project. Also his comments to produce my thesis was very useful.

Dr Derek A Palmer — Scientific Director, Kalibrant Limited

He was always positive to stand by my side in laboratory, he kindly provided useful literature and advised me with the basic concepts of immunoassay.

Dr Mark Evans — Assay Development, Kalibrant Limited

He was always friendly and helped me to be familiar with the facilities in the initial period. Furthermore he provided many chemical reagents to complete the practical investigation.

G Hussian Sarpara, Stephanie Berreau, Mark Joyce were my nice colleagues with whom I have stayed in the same laboratory for two years, and Dr Colin Farrell is one of my current colleagues at Kalibrant Ltd. They give me not only with knowledge but also in communication skills.

Abstract

Long wavelength (>600nm) fluorescence has many advantages in analysis, including the presenting possibility of building compact, robust, yet sensitive instrumentation, where measurements can be made with minimal autofluorescence and scattered light from biological samples. With the requirement for high sensitivity in immunoassays, e.g., for environmental monitoring, clinical analysis and therapeutic drug monitoring, a novel, compact, fluorescence detection system (NFDS) was successfully constructed using several pulsed diode lasers as excitation sources, and a photodiode as optoelectronic sensor. It has the following characteristics:

1. Excitation source range: 600 nm– 900 nm, and emission wavelength range: 650 nm – 1000 nm.
2. Utilisation of various cut-off filters to eliminate undesirable background radiation and to define the fluorescence wavelength band.
3. Emission beam detection by means of an efficient, high speed and large area silicon photodiode.
4. An adjustable laser pulse frequency and linear optoelectronic amplification.
5. Digital display, output for a digital multimeter or a chart recorder, and analogue to digital converter (ADC) for connecting to a PC with a suitable data handling package.

A 635 nm-laser diode with the output power of 2 mW and a 650 nm cut-off filter were used to test the detection limit of the naphthofluorescein fluorescence dye (NF) in 0.50 M Tris buffer (pH 8.8), containing 2.5% (w/v) 3-[(3-cholamidopropy)-dimethylammonio]-1-propanesulfonate (CHAPS). A 645 nm laser diode with the output power of 2mW and a 665 nm cut-off filter were used to test the detection limit

of Cy5 monofunctional dye (Cy5) in 0.50 M Tris buffer (pH8.8). A 670 nm laser diode with the output power of 2mW and a 690 nm cut-off filter were used to test the detection limit of Cy5.5 bisfuncational dye (Cy5.5) in 0.50 M Tris buffer (pH 8.8).

A comparative test was carried out to assess the detection limit of Cy5 in 0.50 M Tris buffer (pH 8.8), using the NFDS with the RACALL-DANA 4009 digital multimeter and the Hitachi F-4500 commercial research grade fluorescence spectrometer.

A flow injection immunoassay was developed using the α-Interferon as the analyte and Cy5 as the label. A calibration curve was obtained using the NFDS with the FlowTEK data capture software.

The potential of this novel fluorescence detector has been demonstrated through hardware experimentation and practical investigation of detection limits and a flow injection immunoassay (FIIA).

Its application could be extended by the use of superluminescent light emitting diodes (SLEDs) at shorter wavelengths (450 nm - 600 nm); a microprocessor based electronic system, and the LabVIEW 5.0 software for data capture.

PUBLICATIONS AND POSTERS

January, 1999

International Patent, Palmer, D. A., French, M.T., HU, S. J., "A Detector"., PCT/GB98/02394 PCT WO99/08096.

January, 1999

A New Long-Wavelength Fluorigenic Substrate for Alkaline Phosphatase: Synthesis and Characterisation, Authors: Sarpara, G. H., HU, S. J., Palmer, D. A., French, M. T., Evans, M., and Miller, J. N., Analytical Communications, Vol. 36, pp.19-20

30 June – 3 July, 1997

Development of Novel Fluorescence Detection System Utilising Long Wavelength and its Application, Poster for Analytical Science, R & D Researcher' Meeting at University of Northumbria at Newcastle, UK

6 June – 9 April, 1988

Development of Novel Fluorescence Detection System Utilising Long Wavelength and its Application, Poster for Analytical Science, R & D Researcher' Meeting at University of Durham, UK

7 June – 12 March, 1999

Development and Application of Novel, Compact Long-Wavelength Fluorescence Spectrometers, Poster for The Pittcon '99 on Analytical Chemistry and Applied Spectroscopy, in Orlando, USA

TABLE OF CONTENTS

CHAPTER FIVE PRACTICAL INVESTIGATION

CHAPTER SIX CONCLUSION AND FUTURE WORK

CHAPTER ONE

INTRODUCTION

1.1 Aim of the Project

Long wavelength fluorescence detection systems have been used in many applications, including flow injection immunoassays for clinical analysis, therapeutic drug monitoring and environmental monitoring. Screening immunoassays enable the analyst to work quickly, cheaply and with a high degree of sensitivity and selectivity.

The aim of this research was to develop a novel very near infrared (VNIR) fluorescence detection system employing laser diodes as the excitation sources, electrooptical detector and a PC with data capture package. The research was carried out in five stages:

1. The study of long wavelength sources utilising laser diodes, and the selection of an efficient photodiode as an electrooptical sensor; the selection of an optical bench structure, a pre-amplifier, a laser pulse driver modulator and a multiple power supply.

2. The construction of a small portable fluorescence instrument with a digital display, signal output to a digital multimeter or a chart recorder, and to a PC with data capture.

3. Investigations into the use of various filters to eliminate undesirable background radiation and to define a wavelength band.

4. The optimisation of the system, in terms of the electronic characteristics and preliminary testing of selected dyes.

5. The practical investigation of detection limits, comparative testing with a commercial instrument, and the development of a typical flow injection immunoassay.

1.2 Background of Research in Fluorescence Spectroscopy

With the development of trace analysis in complex matrices, i.e., body fluids, drinking water, foodstuffs etc., fluorescence spectrometry has grown in importance for many years, and has been applied routinely and successfully to the detection of solutes in flowing system, e.g. HPLC and FIA. However, the problems of such trace analysis in biochemistry and chemistry are among the hardest that analysts encounter: there is a continually growing requirement for better limits of detection, often at $pgml^{-1}$ or lower levels [1]. Although advances in instrumentation, data handling procedures, synthesis of new fluorescent labels and probe molecules have combined to extend the applications, most fluorescence methods still employ the UV/visible region of the spectrum – in practice, ca 250 – 600 nm. However, there are a number of experimental problems in measuring fluorescence in this region including light scattering.

To overcome the existing drawbacks in conventional fluorescence spectrophotometry, a simple detector employing a light emitting diode (LED) and a photodiode (PD), has been developed for use in biomedical analysis [2]. Diode laser-induced fluorescence detectors have been used as a detector in chromatography [3] and have been used for electrophoresis separation [4]. Also, a laser diode fluorimeter has been used for the field measurement of chlorophyll fluorescence [5]. Such results have shown the potential for developing suitable instruments and for extending their applications.
The three main areas of my research include:

a. A novel enzymatic inhibition based assay has been developed utilising the long wavelength label naphthofluorescein, alkaline phosphatase, and a conventional competitive flow injection immunoassay format. This assay provides the analyst

with a tool for a number of applications which include analysing cyclo-toxins, pesticides and drugs, at long wavelengths, thus reducing the fluorescence background associated with this monitoring and allowing the use of simple solid state light sources and detectors.

b. There are several kinds of dye available for biochemical labelling which utilise the advantages associated with long wavelength measurements that are being investigated in this laboratory. Each dye can be detected quickly and routinely at low concentrations.

c. There are several problems associated with the analysis of trace levels of toxins in environmental analysis. Flow injection immunoassays not only offer the potential for rapid screening and quantitative analysis of these toxic compounds in water samples, but can also be made available in a portable format. Although the dyes for labelling and detection of molecules and analytes have been developed recently, there are still many unexplored ways in which they can be used in biochemical analysis. Also, new solid state optical components are continually being developed encouraging further development of miniaturisation of fluorescence detection.

A novel fluorescence detection system (NFDS) has been developed which incorporates a laser diode light source to excite very near infrared (VNIR) dyes, and a high-speed photodiode as a detector that provides low signal noise, and a high level of precise amplification.

1.3 Fluorescence Spectroscopy

Fluorescence spectroscopy differs from absorption spectroscopy in that the optical design must ensure that none of the incident (excitation) light falls directly onto the photodetector, while incorporating the capability to capture the emission beam from the sample. The particular benefits of long wavelength fluorescence spectroscopy are described in 1.3.3.

1.3.1 Theory of Fluorescence

Fluorescence, phosphorescence, chemiluminescence, radioluminescence and electroluminscence are called Luminescence phenomena. *Chemiluminescence* is the emission of light from an excited species formed in the course of a chemical reaction. In *radioluminescence*, the energy is supplied by a radioactive source. *Electroluminescence* is a term applied to fluorescence or phosphorescence generated by the direct application of an electric current.

In molecular photoluminescence molecules absorb photons of electromagnetic radiation are raised to some excited electronic state and then, emit light on returning to the ground state. Emission phenomena include *fluorescence* and *phosphorescence*. In *fluorescence* the associated energy level transitions do not involve a change in electron spin. As a consequence, fluorescence is short lived, with luminescence ceasing almost immediately ($<10^{-7}$ s). In contrast, phosphorescence involves a change in electron spin and is therefore much slower than fluorescence, allowing detection after termination of irradiation, sometimes for several seconds or longer.

The characteristics of fluorescence can be summarised by means of a simple energy level diagram in Figure 1-1.

Figure1-1 **Schematic representation of a partial energy diagram for a photoluminescent system**

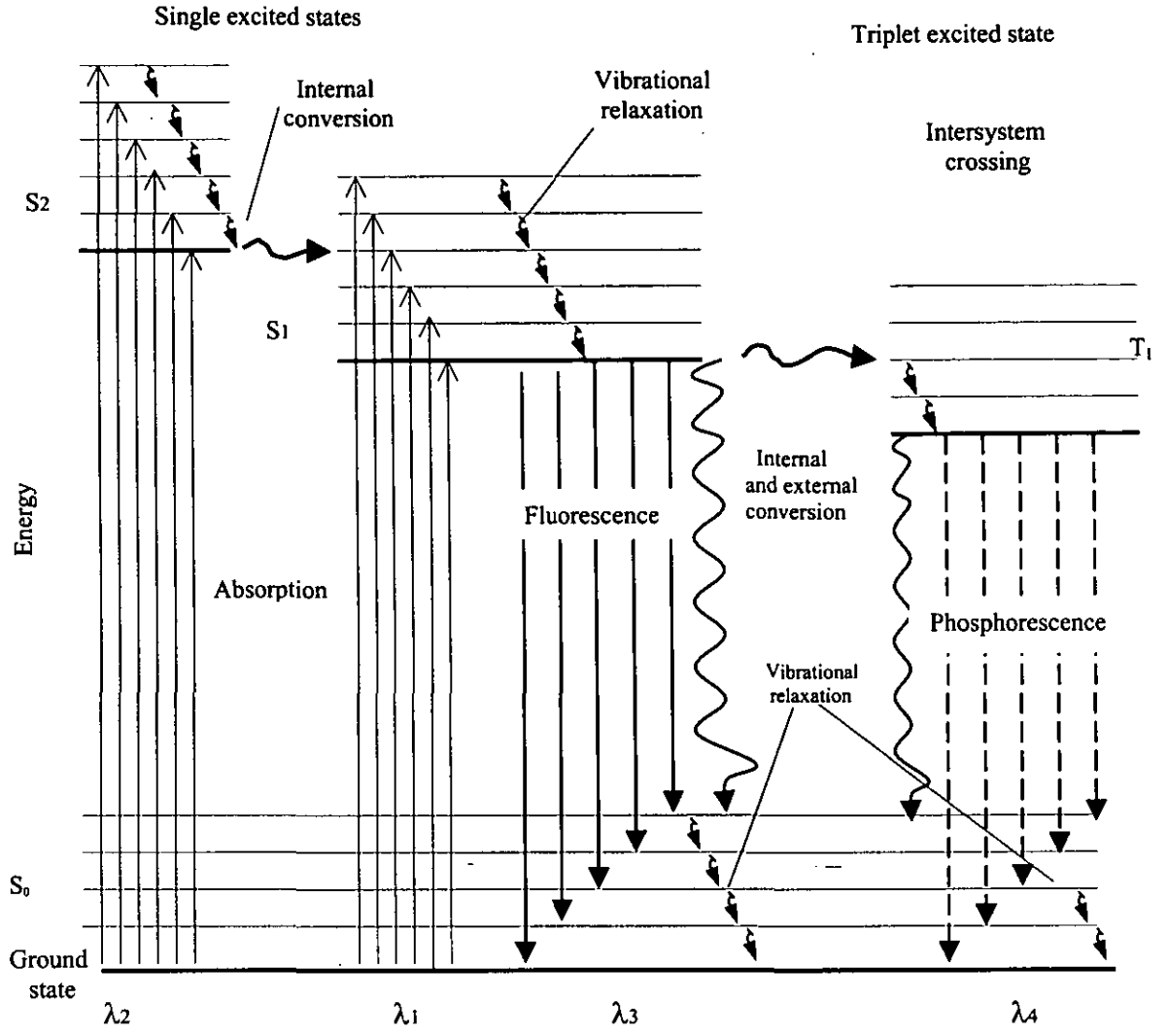

The lowest heavy horizontal line represents the *ground state energy* of a singlet state and is labelled S_0. The upper heavy lines are energy levels for the ground vibrational states of three excited electronic states. The other two lines on the left represent the first, S_1, and second, S_2, excited singlet states. The one on the right, T_1, represents the energy of the first electronic *triplet state*. The energy of first excited *triplet state* is usually lower than the energy of the corresponding singlet state. The excitation of this molecule can be brought about by absorption of two bands of radiation, one centered about the wavelength λ_1 ($S_0 \rightarrow S_1$) and second around the shorter wavelength λ_2 ($S_0 \rightarrow S_2$) [6].

In Figure 1-1, *fluorescence* is the radiative transition from the lowest vibrational level of singlet excited state (S_1) to the ground state (S_0) in 10^{-7}s to 10^{-12}s even less. It has a longer wavelength lower energy than the incident radiation. This shift in wavelength is called a S*tokes shift*. A large *Stokes shift* in nanometers means that there is a large difference between the excitation and emission wavelengths. For example, Alexa Fluor 430 has a maximum excitation wavelength at 430 nm and a maximum emission wavelength at 541 nm, which *Stocks shift* is over 100 nm.

Vibrational relaxation indicates that a molecule may be promoted to any of several vibrational levels during the electronic excitation process. This relaxation process is so efficient that the average lifetime of a vibrationally excited molecule is 10^{-12} s or less, a period significantly shorter than the average lifetime of an electronically excited state. Fluorescence from solution, when it occurs always involves a transition from the lowest vibrational level of an excited electronic state. *Vibrational relaxation* is that fluorescence from a solution which always involves a transition from the lowest vibrational level of an excited state to any one of the vibrational levels of the ground state (see Figure 1.1).

Internal conversion may also occur: those intermolecular processes by which a molecule passes to a lower-energy electronic state without emission of radiation. *Internal conversion* appears to be particularly efficient when two electronic energy levels are sufficiently close to overlap in vibrational energy levels. Other non-radiative transitions may occur where energy is lost in collisions or through external molecular processes such as energy transfer.

Intersystem crossing is a process in which the spin of an excited electron is reversed and a change in multiplicity of the molecule results, i.e. it moves to a triplet state. This

phenomenon is most common in molecules that contain heavy atoms (e.g. Br, I). In *phosphorescence*, the energy transition from triple excited state to the ground state causes longer wavelength and longer lifetime ($>10^{-4}$s) emissions than fluorescence.

These processes directly affect the efficiency of fluorescence as they affect the number of molecules to go back to the *ground state* via fluorescence. The quantum efficiency ***K'*** defines the efficiency of the fluorescence process as follows:

$$F = K'(P_0 - P) \qquad (1\text{-}1)$$

Where: ***F*** is the radiant power of fluorescence.

Po is the radiant power incident on the sample.

P is the radiant power transmitted by sample.

Po-P is therefore assumed to be the radiant power absorbed by the sample.

Quantum efficiency ***K'*** is simply the ratio of [7]:

$$K' = \frac{\text{Photons emitted as fluorescence}}{\text{Photons absorbed}} \qquad (1\text{–}2)$$

The theoretical range for ***K'*** is thus between zero and one, but in practice it rarely exceeds 0.9. In general, the greater the number of processes competing with fluorescence for deactivation of the lowest excited singlet state and the greater their rate constants, the shorter will be the actual lifetime of the lowest excited singlet state [8].

1.3.2 Relationship Between Fluorescence and Concentration

The relationship between fluorescence intensity and molecular properties related to the transition can be derived from the equation 1-1.

$$F = K'(P_0 - P) \qquad (1\text{-}3)$$

As known above, F is the power of fluorescence emission that is proportional to the radiant power of excitation beam.

K' is the constant of the quantum efficiency of the fluorescence process.

P_0 is the power of the beam incident upon the solution.

P is its power after traversing a length b of the medium.

In order to relate F to the concentration c of the fluorescing species, following formula can be written from Beer's law:

$$\frac{P}{P_0} = 10^{-\varepsilon bc} \qquad (1\text{-}4)$$

Where: ε is molar absorptivity of fluorescing molecules.

b is path length of medium and c is molar concentration.

εbc is the absorbance A.

By substitution of the equation 1-3 into the equation 1-4, a new equation will be obtained as follows:

$$F = K'P_0(1 - 10^{-\varepsilon bc}) \qquad (1\text{-}5)$$

Furthermore, the equation 1-5 can be expanded as a series to:

$$F = K'P_0[2.303\varepsilon bc - \frac{(2.303\varepsilon bc)^2}{2!} + \frac{(2.303\varepsilon bc)^3}{3!} .....] \qquad (1\text{-}6)$$

Provided $2.303\varepsilon bc = A < 0.05$, all the subsequent terms in the brackets are small with respect to the first; under these conditions, the maximum relative error caused by dropping all but the first term is 0.13%. Thus, the equation may be written as:

$$F = 2.3K'2.303\varepsilon bc\, P_0 \qquad (1\text{-}7)$$

Or at constant P_0,

$$F = Kc \qquad (1\text{-}8)$$

Thus, a plot of fluorescence power of a solution versus concentration of the emitting species should be linear at low concentrations.

When c is great enough so that the absorbance is larger than about 0.05, the higher order terms in the equation 1-6 become importance, and the linearity is lost; then F lies below an extrapolation of the straight-line plot.

Two other factors, also responsible for negative departures from linearity at high concentration, are *self-quenching* and *self-absorption*. *Self-quenching* is the result of collisions between excited molecules. *Self-absorption* occurs when the wavelength of emission overlaps an absorption peak; fluorescence is then decreased as the emission traverses the solution and is reabsorbed by other fluorescent molecules.

1.3.3 Quenching

Fluorescent compounds are often very sensitive to changes in their environment. Even minor changes in pH, polarity, the vicinity of quenching or enhancing groups such as heavy atoms, or absorbing groups, can change their fluorescence yields or shift wavelengths. Non-specific binding to proteins often quenches the fluorescence to some extent, and light-absorbing molecules in serum can absorb either the excitation or the emission energy. The close proximity of two fluorescent probes in the protein can even cause self-quenching if their absorption and emission spectra overlap.

1.3.4 Light Scattering

The major disadvantage of UV/visible fluorescence methods is the presence of unwanted background signals. Light scattering may contribute significantly to this background, leading to a situation in which fluorescence analysis involves detecting a small difference between two large signals: the fluorescence technique then loses its principal theoretical benefit over other techniques. Light scattering in practical fluorescence analysis could be of two types.

1.3.4.1 Rayleigh – Tyndall Scattering

Rayleigh scattering is caused by molecules or aggregates of molecules with dimensions smaller than the wavelength of radiation. Its intensity is readily related to wavelength as an inverse fourth-power effect [9], and the scattering is elastic, i.e. the wavelengths of the unwanted and scattered light are equal.

Figure 1-2. **Rayleigh scattering: Plot of intensity as a function of wavelength**

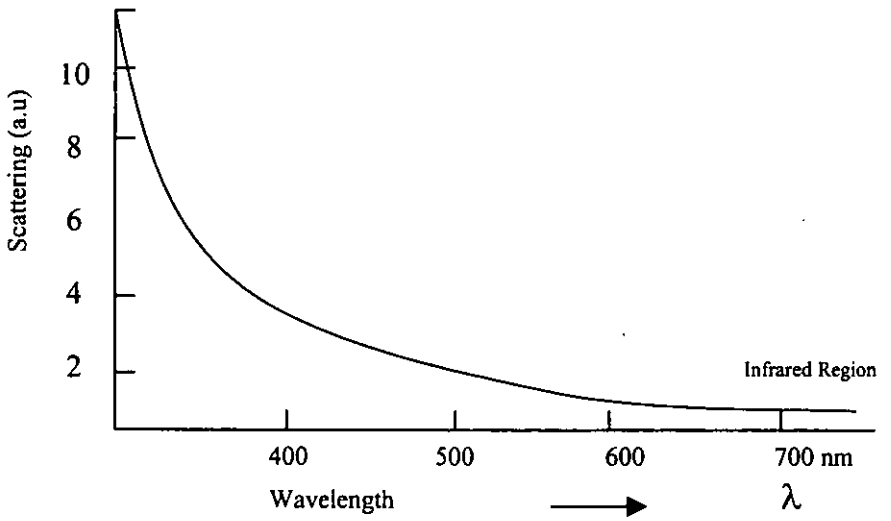

Note: a.u is arbitrary unit.

Tyndall scattering may occur via, for example, particles in a colloidal suspension. The particles have dimensions greater than a tenth and less than 1.5 times the wavelength of incident radiation [10].

In instruments that employ a xenon arc lamp or a pulsed xenon lamp as the excitation source, the combination of this wavelength dependence and that of the light source intensity means that the *Rayleigh* signal is largest when an excitation wavelength of ca.350 nm is used. Unfortunately, this wavelength region is one where many common fluorophores are excited. Therefore the background effect can be serious despite all precautions.

1.3.4.2 Raman Scattering

Raman scattering results from vibrational-energy-level transitions occurring in the molecules as a consequence of the polarisation process [11]. *Raman scattering* is normally only observed from the solvent as it is a much weaker effect than *Rayleigh scattering.* But it can be just as damaging in practice, as the scattered light has a longer wavelength than the incident light. It may therefore be beneficial to run a solvent blank prior to analysis to check where the *Raman* peaks occur.

Most fluorescence experiments in biochemistry and chemistry utilise aqueous solutions: when an excitation wavelength of 350 nm is used the principal water *Raman band* occurs at 397.5 nm where it can interfere with the genuine fluorescence signals.

1.3.5 Long Wavelength Fluorescence

A major drawback of UV/visible fluorescence methods is the high background signal from light scattering and from other fluorophores in this region of the spectrum. At

longer wavelengths the light scattering intensity is diminished, and at wavelengths over 600 nm light emitting diodes (LEDs) and other laser diodes, already used in optical communications, are available as light sources [12]. In this thesis, fluorescence at the wavelengths above 600 nm is defined as "long wavelength fluorescence". The advantages of working in this wavelength region can be summarised as follows:

1. The intensity of *Rayleigh scattering* using an excitation wavelength of 600 nm is only 10% of that at 340 nm in the same sample. Excitation at 800 nm would reduce background signal by further factor of three [13].

2. Excitation for analysing an aqueous sample at 600 nm would produce the principal water *Raman band* at ca 754 nm, a large *Stokes shift* and with much lower intensity than with lower wavelength excitation. With excitation at 830 nm, the same water Raman band is at 1150 nm, well beyond any capacity to interfere with any fluorescence excited at the same wavelength [14].

3. The major advantage of working in the 600-1000 nm region is that there are only a few intense fluorophores in that region. Theory predicts that fluorescence quantum yields should indeed decrease as the energy difference between the ground and excited state decreases. In practice what seems to happen is that there is a relatively small number of bright fluorophores in this region and, compared with the UV/visible region, a much larger number of non-fluorescent or feebly fluorescent organic compounds. The combination of this reduced endogenous fluorescence with the reduced scattering effect means that a biochemical sample has a fluorescence background at 700 nm of emission an order of magnitude less than at 500 nm of emission.

4. Numerous practical applications of long wavelength fluorescence based on the use of solid state detectors have been described [15]. Conventional xenon light sources require high voltage power supplies, and photomultiplier detectors are large and delicate. By contrast, long wavelength detectors can be constructed from a simple solid state light source, e.g. a laser diode or super luminescent light-emitting diode (SLED), a simple optical filter. Additionally an excellent photo sensor, e.g. a charge coupled device (CCD), a charge injection device (CID), a photodiode array (PDA) and a photodiode (PD) can be applied in detecting fluorescence. Yet another reason is that there are possibilities of making the detector more flexible by using low cost and efficient fibre optics. With data capture and handling package in a PC, such a fluorescence detector would be a versatile and easy-to-use analytical tool in flow injection immunoassay and other applications. The development of a long wavelength detection system for fluorescence measurements has been described in Chapter Four and Five in detail.

1.4 Approach to Development of Very Near Infrared (VNIR) Fluorescence Detection System

The latest shift towards increased utilisation of fluorescence detection is due to a combination of recent developments. These include:

1. Improved instrumentation, for example, the use of lasers, e.g. laser diodes, to increase light input, novel electrooptical devices to improve the ability of emission beam light capture.

2. Availability of fluorescence probe molecules, which can be added deliberately to biological material to label at the molecular level. This procedure has also been developed into a number of long wavelength dyes.

3. Some methods of detecting and analysing the fluorescence have been published [16-18] and these improved techniques have been described in detail.

Obviously, instrumentation development now plays a major role in high throughput analysis such as flow injection immunoassays (FIIAs).

1.4.1 Requirement of Novel Fluorescence Detection System (NFDS)

Recently, an improved fluorescence detection system using a laser diode has been developed, in which it was possible to detect single photo events and the decay half lives of the fluorescence of the order of 1 to 1.5 nanoseconds [19]. Yet another advance in fluorimeter instrumentation was an acousto-optic tunable filter (AOTF) to determine the solvent polarity in a flow injection system [20]. However, the flow injection immunoassay system still needs an efficient, simple, economic, robust,

reliable and sensitive fluorescence spectrophotometer for many other applications. The portable instrument should perform several functions:

a) Excitation range: 600 – 900 nm; and emission range: 650 – 1000 nm.

b) The laser pulse generator provided electronic time gating approach (7Hz – 1.4 MHz).

c) Optical system with a short wavelength cut-off filter demanded for fluorescence detection

d) Output for a chart recorder or digital multimeter, a digital display and an analogue to digital converter (ADC) for a PC.

e) Data capture software to display and collect the raw data for all analytical procedures

The diagram of a NFDS that was designed and constructed is shown in Figure 1-3.

Figure 1-3 **Overview of fluorescence measurement system**

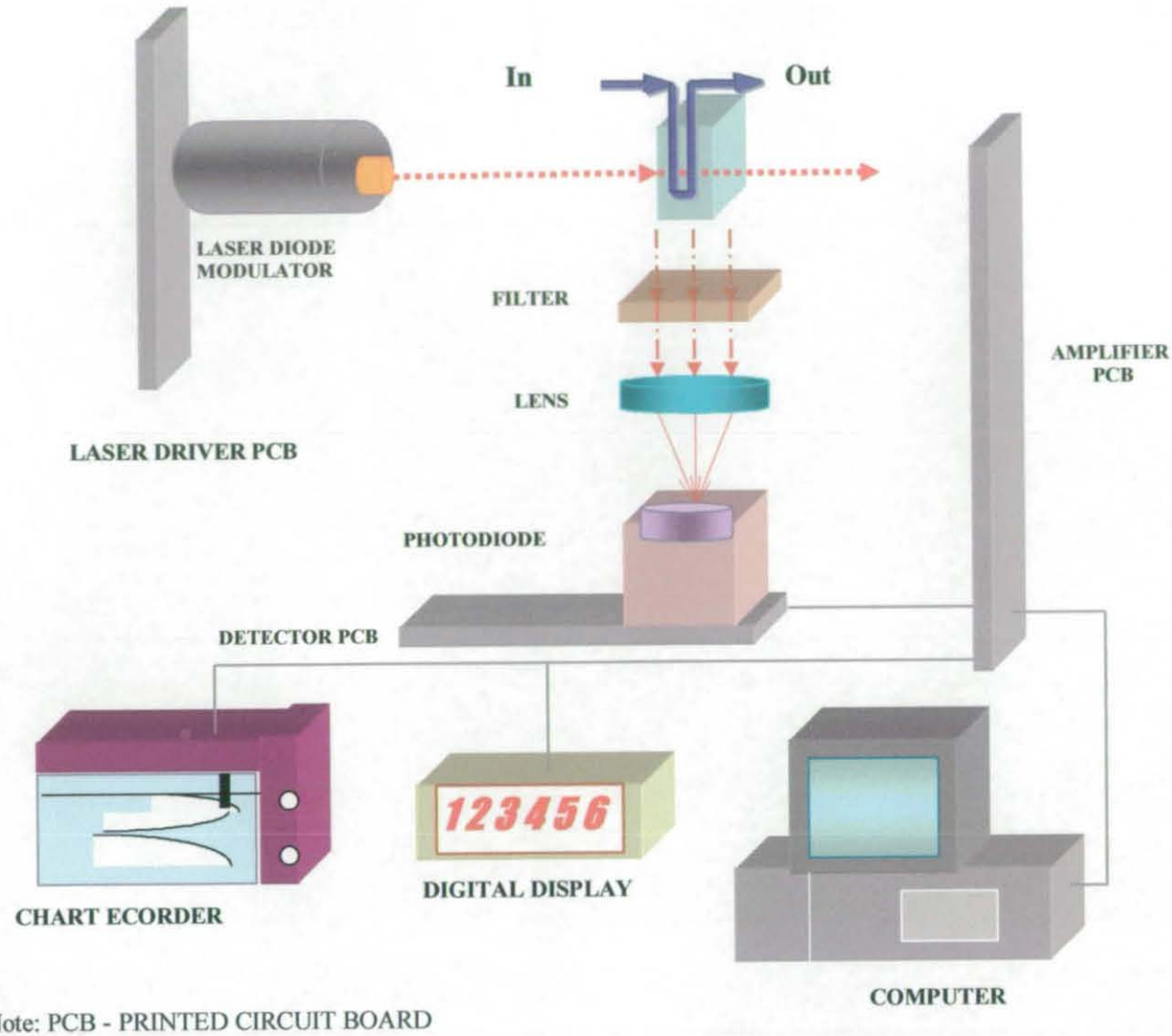

Note: PCB - PRINTED CIRCUIT BOARD

In Figure1-3, a laser diode (various long wavelength options) provides the excitation source, which is modulated and requires a 5 volt DC power supply. A laser pulse generator (self-made) which has 5 pulse speed options drives the laser. Many short-wavelength cut-off filters were selected to minimise fluorescent signal loss. A laser beam at a selected wavelength excites the fluorophore of the sample in the sample holder (cuvette or flow cell). The emission beam from the sample, passes through a biconvex lens onto the surface of the fast speed photodiode. The lens focuses the

emission beam onto the photodiode (Centronic, Inc.) through the short wavelength cut-off filter for detection. The analogue signal from the photodiode would be linearly amplified to the digital display or the chart recorder output, and converted into a digital signal output onto a PC.

Compared with a conventional filter fluorometer and fluorescence spectrophotometer, there are several differences in the construction. These include:

A. In a filter fluorometer, a mercury lamp is used as an UV excitation source and a tungsten lamp as visible excitation source; a primary filter is used to transmit the desired excitation wavelength to the sample cuvette. A photomultiplier tube (PMT) measures the fluorescence emission. The secondary filter between the sample and the photodetector is selected to transmit the fluorescence and to absorb scattered excitation radiation [21].

B. In a spectrofluorometer, the extended analytical scope of fluorescence analysis is achieved by replacing filters with a grating monochromator to provide scanning wavelength selection throughout the region 200 – 800 nm. The instrument usually incorporates grating monochromator that use gratings with 600 grooves/mm. The excitation monchromator is located between the radiation source and the sample, and the emission monchromator is between the sample and the photomulitipler tube (PMT). A Xenon lamp is mostly employed as an excitation source [22-23]. There are a number of these types of instruments already commercial available.

Laser diodes that were initially used in telecommunications and data processing are now employed as an excitation source in the NFDS. There are some obvious advantages of a fluorescence detector using a laser diode as excitation source

compared to gas-discharge lamp excited fluorescence. Lasers have a monochromatic output, which provides selective excitation and easy isolation of the fluorescence from *Rayleigh* and *Raman scatting*, but the most important advantage is a high efficient output of laser at a selected wavelength. Furthermore, a laser diode is smaller than the conventional lasers and has a long life ($>10^5$ hours). This characteristic can be used advantageously in two ways: firstly, it allows the use of small detection volumes, which is necessary in a small flow cell. Secondly, a high irradiation (W/m^2) of the sample can be achieved because of the small irradiated area.

1.5 Scope of Application Areas

Since long wavelength detectors for fluorescence analysis have tremendous advantages in sensitivity and reliability, in theory it can carry out most of measurement as same as the conventional detector. Generally, most of the routine applications fall into one of the following three groups:

I. Direct methods- in which the natural fluorescence of the assay itself is measured, e.g. cyanine family of dyes, i.e. Cy5 and Cy5.5 for testing the detection limit of the detector, and the α-interferon.

II. Derivatisation methods - in which the compound of interest is non-fluorescent but is converted into a fluorescent derivative.

III. Quenching methods – in which the analytical signal is the reduction in the intensity of some fluorescent species due to the quenching action of the assay.

Each of these groups can be further sub-divided according to the chemical or biochemical nature of the assay or the experimental method used. However, flow injection immunoassays concerned with the above methods use such a detector and have wide application not only in clinical analysis but also in extending into environmental monitoring.

1.5.1 Clinical Routine Analysis

Immunoassays are defined as analytical techniques that use antibody or antibody-related reagents for the determination of sample components and they continue to play a major role as diagnostic tools in clinical chemistry. With the increase of readily

detectable labels used in immunoassay there is a need to provide many of these methods with extremely sensitive detection systems which are used widely in both clinical analysis and environmental monitoring. Flow injection immunoassays provide a fully robust method for immunoassay, with the possibility of automation [24-25]. Such properties, plus the relatively low cost involved with most of these techniques, make immunoassays the method of choice for many clinical applications. However, an increased emphasis on the development of improved flow injection immunoassay reagents and better assay protocols has continued up to the present, as well as exploring the NFDS in the long wavelength region.

Therapeutic drug monitoring is the continuous measurement of drugs used in the management of certain disease states. Drug determination in biological fluids can be undertaken for drug overdose, screening for drugs of abuse and compliance testing. Also, it is obvious that the potential beneficial effects need to be separated from the possible harmful ones [26]. In practical therapeutic drug monitoring, TLC, GC, HPLC methods and immunoassay are employed as the principle techniques. In practice, the drugs used have very narrow therapeutic indices, i.e. a small difference between safe and toxic concentration range. Furthermore the analysis is normally performed on biological samples which can cause problems due to the matrix. Immunoassays using a fluorescence detector have excellent selectivity and sensitivity compared to TLC, GC and HPLC methods. Additionally, with the availability of novel solid state devices, i.e. laser diodes as excitation sources, charge coupled devices (CCDs) as optical sensors, the combination of immunoassays with labelled dyes, these solid state devices and data handling techniques makes for analyte flexibility and overall versatility. These devices allow the analyst to examine lower levels of sensitivity than were achievable previously [27].

Currently, Amersham Co. USA [28] produces a range of fluorescent products for detection of biological molecules that are pre-labelled products available under the brand name CyDye™ with the excitation wavelength range 400 nm to 750 nm and the emission wavelength range between 450 nm to 800 nm. Amersham Co. USA provides a number of labels, which utilise long wavelength detection, and have less interference problems as compared to UV/visible spectrum.

1.5.2 Environmental Monitoring

With an increasingly greater role in the field of environmental monitoring, there is a continuing trend towards lower threshold limits as a result of legislation related to environmental monitoring. However, after having developed some powerful methods in 1970's new threshold limits, e.g. for pesticides, even less than 100 ppt for a single compound [29] using accepted techniques, i.e. GC, GC-MS or HPLC have been developed [30]. The general trends towards lower threshold limits and higher analysis speed has been following by the next generation of emerging analytical technologies: establishment of powerful computing and immunoassay. Since flow injection immunoassays offer the potential for rapid screening and quantitative analysis of organic compounds in aqueous sample, more and more pollution monitoring have been undertaking using these techniques, i.e. pesticide monitoring and foodstuff analysis [31-32]. In general, there are two main applications:

1. The portable NFDS provides a vital tool for field monitoring which enables rapid determination of target compounds needing field analysis quickly and accurately. Pesticides have been the primary focus of immunoassay developmental work. However, some work has been extended toward industrial chemicals and pollutants leaking from underground gasoline storage tanks [33] and landfill. With

Such a NFDS, the field sample tests can be performed initially on site without requiring sample transfer to an analytical laboratory [34].

2. With this portable NFDS, many immunoassays can be developed for environmental compounds that are difficult to detect by conventional methodologies. Further more, with immunoaffinity chromatography, it is very useful for specific separations of target compounds in complex matrices thus the same antibodies used in an immunoassay can be used to develop immunoaffinity techniques. In such a procedure, specific antibodies immobilised onto a chromatography column make it possible to preconcentrate specific compounds from environmental sample before determination. For instance, using some near infrared dyes with selected enzyme, the immunoassays have already been evaluated [35], which could be developed to determine cyclo toxins and pesticides [36], and possibly use this portable detector. Currently, a number of environmental monitoring methods concerned with immunoassay have been described in several publications [37-39].

1.5.3 Flow Injection Immunoassays with Long Wavelength Fluorophores

Recently, amongst many developments in fluorescence spectrometry, the rapidly increased use of long wavelength probes and labels is one of the most important [40]. Since many biological samples fluoresce in the region between 200 nm and 600 nm, long wavelength fluorescence detection using laser diode as sources, and solid state detectors in small, low cost and robust instruments gives better sensitivity and more ease of operation.

Nathphofluorescein monophosphate with CHAPS was preliminarily investigated using both the NFDS and a research grade fluorescence detector. The NFDS can detect nathphofluorescein at the level of 10^{-9} M sufficient to determine the drug at the therapeutic (μgml^{-1}) level [41]. Using the NFDS with the LabVIEW data capture software, further studies of nathphofluorescein based substrates for the determination of esterase and other enzymes are currently being carried out in the laboratory, and are expected to be of importance in high throughput screening applications.

With the movement toward automation in immunoassays, more and more research is being done with continuous-flow analytical techniques, especially flow injection. With respect to immunoassays, flow injection offers: precise control of reaction times; compatibility with any homogeneous and heterogeneous format; compatibility with a wide range of detector; reuse of supports and reagents; improvement in accuracy and precision with a sensitivity similar to batch methods; dramatic reduction of analysis time close to real time performance; flexibility; on-line coupling to industrial processes. Additionally, FIIAs are easy to calibrate and there is possibility of integration of reaction, separation, and detection processes used with different formats, use of kinetic and differential measurements, and application as routine methods and screening.

FIIA is a powerful tool and a simplified system of automation [42] for the development of analytical protocols, and the application of flow injection techniques is expected to be an enormous contributor to improved speed and quality of immunoassays.

1.6 References

[1]. Miller, J. N., Immunoassay: The ideal trace organic analysis method, Phil Trans Royal Society of Chemistry, London, (1990), 333, pp.71-83.

[2]. Brown, M. B., Edmonds, T. E. and Miller, J. N., Novel instrumentation and biomedical application of very near infrared fluorescence, Analyst, (1993), Vol.118, pp.407-410.

[3] Mank, A. J. G., Lingema, H. and Gooijer, C., Diode Laser – induced fluorescence detection in chromatography, Trends in Analytical Chemistry, (1992), Vol.11. No.6, pp.210-216.

[4] Baars, M. J. and Patonay, G., Interfacing a high-sensitivity, near-infrared laser-induced fluorescence detector with a commercial capillary electrophoresis instrument, Applied Spectroscopy, (1998), Vol.52, No.12, pp.1619-1622.

[5] Mazzinghi, P., Laser diode fluorometer for field measurement of the F685/F730 chorophyll fluorescence ratio, Review of Scientific Instrument, (1996), Vol.67, No.10, pp.3737-3744.

[6] Skoog, D. A. and Leary, J. J., Theory of fluorescence and phosphorescence, Principles of Instrumental Analysis, Philadelphia, Saunders College, (1992), pp.175-177.

[7] Willard, H. H., Merrit, Jr. L. L., Dean, J. A. and Settle, Jr. F. A., Fluorescence and phosphorescence spectrophotometry, Instrumental Methods of Analysis, Belmont, Wadsworth Publishing Company, (1988), pp.201.

[8] Belcher, R. and Freiser, H., Photophysical processes in isolated molecules, Fluorescence and Phosphorescence Spectroscopy: Physicochemical Principles and Practice, Pergamon Press, (1977), pp.36-37.

[9] Skoog, D. A., Holler, F. J. and Nieman, T. A., An introduction to spectrometric Methods, Principles of Instrumental Analysis, Philadelphia; Harcourt Brace, (1998), pp.136-137.

[10] Meyer-Arendt, J. R., Light Scatting, Introduction to Classical and Modern Optics, Prentice Hall, (1995), pp.277.

[11] Christian, G. D. and O'Reilly, J. E., Infrared and Raman spectroscopy, Instrumental Analysis, Allyn and Bacon, Inc., (1986), pp.215 – 217.

[12] Adams, M. J., Steventon, A. G., Reliability of long wavelength laser, Semiconductor Lasers for Long-Wavelength Optical-Fibre Communications Systems, Peter Peregrinus Ltd, UK, (1987), pp.80.

[13] Brown, M. B., The Use of Long Wavelength Fluorescence in the Study of Ligand-Protein Interactions, Ph.D. Thesis, Loughborough University, (1987), pp36-38.

[14] Brown, M. B., The Use of Long Wavelength Fluorescence in the Study of Ligand-Protein Interactions, Ph.D. Thesis, Loughborough University, (1987), pp38-40.

[15] Miller, J. N., Long wavelength fluorescence spectroscopy, Spectroscopy Europe, (1993), 5/2, pp.34-36.

[16] Hindocha, R K., Miller, J N. and Seare, N. J., On-line liquid-liquid extraction with near-infrared fluorescence detection, Analytical Proceedings, (1994), Vol.31, pp.185-186.

[17] Imasaka, T. and Ishibashi, N., Diode lasers and practical trace analysis, Analytical Chemistry, (1990), Vol.62, No.6, pp.363A-371A.

[18] Sauda, K., Imasaka, T. and Ishibashi, N., Determination of protein in human serum by high-performance liquid chromatography with semiconductor laser fluorimetric detection, Analytical Chemistry, (1986), Vol.58, pp.2649-2653.

[19] Brown, M. B., Miller, J. N., Riley, D. P. and Seare, N. J., Novel instrumentation and biomedical applications of very near-infrared fluorescence, Analytical Proceedings, (1993), Vol.30, pp.157-159.

[20] Studholme, R. M. and Blau, D.A., Background of the invention, Fluorimeter Detection System, International Patent Classification 5: G01N21/64, (1993), pp.1-3.

[21] Tran, C. D. and LU, J., Detection of flow analysis by acousto-optic tunable Filter-based fluorometry and its application in the determination of solvent polarity, Applied Spectroscopy, (1996), Vol.50, No.12, pp.1578-1580.

[22] Willard, H. H., Merrit, Jr. L. L., Dean, J. A. and Settle, Jr. F. A., Fluorescence and Phosphorescence Spectrophotometry, Instrumental Methods of Analysis, (7^{th} Edition), Wadsworth Publishing Company, (1988), pp.207.

[23] Rendell, D., Instrumentation, Fluorescence and Phosphorescence, Chichester: Wiley, (1987), pp.48-49.

[24] Afeyan, N. B., Gordon N. F. and Regnier, F. E., Automated real-time immunoassay of biomolecules, Nature, (1992), Vol.358, pp.603-604.

[25] Liao, N. L., Rapid determination of atrazine in environmental samples using automated flow injection immunoassay, Abstracts of Papers of the American Chemical Society, (1996), Vol.211, Pt.1, pp.10.

[26] Evans, M., The Development of A Fully Automated Immunoassay for Phenytoin Utilising Fluorescence Detection, Ph.D. Thesis, Loughborough University, (1996), pp.35-39.

[27] Li, Y. Q., Sasaki, Shin-Yi,, Inoue, T., Harta, A. and Ogawa, T., Spatial imaging identification in a fiber-bundle confocal fluorescence microspectrometer, Applied Spectroscopy, (1998), Vol.52, No.8, pp.1111-1114.

[28] Hatano, T., Kaneta, T. and Imasaka, T., Application of optical chromatography to immunoassay, Analytical Chemistry, (1997), Vol.69, No.14, pp.2711-2715.

[29] Johnson, J., Fluorescence technology: a bright future, Life Science Issue 23, (1997), pp.5 – 6.

[30] Hernandez, F., Beltran, J., Forcada, M., Lopez, F. J. and Morell, I., Experimental approach for pesticide mobility studies in the unsaturated zone, International Journal of Environmental Analytical Chemistry, (1998), Vol.71, No.1, pp.87 – 103.

[31] Maquieira, A., Puchades, R. and Gonzalez-Martiez, M. A., On-line immunoanalysis for environmental pollutants: from batch assays to automated sensors, Trends in Analytical Chemistry, (1999), Vol.18, No.3, pp.204 – 218.

[32] Dietrich, R., Usleber, E., Martlbauer, E. and Gareis, M., Detection of the nephrotoxic mycotoxin citrinin in foods and food colorants derived from moascus spp, Archiv Fur Lebensmittelhyfiene, (1999), Vol.50, No.1, pp.17 –21.

[33] Niessner, R., Immunoassays in environmental analytical chemistry: Some thoughts on trends and status, Analytical Methods and Instrumentation, (1993), Vol. 1 No. 3, pp.134-144.

[34] Jeanette, M., Emon, V. and Viorica Lopez-Avila., Immunochemical methods for environmental analysis. Analytical Chemistry, (1992), Vol. 64, No.2, pp.79A-88A.

[35] Boyer, A., Lipowska, M., Zen, J., Patonay, G. and Tsang, V. C. W., Evaluation of near infrared dyes and labels for immunoassays utilising laser diode detection: Development of near infrared dye immunoassay (NIRDA), Analytical Letter, (1992), Vol. 25, No.3, pp.415-428.

[36] Wittmann, C. and Schmid, R. D., Development and application of an automated quasi-continuous immunoflow injection system to the analysis of pesticide-residues in water and soil, Journal of Agricultural and Food Chemistry, (1994), Vol.42, No.4, pp.1041-1047.

[37] Leon-Gonzalez, M. E. and Townshend, A., Flow-injection determination of paraoxon by inhibition of immobilized acetylcholinesterase. Analytical Chimica Acta, (1994), Vol. 236, No.2, pp.267-272.

[38] Wortberg, M., Middendorf, C., Katerkamp, A., Rump, T., Krause, J. and Cammann, K., Flow-injection immunosensor for triazine herbicides using Eu(III) chelate label fluorescence detection, Analytical Chimica Acta, (1994), Vol. 289, No.2, pp.177-186.

[39] Marco, Maria-Pilar., Gee, S. and Hammock, B. D., Immunochemical techniques for environmental analysis II. Antibody production and immunoassay development, Trends in Analytical Chemistry, (1995), Vol.14, No.8, pp.415-425.

[40] Miller, J. N., Brown, M .B., Seare, N. J. and Summerfield, S., Analytical application of very near-IR fluorometry, Fluorescence Spectroscopy, New Methods and Applications, Springer-Verlag, Berlin, (1993 edited), pp.189-196.

[41] Sarpara, G. H., Hu, S. J., Palmer, D. A., French, M. T. and Miller, J. N., A new long-wavelength fluorigenic substrate for alkaline phosphatase; synthesis and Characterisation, Analytical Communications, (1999), Vol. 36, pp.19-20.

[42] Fintschenko, Y. and Wilson, G. S., Fundamental review flow injection immunoassay: a Review, Mikrochimica Acta, (1998), Vol.129, No.1-2, pp.7-18.

CHAPTER TWO

PRINCIPLES OF INSTRUMENT DEVELOPMENT

2.1 Introduction

The development of a novel fluorescence detection system (NFDS) involved the use of optical physics, electronics and computing technology.

The aim of the project was to develop a long wavelength fluorescence spectrometer to detect fluorescence between the wavelengths of 600 nm to 900 nm. Photon detectors, such as the photomulitipler vacuum tubes (PMTs), photodiode arrays (PDAs), photodiodes (PDs) and a charge couple devices (CCDs), can capture fluorescence from the sample. A large active area, high sensitivity silicon photodiode was chosen as the detector and a laser diode was chosen as an excitation source; this had a narrow spectral band, high luminescent efficiency, low power consumption and compatible size. A cut-off filter was used to remove any scattered laser light, and to minimise unwanted background fluorescence. A collimating lens was used to focus the fluorescence on to the detector.

The electronic and electrical parts of the NFDS included a multiple power unit, which transformed the main alternating current (AC) to the direct current (DC) and distributed it to each circuit. A linear operational amplifier collected the electrical signal from the PD. A laser driver with pulse generation was used to drive the laser diode in a pulsed mode. In order to achieve sensitive detection, a pulse format raising from several hertz to megahertz was used. An analogue signal to digital signal converter (ADC) was also used to transform the measurement data into a format that was compatible with a PC. This was to enable the data to be analysed.

2.2 Fundamental Operation of Fluorescence Detection System

The fluorescence detector is a spectroscopic optical instrument. Like an ordinary spectrometer, a fluorescence detection system detects light changes for quantitative analysis.

Light is just one portion of the various electromagnetic waves flying through space. The electromagnetic spectrum covers an extremely broad range, from radio waves with wavelengths of a meter or more, down to x-rays with wavelengths of less a manometer. Optical radiation lies between radio waves and x-rays on the electromagnetic spectrum, exhibiting a unique mix of ray, wave, and quantum properties.

Figure 2-1 **Optical portion of the electromagnetic spectrum**

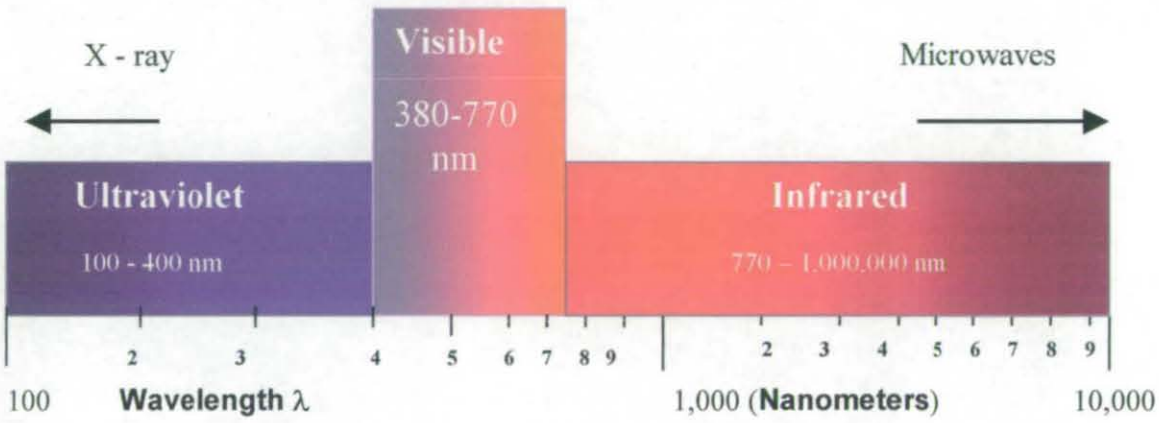

At x-ray and shorter wavelengths, electromagnetic radiation tends to be quite particle-like in its behaviour, whereas toward the long wavelength end of the spectrum the behaviour is mostly wave-like. The visible portion occupies an intermediate position, exhibiting both wave and particles in varying degrees. Like all electromagnetic waves, light waves can interfere with each other, become directionally polarised, and bend

slightly when passing an edge. These properties allow light to be filtered by wavelength or amplified coherently as in a laser.

In radiometry, light's propagating wavefront is modelled as a ray travelling in a straight line. Lenses and mirrors redirect these rays along predictable paths. Wave effects are insignificant in an incoherent, large scale optical system because the light waves are randomly distributed and there are many photons [1].

In this research, the excitation wavelength is selected in the region between 600 nm and 900 nm, i.e. the visible to near infrared light region (near-IR). Fortunately, the fluorescence wavelength of the emission beam is also in this region.

Hence, the fundamental idea of the fluorescence detection system is the same as in common luminescence spectroscopic instruments. Five basic functions are as follows:

I. Light sources.

Luminescence intensity is directly proportional to the intensity of the light source (see Equation 1-7), and high intensity sources can therefore be used to increase sensitivity and to lower detection limits in luminescence analysis. Laser diodes in this project have provided such high intensity excitation sources.

II. Sample holder.

A transparent container for holding the sample, i.e. cuvette or flow cell. Quartz cuvette or flow cell are used for measurements in the UV-Visible region, and less expensive glass cuvette or flow cell can be used for measurements in the visible region only. A various sample volumes of flow cell are available dependent on the requirement of measurement.

III. Wavelength selection.

Either filters or monochromators can be used for wavelength selection. Filters offer better detection limits and are therefore well suited to quantitative analysis, but do not provide wavelength-scanning capabilities desirable for acquisition of spectra. Monochromators provide wavelength-scanning capabilities as acquisition of spectra. Laser diodes can provide monochromatic light and do not require wavelength selectors except to isolate one of several lines if there is multiline output.

IV. A radiation detector.

Photon detectors convert radiant energy to a usable signal (usually an electrical signal). In general, PMTs are the most common detector which are sensitive in the range of 200 nm – 600 nm. Improved red-sensitive PMTs are also available for detection above 600 nm. PDs which provide high sensitivity and are robust solid state devices have been widely used in measurements of wavelength region 400 nm – 1000 nm. CCDs which are another kind of multichannel semiconductor solid state devices, offer more sensitive measurements in the most UV-visible region than PDs.

V. Readout and signal processor.

The output single is often transduced on a digital multimeter or a chart recorder, or is frequently interfaced to a PC with an appropriate data capture package.

The configuration of fluorescence detection system is illustrated in Figure 2-2.

Figure 2-2 **Configuration of novel fluorescence detection system**

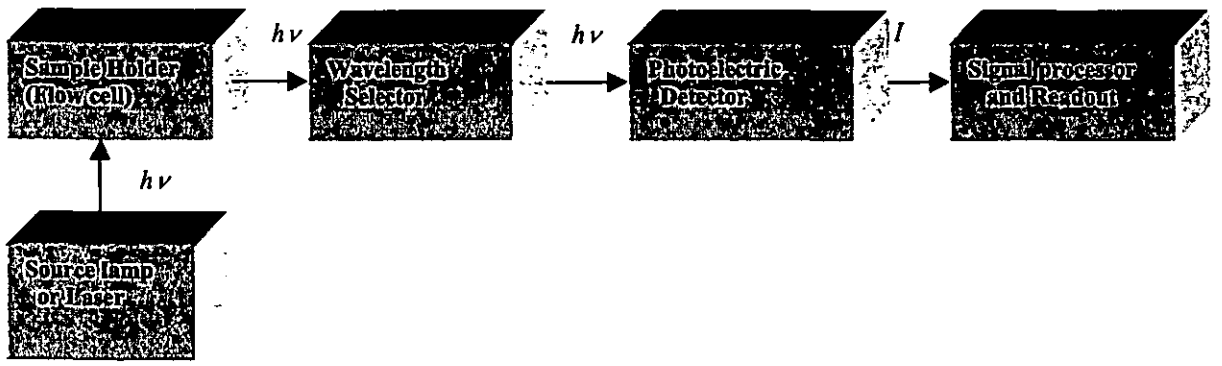

The light intensity I is proportion to the energy of the photon $h\nu$ (where h is Planck's constant, 6.62×10^{-34} J·s; ν is the frequency of the electromagnetic radiation). The performance of the system requires each component to co-ordinate in operation.

2.2.1 A Laser Diode as an Excitation Source

The term laser is an acronym that stands for "Light Amplification by Stimulated Emission of Radiation". As a consequence of their light-amplifying characteristics, lasers produce spatially narrow, extremely intense beams of radiation. The process of stimulated emission, produces a beam of highly monochromatic and remarkably coherent. Because of those unique properties, lasers have become sources for use in UV, visible and infrared regions of the spectrum.

Laser action can be explained by considering the four processes; (a) pumping, (b) spontaneous emission (fluorescence), (c) stimulated emission, and (d) absorption. The principle concepts of laser have been well summarised in Skoog's book (1999) [2].

The laser diode is fabricated with a semiconductor *pn* junction, which was first developed in the 1960's. The phenomenon of lasing, as it occurs in semiconductors, is

this. A radiative transition of an electron from the conduction band to the valence band, emitting a given wavelength of the light, can be stimulated to occur by an incident beam of radiation of the same wavelength.

Normally, the emission of radiation, as an electron falls from the conduction band to the valence band, is a random process and is referred to as spontaneous emission. The transitions occur at unrelated instants, so the overall radiation, although almost monochromatic, is incoherent. Stimulated emission is not only at the same frequency as the incident beam, it also occurs in phase with it, so that the resulting radiation is both monochromatic and coherent.

Figure 2 – 3 **The Heterostructure of (a) a LED and (b) a Laser Diode**

(a) The Heterostructure of a LED

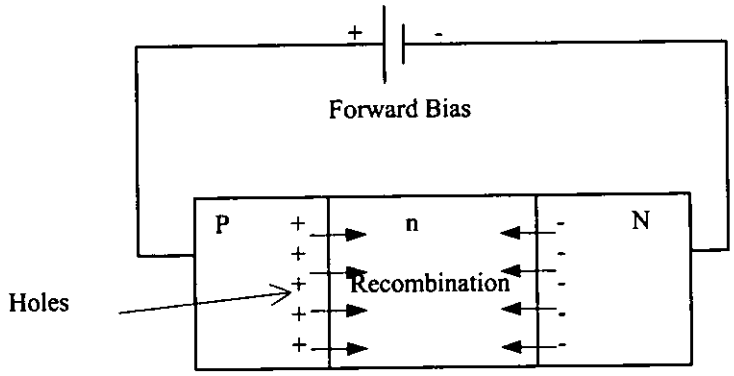

Note: P – P-type indium phosphide, N – type indium phosphide, n – n type indium gallium arsenide phosphide.

(a) The Heterostructure of a laser diode

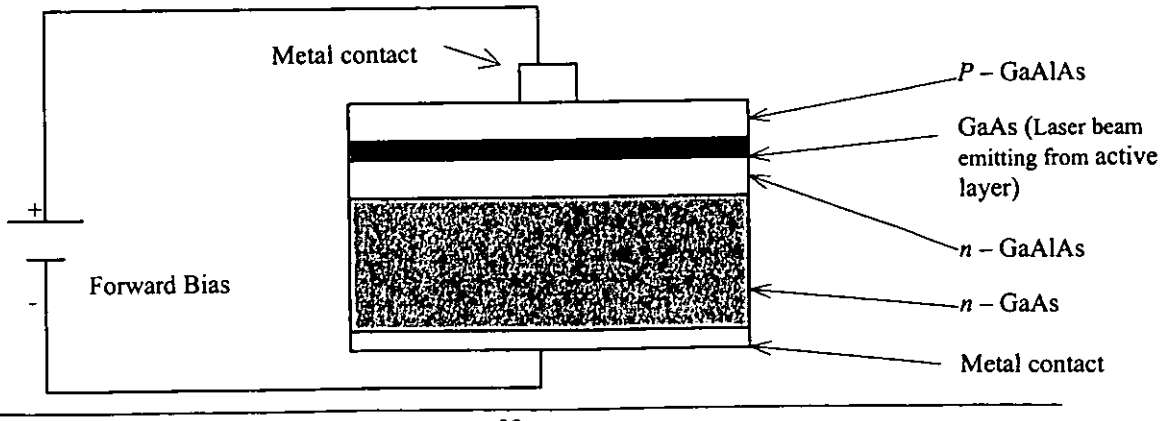

Understanding the principle of LED helps easily to explain the principle of laser diode. In operational principle of LEDs, when a voltage is impressed across a semiconductor diode in the forward direction, electrons are excited into the conduction band, hole-electron pairs are created, and the diode conducts. Ultimately, some of these electrons relax and go back into the valence band, the energy is released that corresponds to the band-gap energy $E_g = h\nu$ (h Plank's constant 6.62×10^{-34} J·s). Some of the energy is released in the form of electromagnetic radiation of the frequency $\nu = E_g h^{-1}$. Diodes that are fabricated to enhance the production of the light are called light emitting diodes (LEDs). Yet, the way for laser diode to achieve amplification is to ensure that there is high concentration of the hole-electron pairs to recombine. The impinging beam will then stimulate a more intense emission of radiation than the original beam. The structure of a semiconductor laser is much the same as the LED expect that light is allowed to emerge from the ends of the central region of the device so the narrow n-type layer. The heterojunctions run the full length of the device so the narrow n-type layer contains a concentration of the holes and electrons waiting to recombine all along its length. All that has been achieved is an 'edge-emitting' LED. The light generated spontaneously within the region is then reflected back and forth along the region causing stimulated emission to occur. A favored design is double heterostructure, like that of the edge-emitting LED but with both end faces made reflective – the output end has to be only partially reflective so that a fraction of the light can emerge at each reflection. In practice, a photodiode placed at one end can be used to monitor the light intensity and to control the current through the diode. Since this current creates the clouds of the holes and electrons, it is a convenient means of keeping the light intensity of the source constant [3].

Therefore, most laser diodes take advantage of the high efficiency of radiative emission from electron-hole recombination directly across the band-gap. The lasing requirement for population inversion is obtained by applying a forward bias such that electrons and holes are forced at high concentrations into the depletion layer formed by the space charge at the junction [4].

Figure 2-4 **Elliptical output beam of a typical laser diode**

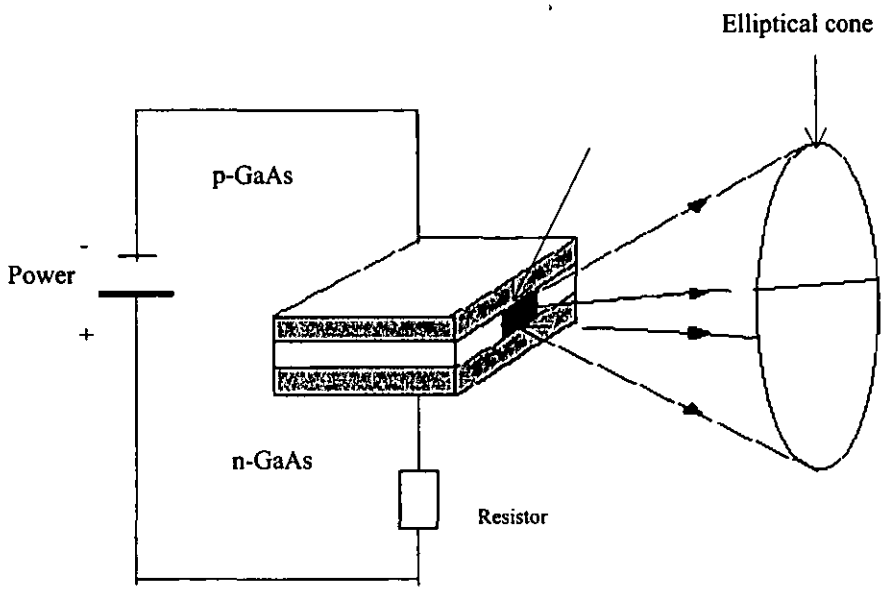

The elliptical cross section of the beam is a result of the rectangular shape of the beam emission facet of the laser diode. This characteristic prevents the beam from being entirely collimated, allowing quasi-collimation only. Also, astigmatism is in fact another result of the rectangular facet of the laser diode. The existence of astigmatism means that when using a single standard aspheric lens, the beam can be collimated only in one direction. However, most manufacturers have considered these characteristics and they incorporate a basic single-element aspheric lens to produce a quasi-collimated beam — "constant optical output power operating mode" [5].

Therefore, the electro-optical characteristics are important to evaluate the laser diode's behaviour.

Figure 2-5. **Electro-optical characteristics of laser diode**

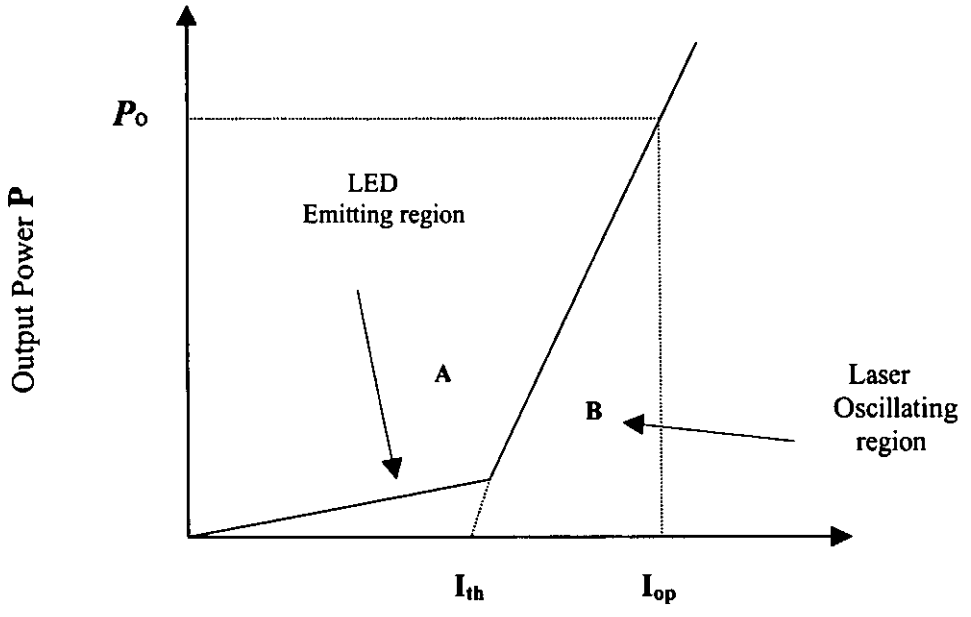

a. The curve distinguishes the LED light emitting region *A* from the laser oscillating region *B*, the current level that triggers laser oscillation is the threshold current ($\mathbf{I_{th}}$). In fact, $\mathbf{I_{th}}$ is defined as the point where the straight line in region B intersects the X axis.

b. Light output power (P_o) varies with the current during continuous operation.

c. Operation current ($\mathbf{I_{op}}$) in the forward direction is required to generate rated light output power.

In the NFDS, the modulated laser diode was employed to generate a narrow excitation beam even without a lens being between the sample and the light source. There is a great deal of literature concerned with the qualitative comparison of linewidths for

laser emission and spontaneous emission involving the same pair of energy levels in an atom. The broad peak is the lineshape of spontaneously emitted light between energy levels E2 and E1 before lasing begins. The sharp peak is the lineshape of laser light between levels E2 and E1 after lasing begins. This is illustrated in the following diagram [6].

Figure 2-5 **Qualitative comparison of linewidth for laser emission and spontaneous emission**

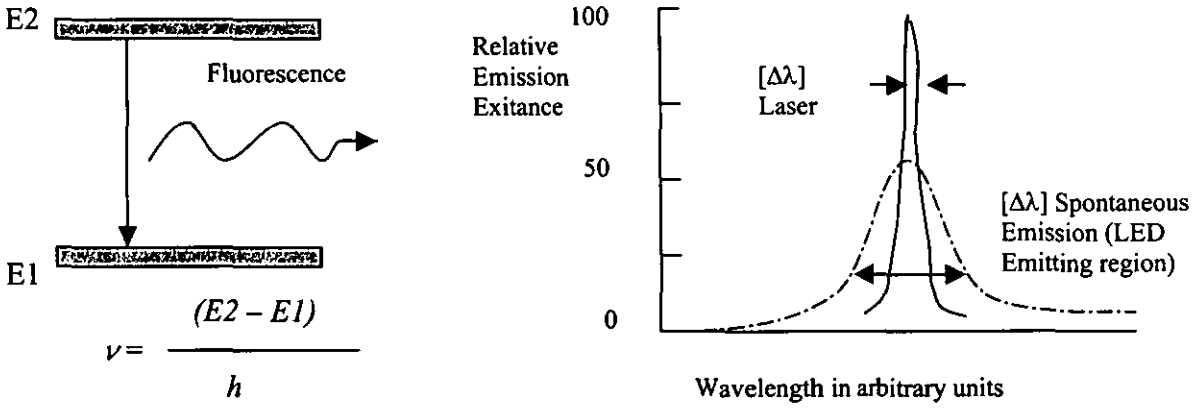

Note: h – Plank's constant, 6.62×10^{-34} J·s; ν – the frequency of the electromagnetic radiation.

Obviously, a laser diode has all the general advantages and convenience of a semiconductor and solid-state devices in the following respects:

1. Excitation in the narrow wavelength as a source.
2 Compact, efficient, low cost and in many ways superior to other laser technologies.
3 Life time exceeding 50,000 hours.
4 Low operating voltage compared with the lamp as an exciting source.
5 The small geometry and nature of the lasing cavity simplifies modulation of the laser output at frequencies up to 1 GHz.

2.2.2 Performance of Electrooptical Devices

An electrooptical device is a transducer that converts electromagnetic radiation into an electron flow, and subsequently, into a current flow or voltage in a readout circuit. The performance of the optical detector is strongly influenced by the incident wavelength whatever the choice of photomultiplier tubes (PMTs), photodiodes (PDs) and charge couple devices (CCDs). Many optical detectors do not respond at all if the wavelength is longer than a certain cut-off wavelength. All optical detectors involve a quantum effect (QE), in which the photon energy is an important parameter. The energy level of each photon Ep is expressed by the following equation:

$$Ep = c\,h/\lambda \qquad (2-1)$$

Where h = Planck's constant = 6.62×10^{-34} J·s.

c = Velocity of light = 3.0×10^{8} ms^{-1}.

λ = Wavelength of light.

For convenience reasons, the photon energy can be given in electron-volts (eV) and wavelength in nanometers (nm). Therefore $c\,h$ = Constant = 1240 eV/nm.

Since the wavelength region in this project is from 600 nm to 950 nm, the energy level of each photon for this region is between 2.1 eV and 1.2 eV (or 199 $kJmol^{-1}$and 116 $kJmol^{-1}$ because 1 J is 6.24×10^{18} eV) according to the Equation 2–1. Nearly all electrooptical effects require that a single photon has sufficient energy to free an electron by overcoming the energy of a chemical bond or trap in a solid. Most bond energies lie in the range of 0.2 to 4 eV (or 19.3 $kJmol^{-1}$ to 385 $kJmol^{-1}$) the minimum photon energy needed is in this range. Practically, trapping energies lower than this

commonly occur in semiconductors, but the trapped charge carriers are released by the thermal energy (approx. 0.025 eV or 2.4 $kJmol^{-1}$ at room temperature) unless the detector is cooled.

Figure 2-6 **Optical spectrum and photon energy**

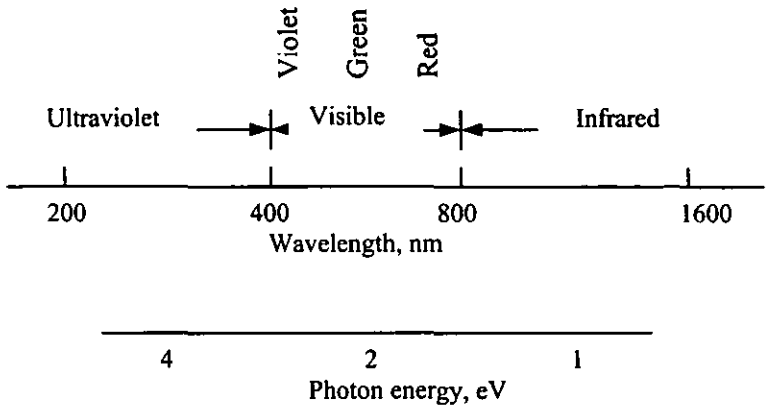

Figure 2-6 indicates that where the longer wavelength of light is located, the lower energy of the photon is required.

Light intensity referring to the amount of power emitted from the source is commonly expressed in watts, which can also be defined as energy or radiant flux, expressed in watts per square meter. Most photon detectors are specified in terms of irradiance with units of watts per square centimeter. Dark current is the current that flows in a photo detector in the absence of incident light. Dark current that increases with increasing reverse bias, is one of most important parameters to evaluate photon detectors.

In fact, the intensity of fluorescence detection using a photodiode in this research was in millivolts, because the response of the light from the photodiode, to the electrical signal, was converted and mostly displayed in voltage using a digital multimeter or a PC with data capture package (see section 4.4.1).

2.2.2.1 Photomultiplier Vacuum Tubes (PMTs)

Despite many advances in semiconductive electrooptical devices, the photomultiplier vacuum tubes (PMTs) are still the most widely employed photodetectors for conventional fluorescence detection.

Figure 2-7 **Structure of a photomulitipler vacuum tube**

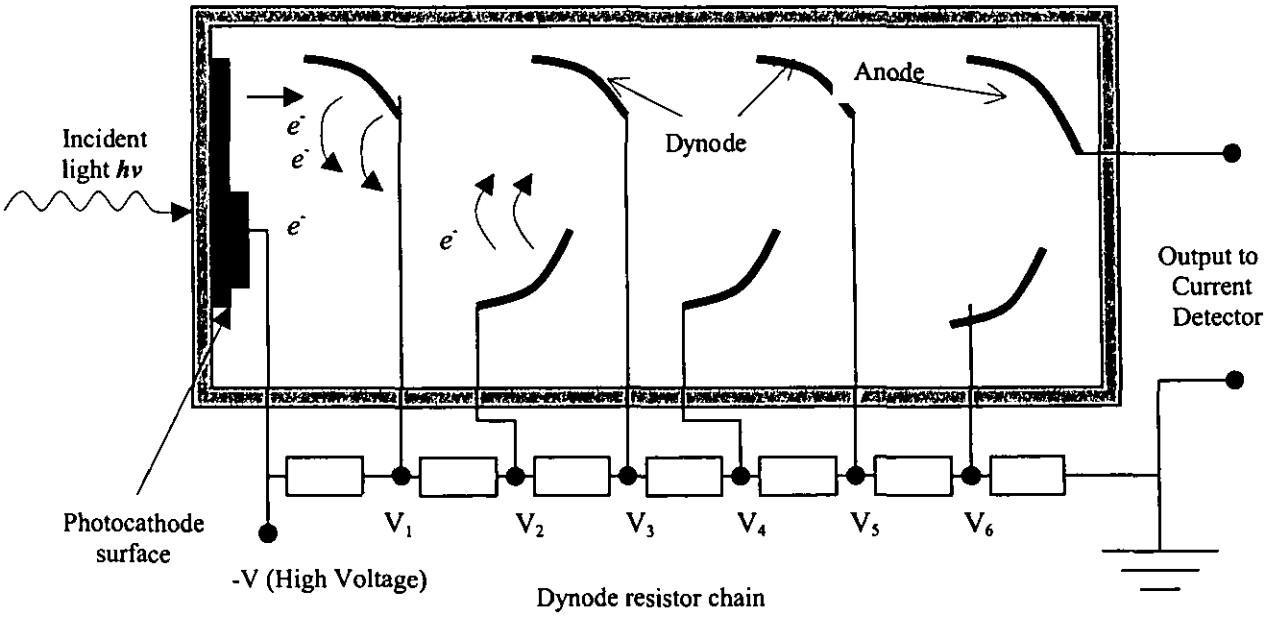

Figure 2-7 shows the structure of a linear focused head, which is one type of PMTs. In this type of photosensor, there are a number of positively charged anodes, called dynodes that intercept the electrons. When light impinges on the cathode, electrons are emitted because of photoelectric effects. They are accelerated through a positive high-voltage potential V_1 to the first dynode. They acquire substantial kinetic energy during this transition, so when each electron strikes the metal, it gives up its kinetic energy. In the giving up of this kinetic energy, some is converted to heat, while some is converted to an increased current flow by dislodging additional electrons from the dynode surface. Thus, a single electron causes two or more additional electrons to be dislodged. These electrons are accelerated by a high-voltage potential V_2 and

reproduce the same effect at the second dynode. The process is repeated several times, and each time several more electrons join the cascade for each previously accelerated electron. Eventually, the electron stream is collected by the last dynode or a separate anode and can be used in an external circuit.

Most PMTs are used in the UV and visible region, and are more sensitive here than in the long wavelength region. Some improved PMTs are being employed in long wavelength fluorescence detection, but they are costly and still need high voltage supplies.

2.2.2.2 Photodiodes (PDs)

There are mainly two types of photodiodes used in fluorescence detection, silicon photodiodes and avalanche photodiodes. Despite the avalanche photodiode having high sensitivity, low noise and high speed, the extremely small active area of the fastest devices in fluorescence studies primarily limited its application. Large area avalanche photodiodes (LAAPDs) have been recently available, but their cost is still over expected in this research.

Figure 2-8. **Configuration of a silicon photodiode geometry**

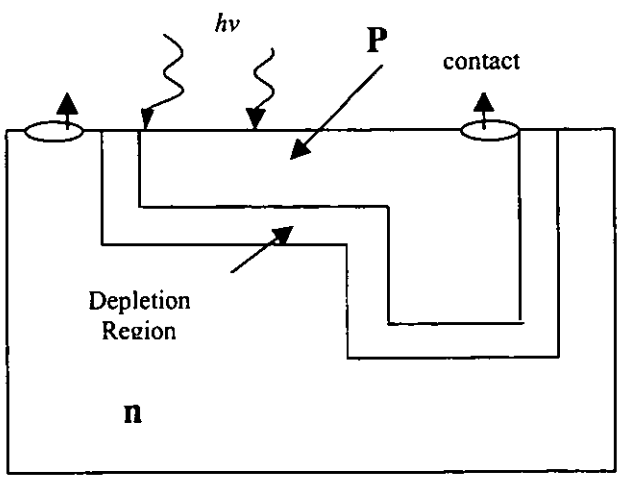

Such *planar* diffusion type silicon photodiodes are perhaps the most versatile and reliable sensors available. The fundamental principle upon which the photodiode operates is a quantum effect. The basic construction is shown in Figure 2-8.

If the light is absorbed in a semiconductor with a certain probability, an electron is excited into the conduction band. If the extra charge carriers are produced a long way from the junction it causes a slight increase in conductivity/photoconductivity. This is negligible if the diode is reverse-biased. A minority of carriers are produced near the junction in the depletion region, and have a marked effect because they are drawn by the field through the junction and contribute to the reverse current, which is very small in the dark. The junction must be close to the surface (P region should be thin), since light is absorbed as it passes through silicon. The energy absorption is the first step in a photoelectric conversion, since standard photodiode chips are small. A glass or plastic lens is often used to focus the light onto the active area [7].

In practical circuits, the current magnitudes are of more significance than the number of the charges present. The current is the charge flow rate. This idea is used to develop the equation 2 – 2 for the photo-generated current in a quantum photodiode [8].

$$I_P = \eta H_o A \frac{e\lambda}{hc} \qquad (2-2)$$

Also, for most engineering, a useful parameter to define for a photodiode is the flux responsivity, R.

$$R = \eta \frac{e\lambda}{hc} \qquad (2-3)$$

Where I_P is the amount of photo current in amps.

η is the ratio of electrons to photos (quantum efficiency, QE).

H_o is the flux density, in watts per unit area.

A is the active area of the photodiode, mm^2.

e is the charge of the one electron, 1.60×10^{-19} eV.

λ is the photo wavelength in nm.

h is Planck's constant, 6.62×10^{-34} J · s.

c is the speed of the light, 3.0×10^{8} ms^{-1}.

R is the flux responsivity in amps per watt.

As equation 2–2 illustrates the amount of photon current created is directly proportional to the flux density H_o, the active area A of photodiode, and the wavelength λ. Therefore for a photodiode the bigger the quantum efficiency η and active area A, the more amount of photon current I_P, which means more sensitive in operation. The most silicon photodiodes have 45 –55% of quantum efficiency except avalanche photodiode. However the active area A of photodiode varies with the type of the product.

Furthermore, four physical conditions, which are reflection, decreasing absorption of long wavelengths, short wavelength absorption and bandgap limit, cause a photodiode's responsivity R to be different from that of an idealised quantum photodiode. Mooney's book [9] clearly described these four conditions.

Typical silicon photodiode characteristics are shown in Figure 2-9. Note that the current is linearly proportional to the incident light intensity over a wide range. It should be emphasised that that is the reverse current, and not the conductivity of the

device. The current at a given light level is nearly independent of diode voltage [10-11].

Figure 2-9. **Current versus intensity of a photodiode**

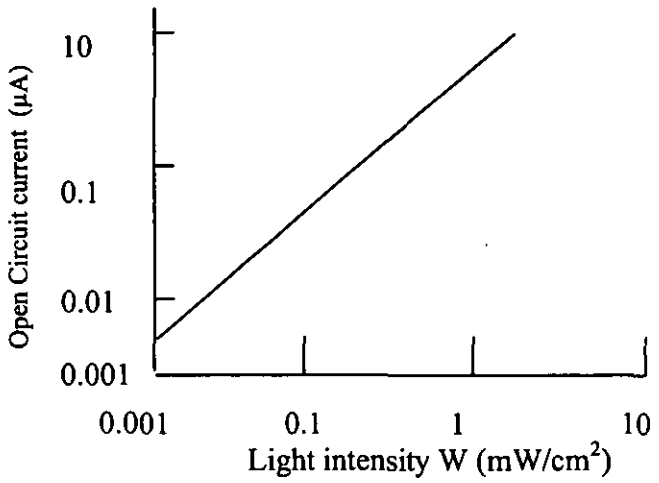

Figure 2-10 **Spectral response of a photodiode**

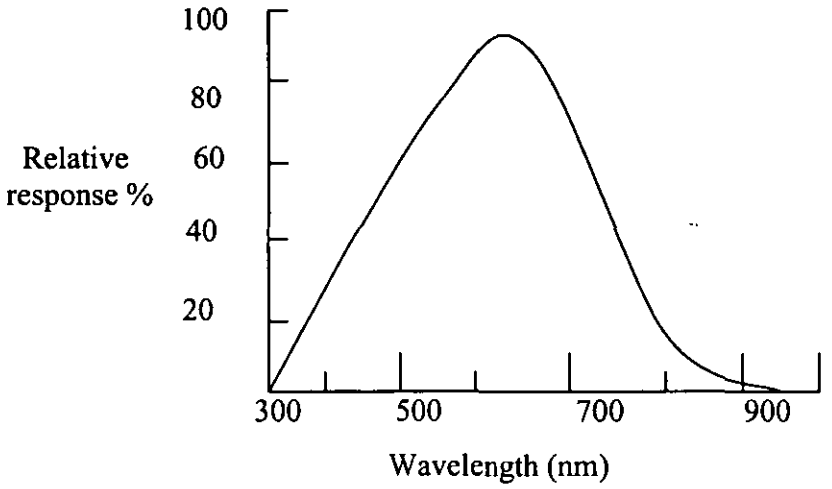

Regularly, a high-input-resistance FET (Field-Effect Transistor) amplifier is applied to photodiode amplifying circuits, or a preliminary amplifier.

2.2.2.3 Charge Couple Devices (CCDs)

CCD is one of multichannel detectors and come in a semiconductor "chip" package. The basic concept of a CCD is a simple series connection of MOS (Metal Oxide Semiconductor) capacitors. The individual capacitors are physically located very

close to each other. To operate the CCD, charge packets are transported from one capacitor to its neighbour by means of digital pulses on the top plates of the MOS structure.

Figure 2-11 **Layout of Charge Coupled Device Detector (CCD)**

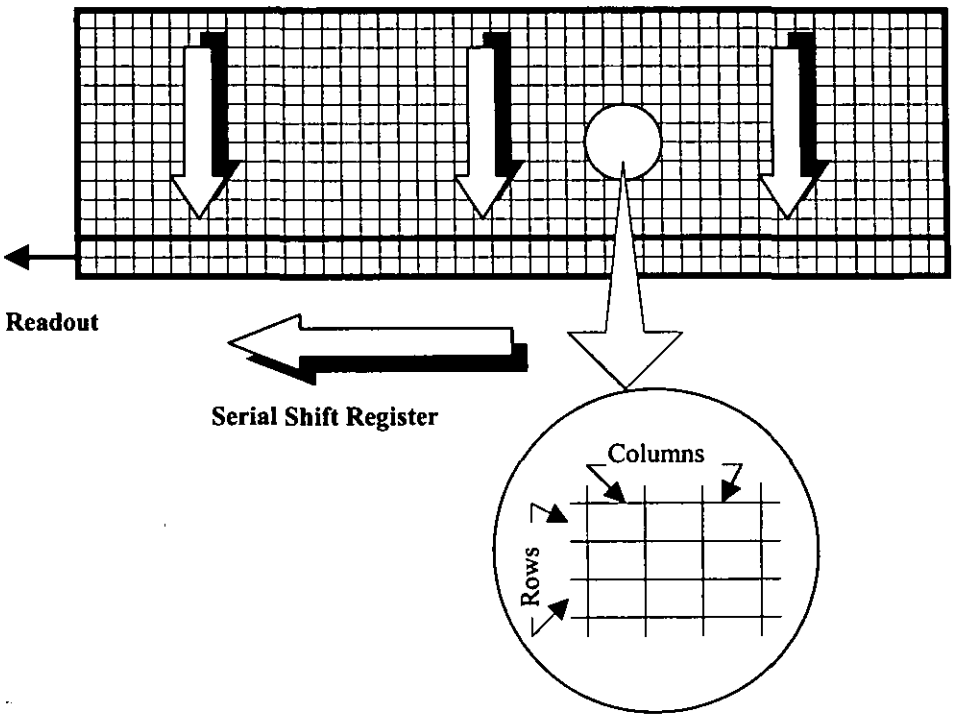

A CCD pixel may be composed of one to four gate electrodes. During the charge collection, or integration period, electrons generated by photons are collected under selected gate electrodes. After collection, the electrons are sequentially shifted between pixels to the readout electronics by cycling the bias on the gates [12].

A typical spectroscopic CCD layout is a two-dimensional array of 1024 by 256 pixels with each pixel 27 μm square. The signal is shifted down sequentially to the register and then read out. The most important benefit of this readout method is that the associated readout noise is very low, about ten electrons per pixel. The CCD is

approximately 100 times more sensitive than a photodiode array (PDA), making it best suited for Raman, luminescence or any very low light applications.

There are mainly two types of CCD chips, i.e. front illuminated CCD and back illuminated CCD. The fundamental operation of these CCDs is same as described above. The CCD not only has the advantage of the solid-state device, but also other excellent features such as resolution, dynamic range, low dark current. In particular, the high sensitivity of the CCD can capture the low fluorescence signals generated in a flow injection system. Advances in electrooptical devices have shown the potential of CCD, such that many spectrophotometers will use CCD to achieve highly sensitive levels of detection.

However, there are still some limitations in the use of current CCD technology for fluorescence detection in our application. For instance, high pixel density restricts the continuously fast capture of exposed incident light. At the moment, the spectral speed using a CCD device is approximately several hertz to a hundred hertz.

2.3 Electronic System

With the exception of fluorescence detection, most analytical radiation signals are analogue signals that vary continuously and can assume any of an infinite number of values between certain limits. Therefore, transducers in a fluorescence spectrometer have to be employed to convert analogue light signals to analogue electrical signals, which are then processed, and displays may take the form of the intensity of fluorescence through a chart recorder or the screen of a PC with data capture software. In particular, a laser pulse generator is utilised to generate the variation of pulse format to produce an electronic gating approach, which can increase the sensitivity for fluorescence detection. In addition, a multiple power supply unit is designed for the entire electronic system.

2.3.1 Operational Amplifiers to Produce the Potential Signals

As the current conversion of the photons to the potential in voltage takes place in a photodetector, operational amplifiers can be generally used in the precise measurement of variation of voltage in the fluorescence detector.

It is important to properly utilise an operational amplifier chip in order to be suitable for such a process. Basically, there are many types of integrated circuit chip (IC chips).

Firstly, a field-effect Transistor (FET) has very high input impedance so it makes a good voltage amplifier [13]. However, FET devices are generally used as amplifiers and switches in non-linear circuits such as mixers. Furthermore, improved junction field-effect transistors (JFET) are commercially available. Secondly, another type of IC chip, complementary metal oxide semiconductor field-effect (CMOS) devices,

offer the advantages of reduced power consumption and excellent noise immunity compared with regular MOS components.

The operational amplifier circuit is one basic component of most analogue signal modifiers. It should be a high-gain amplifier that, when connected to an electrooptical sensor, can perform a variety of mathematical operations on the analogue signal. The desirable characteristics of such an amplifier are derived from two properties; high-gain DC amplification and the provision for external feedback. The combination of high gain and feedback allows the output signal produced, to depend primarily on the components in the external feedback circuit. In addition, the properties of high input impedance, low output impedance, and good response to high-frequency input signals are required for the amplifier to function properly. The basic principle of the operational amplifier can be illustrated in Figure 2-12. Schematically the operational amplifier is represented by a triangle with inputs and outputs.

Figure 2-12. **Operational amplifier with external components**

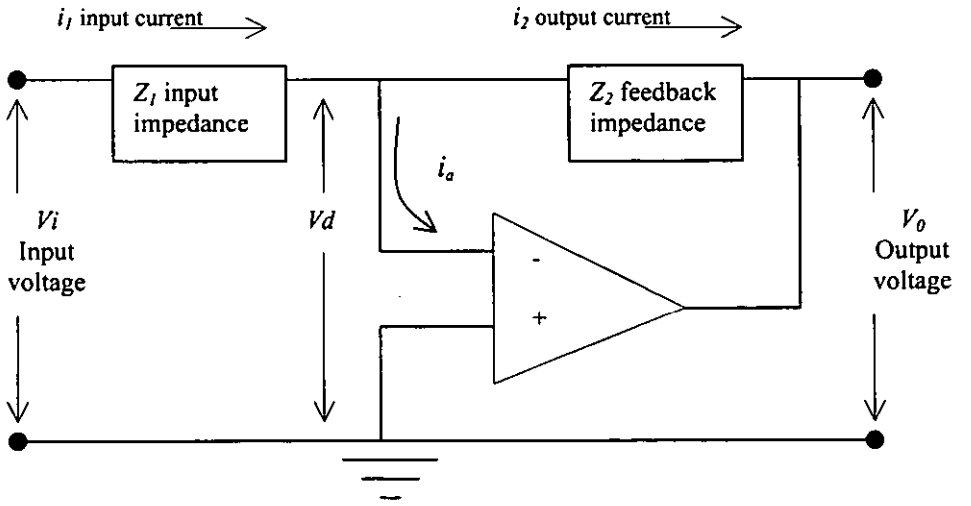

When the operational amplifier is used for the detector of signal transformation, it is normally used in the closed-loop configuration where the impedance Z_1 and Z_2

generally consist of resistors and/or capacitors external to the operational amplifier. Since the input impedance of the amplifier itself is very large, the current into the operational amplifier i_a is practically zero and can be neglected, thus $i_1 = i_2$.

The normal operation of the operational amplifier requires that the two inputs be at essentially the same voltage, $Vd = (V+ - V-) \cong 0$. The allowable difference at the inputs then depends upon the open-loop gain G and limiting output voltage V_0. With a differential input, $V_0 = G(V+ - V-)$, that has a maximum of approximately 10 Volts and a very large gain, the input different $(V+ - V-)$ must be close to zero. Thus:

$$i_1 = \frac{1}{Z_1}(Vi - Vd) = \frac{Vi}{Z_1} = i_2 = \frac{1}{Z_1}(Vi - Vd) = \frac{V_0}{Z_2}, \qquad (2-4)$$

and therefore:

$$V_0 = -\frac{Z_2}{Z_1} Vi \qquad (2-5)$$

This operational amplifier is the basis for many signal-modifying circuits and extended in many applications. The composition of $Z1$ and $Z2$ determines the relationship between the input and output voltage signals [14]. In this research, such an operational amplifier can (1) generate required voltage ramps, (2) provide the accurate voltages required for precise measurements and (3) amplify the resulting current.

2.3.2 Analogue to Digital Conversion

Since the data handling takes place by the means of the computer, more and more data handling software have become commercially available, and has caused a revolution in routine analysis compared to the conventional methods. However, the data handling software still depends upon the source of signals from the detector. It is therefore necessary to set up the relationship between the analogue signal from the detector and the digital data from a PC. A digital circuit offers some important advantages over its analogue counterparts. Digital circuits are less susceptible to environmental noise, and digitally encoded signals can usually be transmitted with a higher degree of signal integrity. Digital signals are also compatible with digital computers, which means that software approaches can be used for the extraction of information from a chemical signal, i.e. fluorescence signal from a flow cell/cuvette.

Since the input transducers initially produce analogue signals, an analogue to digital converter (ADC) produces the digital representation of analogue input signals. For example, the intensity of fluorescence in the flow cell/cuvette is often measured with a photon detector that converts the radiant energy into an analogue current, which can vary continuously over a considerable range. However, at low radiation intensity, a properly designed detector can respond to the individual photons and produce a signal that consists of a series of pulses that can be counted by an ADC. Usually, there should be two important parameters, resolution and sampling that characterise to analogue to digital converters.

The resolution:

The number of bits in the digital signal determines resolution, e.g. 10 bit, 1 part in 1024 and 12 bit, 1 part in 4096. Thus for an ADC converter with a maximum range

from 0 to 5 V dc and 12 bits of output, the smallest change that can be detected in the digital output is 5V/4096 = 4.88 mV. The ADC sets the limit on resolution of the system; greater resolution translates into more bits of digital data, which means higher accuracy.

The rate of sampling:

Nyquist frequency rule states that the rate of sampling must be greater than twice the highest frequency component of the analogue to digital (A/D) input.

The parameters are determined by the detection system used for the analogue-to-digital conversion, which may be achieved by several methods. The following diagram shows the basic procedure.

Figure 2-13 **Analogue-to digital converter block**

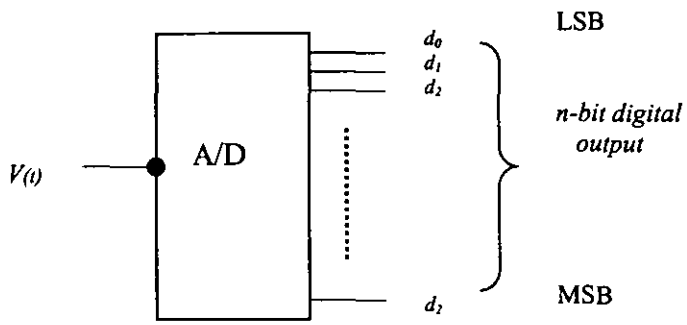

Note: LSB – Least signal bit; MSB - Most signal bit; *V(t)* – the input voltage in volt.

A complete A/D conversion system could be used as an interface for a computer system. However, the most important characteristics of ADC are speed and accuracy of conversion.

2.3.3 Laser Pulse Generation

Theoretically, a fluorescence detector is capable of being the most sensitive of all analytical tools that detect single photon events, with the possibility of re-exciting a fluorophore to confirm the analysis. However, the problem, which has plagued fluorescent signal detection, is distinguishing the signal of interest from the background radiation in the system. The problem caused by background radiation is particularly acute in biological systems. Other sources of undesirable background radiation include ambient radiation and various scattering mechanisms. Earlier attempts to overcome these problems of background radiation have met with limited success [15]. Generally, a filter is used to reject detected radiation at all but a narrowly defined wavelength band. A second technique attempting to discriminate the desired fluorescent signal from background is the so called *gating approach* which produces an interval pulse of excitation beam to prevent excess light and scattering effects causing interference and is used in many spectrophotometers. Figure 2-14 shows the pulse generation and driving laser as an excite source.

Figure 2-14 **Laser pulse generation to drive an excitation source**

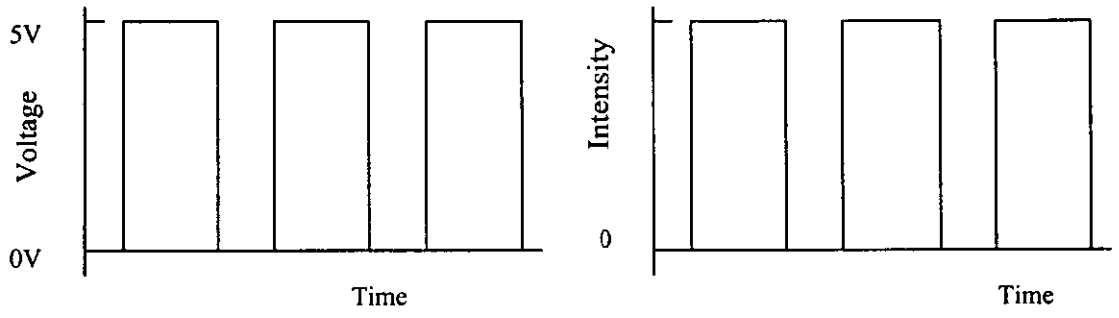

The combination of two above techniques increases the sensitivity of fluorescence detection. Thus, there have been two excitation pulse formats for transient state fluorescent analysis, which is either a single, relatively high power pulse or high-

speed pulse to excite the fluorophore in the sample. With the development of lasers, the excitation source is a laser diode not a lamp. Therefore, the laser pulse generation is required to drive the laser diode, which has many options of pulse speed according to the measurement.

The laser pulse format in this project gave the beneficial aspects as follows:

I. The improvement of the ratio of signal to noise, which is same as the most pulse formats in analytical instrument, in which synchronised gated detection is used.

II. The higher stability of operation could be achieved because the heating in a pulse format is less generated than in a constant wavelength (cw).

III. The potential of pulse format which has be successfully established for a fluorescence detector coupled flow injection immunoassay [16], could be to extend the NFDS for multi analysis using various wavelength laser diodes and time resolved detection.

The most convenient pulse generator, which can be carried out on the pulse of square waveforms, is the astable configuration of the IC timer. Pulse width and frequency F can be controlled by the indicated RC products by adjusting the ratio of R_A to R_B (see Figure 2-15). However, the output signal of pulse from the IC timer can not straightforwardly drive the laser diode. Usually, operational amplifiers are employed to magnify the pulse signal and drive the switching circuit to control the output speed of laser pulse.

Figure 2-15 **Pulse generator based on the astable IC timer**

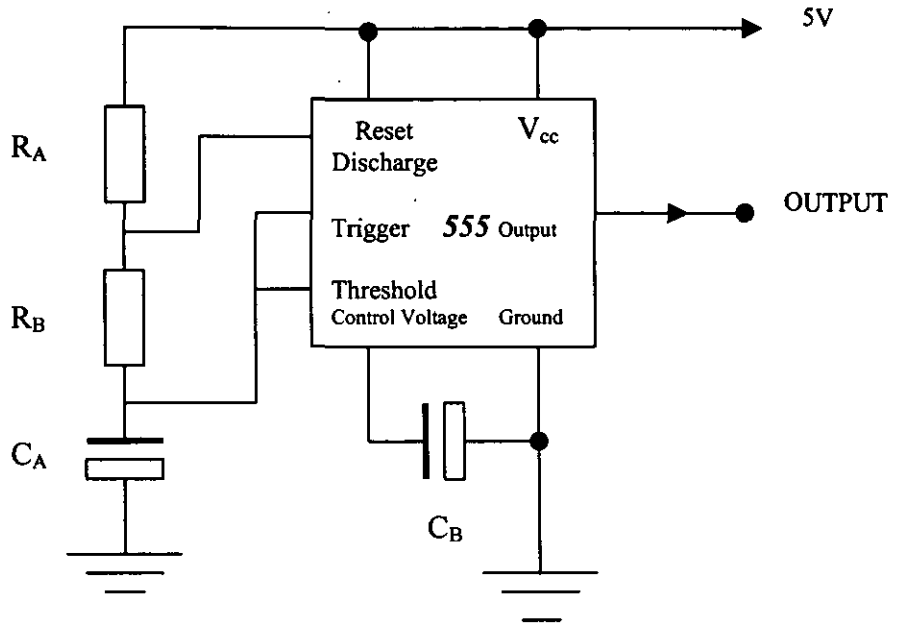

Note: R_A, R_B are resistors respectively; C_A, C_B, are capacitors respectively.

Such astable cofiguration of the IC timer generates only analogue trigger signal not TTL output. However, some IC555 timers, i.e. TLC555 [17] used in this research, have been improved in their behaviours, i.e. the speed (see Section 4.3.3).

Also, crystal oscillators that can generate oscillation between 10KHz to 20MHz are frequently employed as accurate frequency or time references. Actually, there are two types of crystal oscillators, one is quartz crystals and another less accurate ceramic crystals. These piezoelectric crystals are electromechanical devices which exhibit marked electrical resonances at the mechancial resonance frequencies. Conversely, when an ac voltage is applied across the crystal, it vibrates at the frequency of the applied voltage [18]. These crystal oscillators can be built as pulse generators which provide more accurate laser pulse foramtes than IC timer circuits, i.e. IC555 timer. The circuit using crystal oscillators is slightly more complicated than using IC 555 timer.

2.3.4 Design of a Power Supply

Generally, the detector requires a DC power to operate amplifiers and other reactive components, and contains three or four general stages to convert power, which are shown in Figure 2-16.

Figure 2-16 **Simplified block diagram of a power supply**

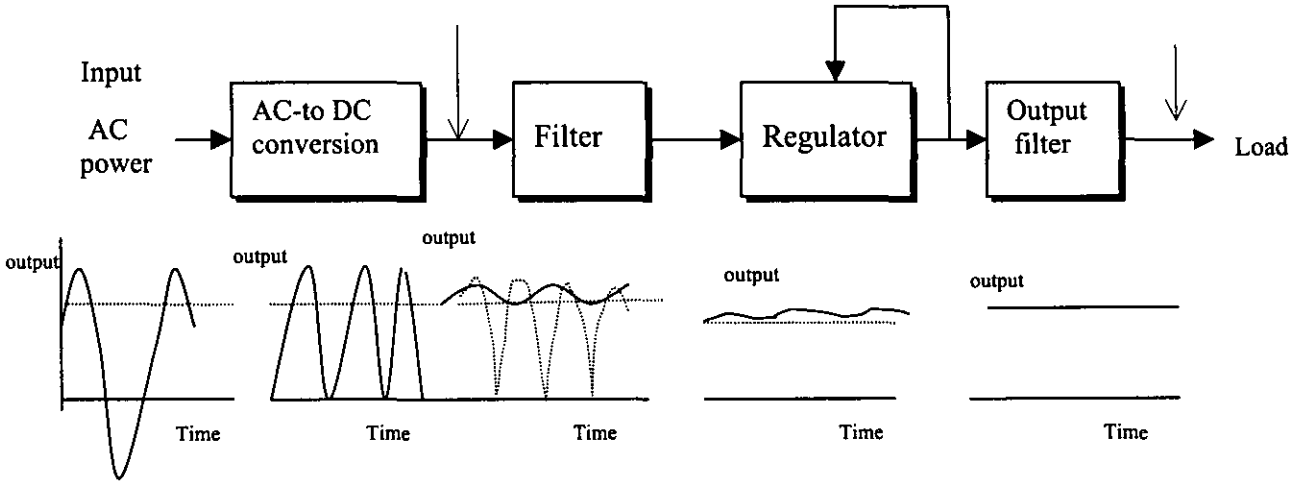

Firstly, the converter transforms the AC power to some intermediate form of the DC power. Then it filters the DC power to remove gross variations in the voltage and supplies the filtered DC power to the regulator. Secondly, the regulation stage uses feedback to control the output voltage level at the load. Finally, the output filter smoothes the variations in the load voltage.

The output power depends upon the consumption of the detection system including a laser pulse generator, an operational amplifier and a digital display etc. The basic formula for estimating the power is:

$$P = VI \qquad (2-6)$$

Where: P is total output power in watt.

V is DC voltage of output in volt.

I is DC current of output in amp.

If there are several distributors in power supply, the formula would be written as follow:

$$P = V_1I_1 + V_2I_2 + V_3I_3 + \ldots V_nI_n.. \qquad (2-7)$$

Where: P is the total output power.

V_1 , V_2 , V_3 .. V_n are the DC voltage of the output in an individual distributor.

$I_1, I_2 , I_3 . I_n$ are the DC current of the output in an individual distributor.

2.4 Elements of Optical System

Conventional optical methods are still widely used in fluorescence spectrophotometers although many advances have been made to instruments by novel solid state components.

2.4.1 Setting up an Optical Bench

The best fluorescence measurement set-up should be in accordance with the principle of a conventional spectrophotometer as well as providing as much flexibility as possible. The idea is to prevent the environmental parameters from influencing the measurement. Otherwise, the measurement would not be repeatable at a different time and place.

Baffles, for example, greatly reduce the influence of stray light reflections. A baffle is simply a sharp edged hole in a piece of thin sheet metal that has been painted matt black. The light outside of the optical beam is blocked and absorbed without affecting the optical path. It is a good idea to leave as much space between the optical path and walls as is practical. Distant objects make weak reflective sources because of the Inverse Square Law [19]. An object that is near to the detector, however, has a significant effect, and should be painted with "black velvet" paint or moved out of view.

The "zero" reading should be made with the sources ON, to maintain the operating temperature of the laser diode as well as measure the emission beam that has defeated the baffling scheme from a cuvette/ flow cell. Accurate distance measurements and repeatable positioning in the optical path are the most important considerations when setting up an optical system. The goal of an optical system is to provide repeatability. It is not enough to merely control the distance from the laser diode source to the flow

cell or the cuvette, since each laser diode has non-uniform beams. A proper photodiode mounting system would provide the adjustment of position and angle in 3-D space, as well as interchangeability into a calibrated position in the optical path.

Another important point of setting up an optical bench is to minimise the environmental vibration. Floor vibration in research environments is typically dominated by random, "broadband" energy, as opposed to pure tone energy consisting of discrete frequencies. Although both broadband and pure tone vibrations will excite the system resonance of an optical bench, the degrees of their excitation will be different.

2.4.2 Selection of a Suitable Optical Filter

Choosing a filter in the fluorescence spectrophotometer is to meet the requirement of practical measurement. A detector's overall spectral sensitivity is equal to the product of the responsiveness of the sensor and the transmission of the filter. Given a desired overall sensitivity and a selected wavelength, the ideal filter transmission covers the detection response range. Filters operate by absorption or interference. Coloured glass filters are doped with materials that selectively absorb light by wavelength [20].

Optical filters can be made of tinted glass, gelatin (Wratten filters) containing organic dyes usually sandwiched between glass or lacquered for protection, a liquid solution of absorbing substances, or they can be interference filters. In general, there are three types of absorption filter for fluorescence applications, neutral tint, cut-off filters and bandpass filters. *Neutral tint* or *neutral density filters* have a nearly constant transmission over a wide range of wavelengths. They are used to decrease the intensity of light uniformly and are used with strongly fluorescent compounds. *Cut-off filters* have a sharp cut-off in their transmittance characteristics, with complete

transmission on one side of the cut-off and little or no transmission on the other. These filters are used to cut-off stray or unwanted light. *Bandpass filters* are filters that transmit or reject only a limited band of wavelengths. They are usually composite filters constructed from sets of cut-off filters.

Interference filters are markedly different from absorption type filters. Destructive interference and reflection in an interference filter eliminate the unwanted radiant energy. An interference filter consists of two highly reflective but partially transmitting films of silver, separated by a spacer film of completely transparent material such as MgF_2. In practice, a narrow range of wavelengths is transmitted through the interference filter. Because little light energy is actually absorbed by the filter, negligible heating of the filter occurs and this type of filter is therefore particularly well suited to use with an intense spectral source.

The selection of a filter should be based on two criteria, peak transmittance and bandwidth at the desired wavelength. Usually, the narrower effective bandwidths which is the bandwidth at half peak height of maximum transmittance, is defined a narrower bandwidth represent better performance of wavelength selectors, i.e. filters, monochromators. *Absorption filte*rs have effective bandwidths that range from 30 – 250 nm. Filters that provide the narrowest bandwidths also absorb a significant fraction of the desired radiation and may have a transmittance of 10% or less at their band peak. *Cut-off filters* have transmittances of 85 – 95% over a portion of the visible spectrum, but then rapidly decrease to zero transmittance over the remainder. *Interference filters* have the bandwidth of 10 – 15 nm, full width at half maximum transmission; the maximum transmission is usually 40 – 55%.

2.4.3 Laser Beam Collimating

A laser diode has been found to have many advantages over other types of laser and can be utilised in a wide range of applications [21]. However, laser diodes also have certain shortcomings. As mentioned in Section 2.2.1, the elliptical cross section of the laser beam and the diode's intrinsic astigmatism are often the most likely cause of problems.

Circularity

The elliptical cross section of the beam is a result of the rectangular shape of the beam emission facet of the laser diode. This characteristic prevents the beam from being completely collimated, allowing for quasi-collimation only. Also, the shape of the elliptical cross sections varies from diode to diode. The difference in θx and θy causes the beam of laser diodes to have an elliptical cross section, as shown in Figure 2-17. In fact, the difference between θx and θy is not consistent even between two laser diodes of the same type. Therefore the shape of the elliptical cross section varies from diode to diode.

Figure 2-17 **The rectangular emission facets of laser diode with an elliptical cross section**

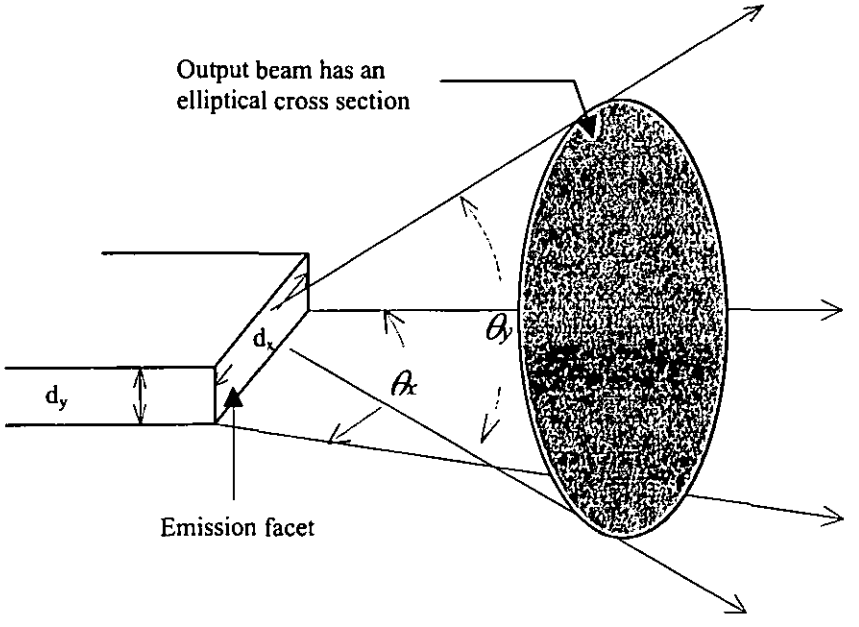

Astigmatism

Astigmatism means that when an object point lies an appreciable distance from the optical axis, the incident cone of rays will strike the lens asymmetrically, giving rise to a third primary aberration [22]. *Astigmatism* is, in fact, another result of the rectangular facet of the laser diode. As illustrated in Figure 2-17, the beam emitted from a small facet is equivalent to the beam emitted by an imaginary point source *P*, whose position can be located by tracing the beam backwards. It can be seen immediately that *Px* is located behind *Py* because θx is smaller than θy. When *dx* is much larger than *dy*, θx is much smaller than θy, and the distance between *Px* and *Py* is therefore very large as well. This phenomenon is called a*stigmatism*, and the distance between *Px* and *Py* is the numerical description of astigmatism.

Figure 2-18 **Illustrating the variation between laser diode and cause of astigmatism**

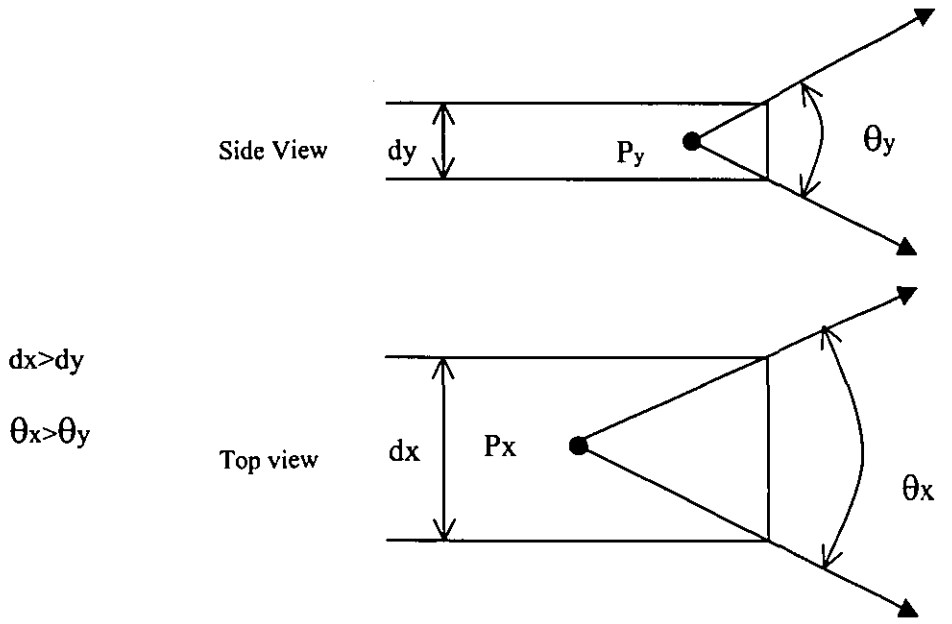

The existence of astigmatism means that when using a single, standard *aspheric lens* laser beam can be *collimated* only in one direction, either in the *x* direction or in the y direction, because Px and Py can not simultaneously converge at the focal point of the collimating lens.

2.4.4 Focusing Emission Beam to a Point

Lenses are often employed to redirect the light or concentrate the optical power. The lens equation defines the image distance s', projected from a point that is a distance, f (the focal length) from the lens. The focal distance is dependent on the curvature and refractive index of the lens. Simply put, all rays parallel to the optical axis pass through the lens and converge at the focal point. The refraction index of the light is dependent upon its wavelength and therefore the focal point various slightly. Chromatic aberration can occur in a simple lens. In this research, the lens is employed to condense the dispersing emission light (fluorescence) from the flow cell or cuvette to a spot on to the surface of the photo detector. For convenience, a biconvex positive lens or an achromatic lens are usually used to produce a focal point as desired the measurement.

When the emission light is made parallel in a single biconvex lens, the focal point F can be located on the surface of a photo detector as shown in Figure 2-19. As the emission light side from the cuvette or the flow cell is brought close to the lens, or moved away from it, the distance of the photo detector side changes accordingly.

Figure 2-19 **Emission Light location and graphical ray tracing**

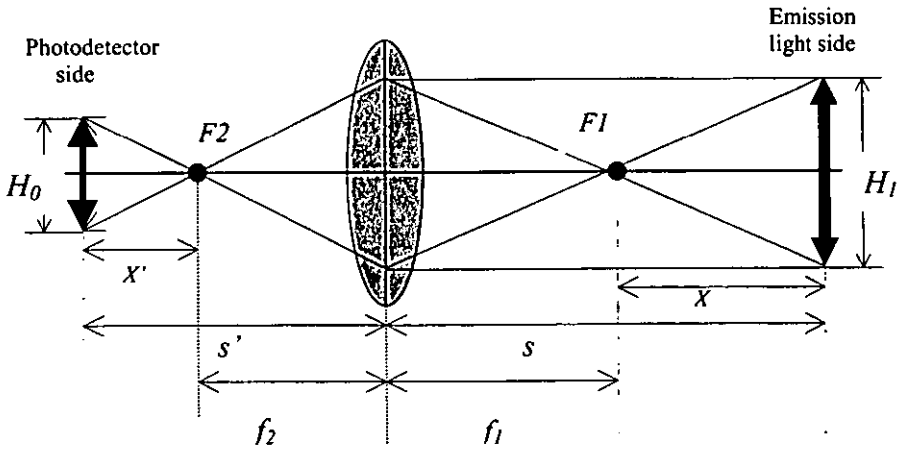

Using the *Gaussian formula*, the lens equation can be written as below [23]:

$$\frac{1}{f_2} + \frac{1}{s} = \frac{1}{s'} \qquad (2-8)$$

or

$$\frac{1}{f_1} + \frac{1}{s'} = \frac{1}{s} \qquad (2-9)$$

where: f_1- the focal length of the emission light side.

f_2 – the focal length of the photodetector side.

s' – the emission light side distance.

s – the photon detector side distance.

Newton's lens equation is:

$$XX' = f_1 f_2 \qquad (2-10)$$

Where: X, X' are extra focal distances.

When using a single biconvex lens $f = f_1 = -f_2$. Therefore:

$$XX' = -f^2 \qquad (2-11)$$

Newton's formula and Gauss's formula can be used to calculate of the distance of emission light side and the distance of photo detector.

Furthermore, the magnification formula of the lens can be described as [24]:

$$m = \frac{H_1}{H_0} = \frac{s'}{s} \qquad (2-12)$$

Where: m – the ratio of the image.

H_I – the window size of the cuvette and the flow cell.

H_0 – the focal point size on to the surface of photo detector.

According to these basic principles, the optical system in a fluorescence detector can be easily established and the optimum performance of fluorescence detection can also be achieved.

2.5 References

[1] Ryer, A., Light Measurement Handbook, International Light Technical Publications Dept., International Light, Inc., USA, (1997), pp.4-8.

[2] Skoog, D. A., Holler, F. J. and Nieman, T. A., Components of optical instruments, Principles of Instrumental Analysis (Fifth Edition), Harcourt Brace College Publishers, (1998), pp. 147 – 153.

[3] Sparkes, J. J., New technologies, Semiconductor Devices (2nd Edition), Chapman & Hall, (1994), pp.200 – 201.

[4] Birch, D. J. S. and Hungerford, G., Instrumentation for red/near-infrared fluorescence, Fluorescence Spectroscopy, Plenum, New York, (1994), Vol.4, pp.397-399.

[5] Fabian, M. E., Introduction to lasers, Semiconductor Laser Diodes, A Users Handbook, Electrochemical Publications Ltd., (1981), pp.1-9.

[6] Pedrotti, F. L., Leno, S. J., Pedrooti, S., Laser basics, Introduction to Optics, Prentice-Hall International, Inc. (1993), pp.440 – 441.

[7] Wobschall, D., Electrooptical devices, Circuit Design for Electronic Instrument, McGraw-Hill Book Company, (1987), pp.79 – 81.

[8] Mooney, W. J., PN junction detectors, Optoelectronic Devices and Principles, Prentice-Hall, Inc., (1991), pp. 250 – 252.

[9] Mooney, W. J., PN junction detectors, Optoelectronic Devices and Principles, Prentice-Hall, Inc., (1991), pp. 253 – 254.

[10] Kano, K., Photodetectors, Semiconductor Devices, Prentic-Hall, Inc., (1998), pp.447-449.

[11] Gage, S., Hodapp, M., Evans, D. and Soresen, H., Photodiode, Optoelectronics Applications manual, McGraw-Hill Book Company, (1977), pp.4.1-4.6.

[12] Harnly, J. M. and Fields, R E., Solid-state array detectors for analytical spectrometry, Applied Spectroscopy, (1997), Vol.51, No.9, pp.337A-338A.

[13] Burns, S. G. and Bond, P. R., Field-effect transistors, Principles of Electronic Circuits, PWS Publishing Company, (1987), pp.150.

[14] Willard, H. H., Merrit, Jr. L. L., Dean, J. A. and Settle, Jr. F. A., Electronic fundamentals and applications of solid-state devices, Instrumental Methods of Analysis, Belmont, Wadsworth Publishing Company, (1988), pp.43-44.

[15] Studholme, R. M. and Blau, D. A., Fluorimeter Detection System, International Patent Classification 5: G01N21/64, (1993), pp.2.

[16] Palmer, D. A., French, M. T. and Hu, S. J., A detector, International Patent PCT WO99/08096, (1999), pp.11 – 14.

[17] TLC555, Low Power Timer, (1999), www.ti.com/sc/docs/products/analog/tlc555.html

[18] Floyd, T. L., Amplifiers and oscillators, Electronics Fundamentals, Prentice Hall, (1998), pp.803-804.

[19] Pedrotti, F. L., Leno, S. J. and Pedrotti, S. Nature of light, Introduction to Optics, Prentice-Hall International, Inc., (1993), pp.11.

[20] Petruzzellis, T., Optical components, Fiber Optics and Laser Cookbook, McGraw-Hill Book Company, (1997), pp.19-22.

[21] Siffvast, W. T., Specific laser system, Laser Fundamentals, Cambridge University Press, (1996), pp.481-482.

[22] Hecht, E., More on geometrical optics, Optics, (3rd Edition), Addison-Wesley Longman, Inc., (1998), pp.164-165.

[23] Meyer-Arent, J. R., Thin lens, Introduction to Classical and Modern Optics, Prentice Hall, (1995), pp.38 –39.

[24] Freeman, M. H., Thin lens, Optics, Tenth Edition, Butterworths, (1990), pp.90 – 93.

CHAPTER THREE

MATERIALS, APPARATUS AND REAGENTS

3.1 Introduction

The components in the NFDS include electronic and optical solid state devices.

The optical components, e.g. a biconvex lens, a short wavelength cut-off filters and a laser diode were fitted on an optical bench to collect the fluorescence onto the surface of large area photodiode. The electronic components, e.g. resistors, capacitors, IC chips etc were placed onto the printing circuit boards (PCB). A multiple power unit, a linear operational amplifier, a digital display and an output distribution unit were constructed to convert the fluorescence into electrical signal then amplified and display or output to a PC. To compare to the NFDS, a LS50 Luminescence spectrofluorometer supplied by Perkin Elmer Corporation and a F4500 Fluorescence spectrophotometer supplied by Hitachi Corporation were employed in this research. The other facilities, i.e. a Gilson Minipuls 3 peristaltic pump, a bench pH meter, a manual injection valve, a 10×10 mm^2 standard cuvette with volume of 4ml and a 10×10 mm^2 flow cell with the volume 100 μl were used in practical experiments.

Elution buffer (Citrate pH 2.5), equilibration buffer (Tris hydrochloride pH 8.8) and assay buffer (PBS/BSA, pH 7.4) were prepared for experimental reagents. The α-Interferon sample and the α-Interferon antibody supplied from Glaxo Wellcome were also selected as a model for a flow injection immunoassay. Cy5 monofunctional dye, Cy5.5 bisfunctional dye and Naphthofluorescein were selected as fluorophores dyes. Furthermore, all selected dyes were prepared to various levels of the concentrations.

3.2 Electronic Components and Equipment

The NFDS measures and displays a physical parameter of the incident light. The current change (electrical parameter) of the photon detector (photodiode) is proportional to the intensity of the incident light (fluorescence), at least over a limited range. It is therefore important to select electrical components, which facilitate the accurate measurement of incident light. Additionally, the correct diagnostic equipment is required to collect the necessary observations and for debugging all electronic circuits in the prototype board [1].

3.2.1 Electronic Components

The NFDS needs electronic and electromechanical components to provide the electrical interface. Each component has its own characteristic properties and failure modes. Furthermore, components can be divided into *active* or *passive*. *Active components* are used to copy (amplify) waveforms and to switch voltages and currents on or off under electrical control. *Passive components* always reduce the power of an input waveform and do not need any additional steady voltage supply to enable them deal with waveform [2]. The electronic circuits used in developing this detection system consist of both active and passive components.

3.2.1.1 Active Components

Active components developed for the fluorescence detection system can be classified as; switches, transistors, diodes, integrated circuit (IC) chips, laser diodes and photodiodes. The details are listed in Tables 3-1, 3–2 and 3-3.

Table 3-1 **Active components or others used in the power supply and digital display**

Name	Specification	Supplier	Notes
Fuse	240V, 1.5A	RS	Not active component
Fuse Holder	240V, 10A	RS	Not active component
Main power switch	240V, 3.5A	RS	Not active component
Transformer	Input: 230-240V (AC) Output: 2×20V, 0.5A (AC)	RS	
	Input: 50V, 1A	RS	Type: DF005M
+5V,Voltage regulator ×2	I/p voltage range 7.4 to35V Fixed +5V, 500mA o/p	RS	Type:MC78M05C
+12v , Voltage regulator ×2	I/p voltage range 14.5 to35V Fixed +12V, 1A o/p	RS	Type:MC78M12
-12v , Voltage regulator ×2	I/p voltage range 7.4 to35V Fixed -12V, 1A o/p	RS	Type:MC7912
2 pole 4 position switch	Contact rating: 60V, 2A Contact resistance: 25mΩ	RS	Type: Enclosed Wafer
Digital indicator	I/p voltage range 5 to 5.5V 4 digit	RS	Type: 31/2 Digit LED DMP

Table 3-2 **Active components used in the photodiode driver and amplifier**

Name	Specification	Supplier	Notes
Photodiode	Response range:350 – 1150nm Noise current: 0.1pA at 0V Dark, rev. bias 10V: 0.5μA	RS (Centronic)	100mm^2 5KHz bandwidth see Chapter 4
BiMOS Operational Amplifier ×2	Input impedance: 1.5TΩ Input current: 10pA at ±15V	Farnell (Harris)	Type: CA3140 Discuss in Chapter 4

Table 3-3 **Active components or others used in the laser pulse generator**

Name	Specification	Supplier	Notes
IC 555 timer	TI LinCMOS™, 200mW O/P Supply voltage:2V – 15V	RS (Taxas Instruments)	Type: TLC555C Discuss in Chapter 4
Operation amplifier ×4	C-MOS versions Supply voltage:12 – 15V	RS (Phillips)	Type: μA741C
Transistor	Switching	RS (SGS Thomson)	Type: 2N3053
Connector×2	75Ω impedance	RS	Bulkhead socket
Slide Switch	Contact rating: 50V a.c/d.c., 2A Contact resistance: 20mΩ	RS	Not active component
2pole 6 position switch	Contact rating: 60V, 2A Contact resistance: 25mΩ	RS	Not active component
635nm Laser diode	Driver voltage:4.5 – 5.5V Output power: 2mW	Laser 2000	Discuss in Chapter 4
645nm Laser diode	Driver voltage:4.5 – 5.5V Output power: 2mW	Coherent	Discuss in Chapter 4
670nm Laser diode	Driver voltage:4.5 – 5.5V Output power: 2mW	Laser 2000	Discuss in Chapter 4

3.2.1.2 Passive Components

Passive components developed for the detection system were widely used in the electronic circuits, i.e. resistors, capacitors, inductors and potentiometers. Each component has its own characteristic properties, mainly arising from the manufacturing processes and materials used. The details are listed in Tables 3-4, 3-5, 3-6 and 3-7.

Table 3-4 **Passive components used in the power supply and display**

Name	Specification	Supplier	Notes
1KΩ resistor ×4	Tolerance: 1%, 0.25W Temperature coefficient: ±50ppm/°C	RS	Type: Metal film
2.2KΩ resistor ×2	Tolerance: 1%, 0. 25W Temperature coefficient: ±50ppm/°C	RS	Type: Metal film
100KΩ resistor	Tolerance: 1%, 0125W Temperature coefficient:±50ppm	RS	Type: Metal film
910KΩ resistor	Tolerance: 1%, 025W Temperature coefficient:±100ppm	RS	Type: Metal film
470μF capacitor ×6	Tolerance:20% Voltage capability: 63V	RS (Panasonic)	Type: General Purpose
10μF capacitor ×6	Tolerance:20% Voltage capability: 50V	RS (Panasonic)	Type: General Purpose
100pF capacitor ×6	Tolerance:20% Voltage capability: 35V	RS (AVX Kyocera)	Type: Tantalum

Table 3-5 **Passive components used in the photodiode driver and amplifier**

Name	Specification	Supplier	Notes
100pF capacitor ×2	Tolerance:5% Voltage capability: 100V(dc)	RS	Type: Epoxy Resin Coated
1KΩ resistor ×2	Tolerance: 1%, 0.125W Temperature coefficient: ±50ppm/°C	RS	Type: Metal film
499Ω resistor	Tolerance: 0.1%, 0.125W Temperature coefficient: ±50ppm/°C	RS	Type: Precision Metal film
511Ω resistor	Tolerance: 1%, 0.125W Temperature coefficient: ±15ppm/°C	RS	Type: Precision Metal film
10KΩ potentiometer	Tolerance: ±20%, 0.25W Temperature. coefficient: ±1000ppm/°C	RS (Bourns)	Type: Conductive Plastic
100Ω potentiometer	Tolerance: ±5%, 1W Linearity better than 2%	RS (AB Elektronik)	Type: Wire wound
1MΩ potentiometer	Tolerance: ±5%, 1W Linearity better than 2%	RS (AB Elektronik)	Type: Wire wound

Table 3-6 **Passive components used in the laser driver and pulse generator (resistors)**

Name	Specification	Supplier	Notes
10KΩ resistor ×2	Tolerance: 1%, 0.25W Temperature coefficient: ±100ppm/°C	RS	Type: Metal film
50KΩ resistor	Tolerance: 1%, 0.25W Temperature coefficient: ±100ppm/°C	RS	Type: Metal film
100KΩ resistor	Tolerance: 1%, 0.25W Temperature coefficient: ±100ppm/°C	RS	Type: Metal film
1MΩ resistor	Tolerance: 1%, 0.25W Temperature coefficient: ±100ppm/°C	RS	Type: Metal film
10MΩ resistor	Tolerance: 1%, 0.25W Temperature coefficient: ±100ppm/°C	RS	Type: Metal film
1KΩ resistor ×6	Tolerance: 1%, 0.25W Temperature coefficient: ±100ppm/°C	RS	Type: Metal film
5Ω1 resistor	Tolerance: 1%, 0.25W Temperature coefficient: ±100ppm/°C	RS	Type: Metal film
10KΩ potentiometer	Tolerance: ±20%, 0.15W Temperature. coefficient: ±1000ppm/°C	RS (Meggitt Piher)	Type: Conductive Plastic
47KΩ potentiometer	Tolerance: ±20%, 0.15W Temperature. coefficient: ±1000ppm/°C	RS (Meggitt Piher)	Type: Conductive Plastic
100KΩ potentiometer	Tolerance: ±5%, 1W Linearity better than 2%	RS (AB Elektronik)	Type: Wire wound

Table 3-7 **Passive components used in the laser driver and pulse generator (capacitors)**

Name	Specification	Supply	Notes
1000pF capacitor	Tolerance:10% Voltage capability: 63V(dc)	RS (Thomson)	Type: Metallised Polyester
2200pF capacitor	Tolerance:10% Voltage capability: 63V(dc)	RS (Thomson)	Type: Metallised Polyester
4700pF capacitor	Tolerance:10% Voltage capability: 63V(dc)	RS (Thomson)	Type: Metallised Polyester
0.01μF capacitor ×2	Tolerance:5% Voltage capability: 100V(dc)	RS	Type: Epoxy Resin Coated
0.022μF capacitor	Tolerance:5% Voltage capability: 100V(dc)	RS	Type: Epoxy Resin Coated

3.2.2 Electronic Equipment

To build and construct a fluorescence detection system, some basic electronic equipment is essential for developing testing periods, making adjustments and carrying out preliminary tests. The most useful and versatile laboratory instruments are the oscilloscopes, employed for monitoring the waveform of electric signal, and the multimeter, used to measure the voltage, current and resistance.

HAMEG HM205-3 Dual-trace storage oscilloscope

A dual-trace oscilloscope manufactured for a general-purpose 20MHz dual channel was used in this research. The oscilloscope had a 6-inch rectangular cathode ray tube with green internal graticule. The following function were available:

1. Triggering mode, includes: Auto, Norm TV field, TV line, TV sync triggering for automatic triggering of TV-V and TV-H signals
2. Linear focus, maintains optimum beam focus
3. Variable hold-off, stable display of periodic waveforms
4. Sensitivity, 1mV to 5V/div in 12 step
5. Timebase, sweep 0.1μs to 0.5s/div in 21 steps
6. 400V (DC + AC peak) max input to CH1 and CH2

RACALL-DANA 4009 Digital multimeter

The digital multimeter (DMM), Mode 4009 supplied by Thurlby Electronics Ltd., UK was high-resolution with 6 LED digit display of accuracy, The following functions were available:

1. Auto-ranging and manual ranging
2. 1μV, 10mΩ and 0.1μA sensitivity

3. 100 reading data logger, holding and storage.

4. Isolated RS232 interface as standard

The discussion is in Section 4.4.1.

3.3 Analytical Instrumentation and Equipment

Evaluation of the NFDS and comparison with commercial detectors and practical investigation were carried out using fluorescence and UV/Vis spectrophotometers, and routine equipment, such as a manual injection valve, a peristaltic pump, a column, a pH meter, some flow injection tubing, and a flow cell or a standard cuvette.

3.3.1 Analytical Instrumentation

LS50 Luminescence spectrofluorometer (LS50)

The LS50 luminescence spectrofluorometer was supplied by Perkin Elmer, UK and was fitted with a R928 photomultipler tube to enable spectra to be taken at the longer wavelengths involved in this research. The excitation source was Xenon Arc Lamp (150 Watts). The LS50 was interfaced to an Epson AX3 personal computer fitted with the Fluorescence Data Manger (FLDM) software package, which controlled all aspects of the spectrofluorometer.

F4500 Fluorescence spectrophotometer

The F4500 fluorescence spectrophotometer was supplied by Hitachi, Wokingham, UK and used a 150 Watt Xenon lamp as an excitation source with the wavelength selection by a monochromator. The fluorescence emitted from a sample is incident on the emission monochromator and transmitted to a photomultiplier. The instrument control and data handling were carried out using the associated the Hitachi software running on a PC.

U-2010UV-Vis Spectrophotometer

The U-2010UV-Vis spectrophotometer was supplied by Hitachi, Wokingham, UK and used a double beam approach, in which a tungsten iodide lamp and a deuterium

lamp were used as excitation sources and operated over the wavelength range from 200nm to 950nm. The condensed beams are focused onto the silicon photodiodes as sensors. The instrument was controlled by a PC which carried out the qualitative and quantitative spectral analysis involving the data handling with Hitachi software [3].

3.3.2 Analytical Equipment

Gilson Minipuls 3 peristaltic pump

A Gilson Minipuls 3 peristaltic pump (Villiers, France) was used, in the flow injection manifold to propel the binding and elution buffer through the NFDS. Different flow rates could be achieved by either altering the speed of rotation of the pump head or changing the internal diameter of the PVC pump tubing.

Manual injection valve

The manual injection valve supplied by Omnifit, Poole Dorset, UK and used for both the one stream and two stream manifolds was a low pressure *Rheodyne 5020* Teflon rotary valve. All parts of the valve in contact with the eluent are of Teflon construction; the remainder is stainless steel and polypropylene. The valve has six ports, which is two ports to form the loop, one port is for injecting the sample, one for excess of injected sample and the others are for inlet and outlet of the eluent from the pump to the detector.

Flow cell

A 10×10 mm^2 quartz flow cell with a 2.5 × 10 mm^2 window and volume of 100 µl was supplied by *Hellma* (Essex, UK). The flow cell was housed in the sample compartment of the detector.

Figure 3 – 1 **Diagram of the flow cell used in the flow injection immunoassays**

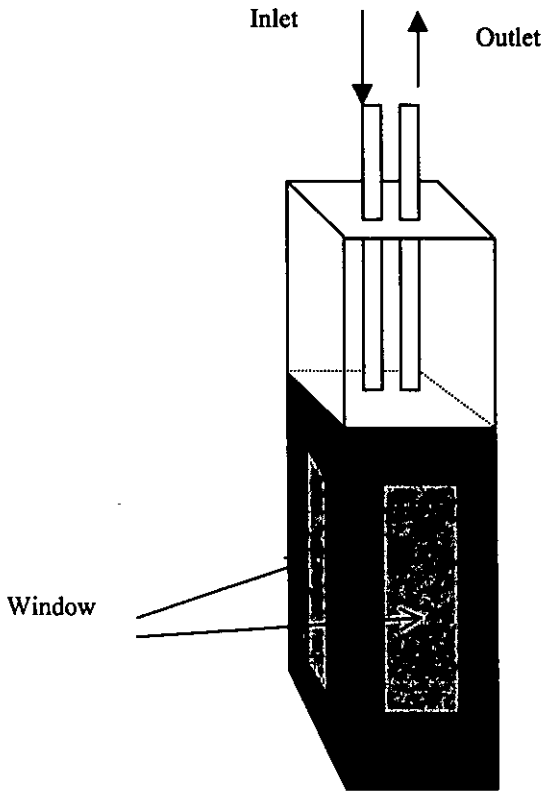

Standard cuvette

A 10×10 mm^2 quartz standard cuvette with volume of 4ml was supplied by *Hellma* (Essex, UK).

Column equipment

A borosilicate glass column supplied by Omnifit Poole, Dorset, UK. 100 mm $\times$ 6.6 mm ($l \times I.D$) with adjustable endpieces was used and packed with 140 µl POROS protein A beads (20 microns).

Novel fluorescence detection system (NFDS)

The detection system used for all the experiments was designed and built in this research. The detail is discussed in Chapter Four.

Analogue to Digital Converter (ADC)

The ADC with FlowTEK^{R} (FlowTEK) software was supplied by Global FIA, Inc., USA. The detail is in 4.4.1 Chapter Four.

Bench pH meter

The *PHA 230* Bench pH meter supplied by Whatman, UK was used to prepare the buffers. All standard BNC electrodes can be accommodated and an advanced microprocessor recognises pre-programmed buffers (pH4.7 and 10) during calibration and offers auto-calibration. Temperature compensation can be either manual or auto from 0 – 100 ^{0}C.

Balance

The Precisa 40SM-200A balance supplied by Precisa Balance Limited, Switzerland, in which operated the weighting range from 0.0001 mg to 99.9999 gram.

Accessories for Optical System

Following Table 3-8 lists the main optical accessories for establish the optical system.

Table 3-8 **Accessories in optical bench**

Name	Specification	Supply	Notes
Precision Biconvex Lens	Diameter: 25.4mm, F/#: 0.7 Focal distance (EFL): 19mm	Newport	Reused lens
Short wavelength cut-off filter	Size: 50×50mm; Thick: 2mm Wavelength: 640nm	Optosigma	
Short wavelength cut-off filter	Size: 50×50mm; Thick: 1mm Wavelength: 650nm	Schott	
Short wavelength cut-off filter	Size: 50×50mm; Thick: 1mm Wavelength: 695nm	Schott	

3.4 Reagents

3.4.1 Preparation of Buffer Solutions

Three buffers were used in the experiments.

Elution buffer (Citrate pH2.5)

0.10 M citrate buffer was prepared in one litre volume as below:

29.26g of sodium chloride (AnalaR grade) and 21.00 g of Citric acid (AnalaR grade) were made up in deionized, triply distilled water. The buffer was adjusted to pH 2.50 with either 0.50M sodium hydroxide or 0.50M hydrochloric acid then stored at 4^0C.

Equilibration buffer (Tris hydrochloride pH8.8)

0.05 M Tris hydrochloride buffer (Tris buffer pH 8.8) was prepared in one litre volume as below:

29.26g of sodium chloride (AnalaR grade) and 7.86 g of Tris hydrochloride (AnalaR grade) were made up in deionized, triply distilled water. The buffer was adjusted to pH 8.8 with either 0.50M sodium hydroxide or 0.50M hydrochloric acid then stored at 4^0C.

Assay buffer (PBS/BSA, pH 7.4)

0.10M of Phosphate buffer was prepared in one litre volume as below:

8.0 g of sodium chloride (AnalaR grade), 0.20 g of potassium dihydrogen orthophosphate (AnalaR grade), 2.90g of disodium hydrogen orthophosphate (AnalaR grade) and 0.20 g of Potassium Chloride (AnalaR grade) were made up in deionized, triply distilled water. The buffer was adjusted to pH 7.4 with either 0.50M sodium hydroxide or 0.50M hydrochloric acid then stored at 4^0C.

Packing materials

The packing material for the adjustable column in flow injection immunoassay was POROS protein A beads (20 μm) that was purchased from PE Biosystems, UK and packed in column prior to utilisation.

α-Interferon sample

The α-Interferon is therapeutic antibody and was supplied as a gift by Glaxo Wellcome, UK. The preparation and storage is described in Chapter 5.

Anti-α-Interferon antibody

The bovine anti-α-Interferon was supplied as a gift by Glaxo Wellcome, UK. The preparation and storage is described in Chapter 5.

Naphthofluorescein (NF)

Naphthofluorescein (NF) was supplied by Molecular Probes, Inc., USA. The preparation and storage is described in Section 3.5.1.

Cy5 Monofunctional Dye

Cy5 Monofunctional Dye (Cy5) was supplied by Amersham Life Science, Cambridge, UK. The preparation and storage is described in Section 3.5.1 and 3.5.2.

Cy5.5 Bisfunctional Dye (Cy5.5)

Cy5.5 Bisfunctional Dye (Cy5.5) was supplied by Amersham Life Science, Cambridge, UK. The preparation and storage is described in Section 3.5.1 and 3.5.2.

3.4.2 Characteristics of Fluorophores Used

3.4.2.1 Naphthofluorescein (NF)

Figure 3 – 2 Chemical structure of naphthofluorescein

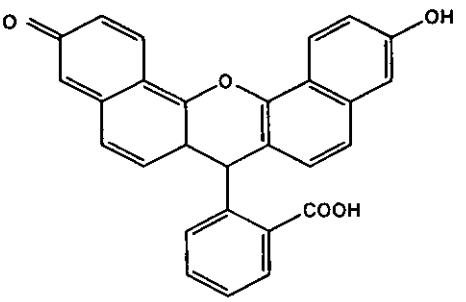

Naphthofluorescein is a xanthine dye. It is sparingly soluble in water but highly soluble at alkaline pH. It can be used as a fluorescent label for biological compounds and is highly fluorescent at alkaline pH. Naphthofluorescein emits fluorescence in the near infrared region of the electromagnetic spectrum.

Figure 3-4 **Naphthofluorescein excitation and emission spectra profile**

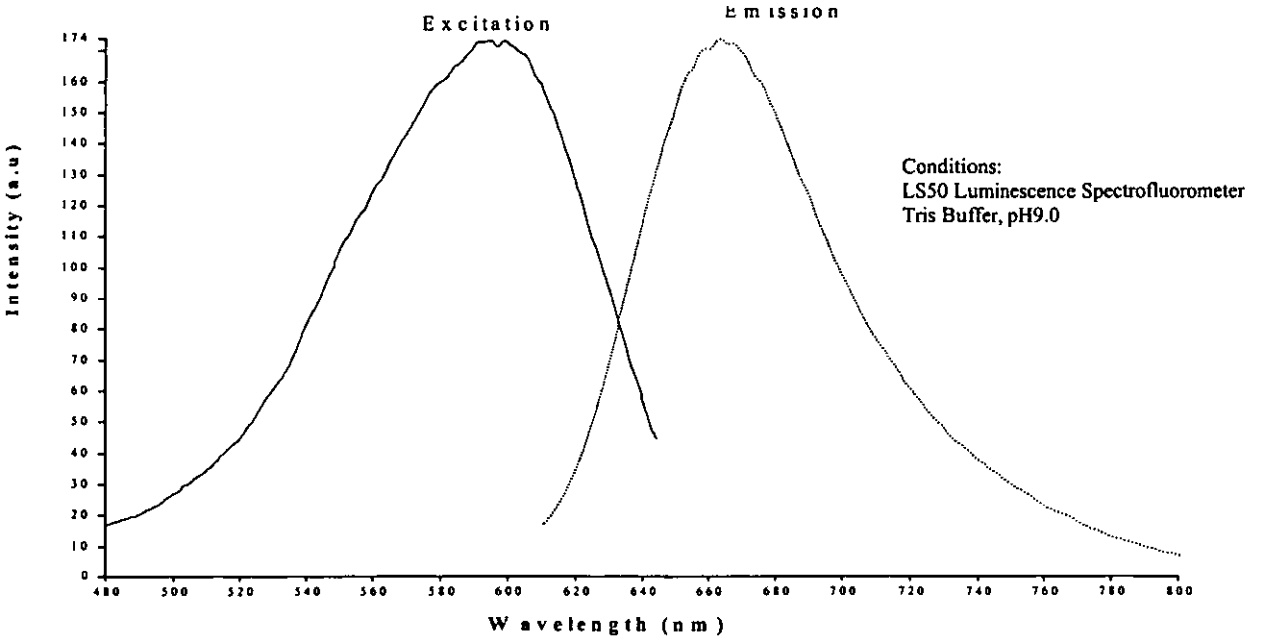

Note: a.u is arbitrary unit.

Characteristics of NF

Formula Weight	432.43
Absorbance Max	595 nm
Extinction Coefficient	$4.2\times10^{4}M^{-1}cm^{-1}$
Emission Max	660 nm
Quantum Yield	>0.15 at pH 9.0

3.4.2.2 FluoroLink™ Cy 5™ (Cy5 Monofunctional Dye)

Figure 3 –4 **The Structure of Cy5 Monofunctional Dye**

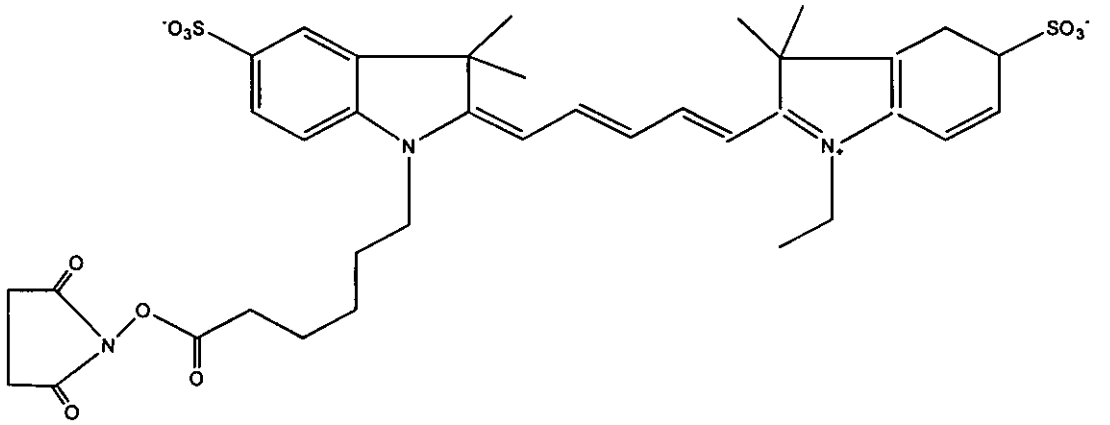

Cy5 monofunctional dye (Cy5) is a member of the cyanine family of dyes, the monofunctional form is NHS-ester that is intensely fluorescent and highly water soluble, it was supplied in a dried, pre-measured form ready for the labelling of compounds containing free amino groups. Figure 3-5 shows the excitation and emission spectra for Cy 5 monofunctional dye [4].

Figure 3–5 **Cy5 Monofunctional dye excitation and emission spectra profile**

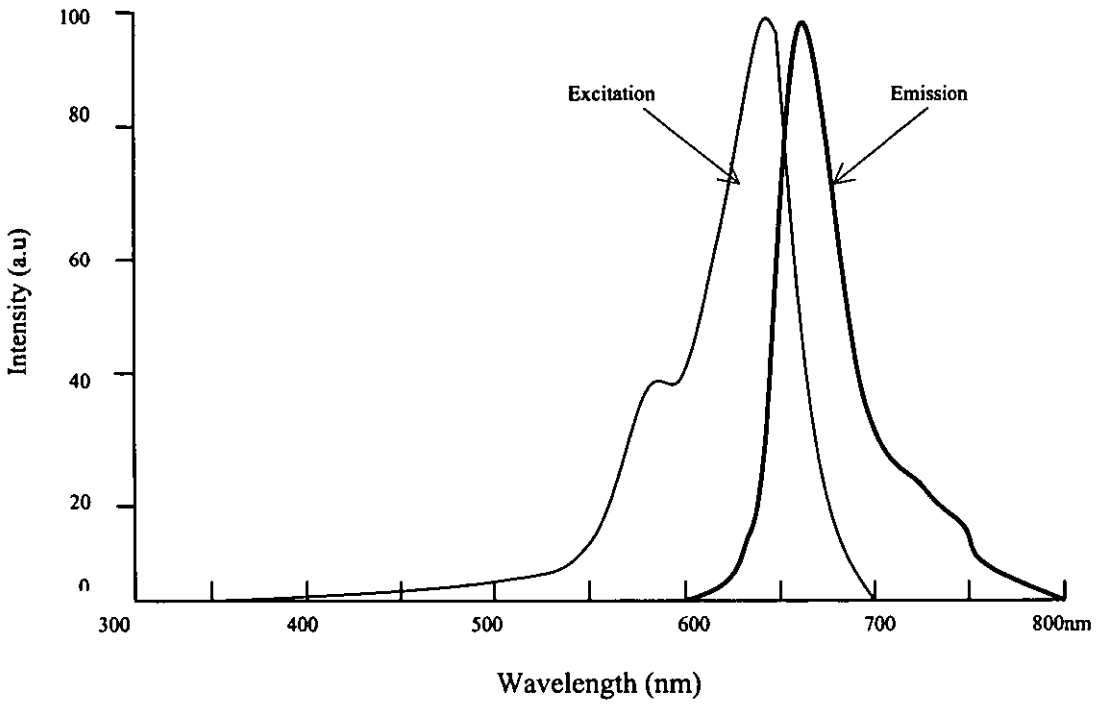

Note: a.u is arbitrary unit.

Characteristics of Cy5 monofunctional dye

Formula Weight	791.99
Absorbance Max	649 nm
Extinction Coefficient	2.5×10^5 $M^{-1}cm^{-1}$
Emission Max	670 nm
Quantum Yield	>0.28 (for labelled proteins, D/P=2)

3.4.2.3 FluoroLink™ Cy 5.5 ™ (Cy5.5 Bisfunctional Dye)

Figure 3 –6 **The Structure of Cy5.5 Bisfunctional Dye**

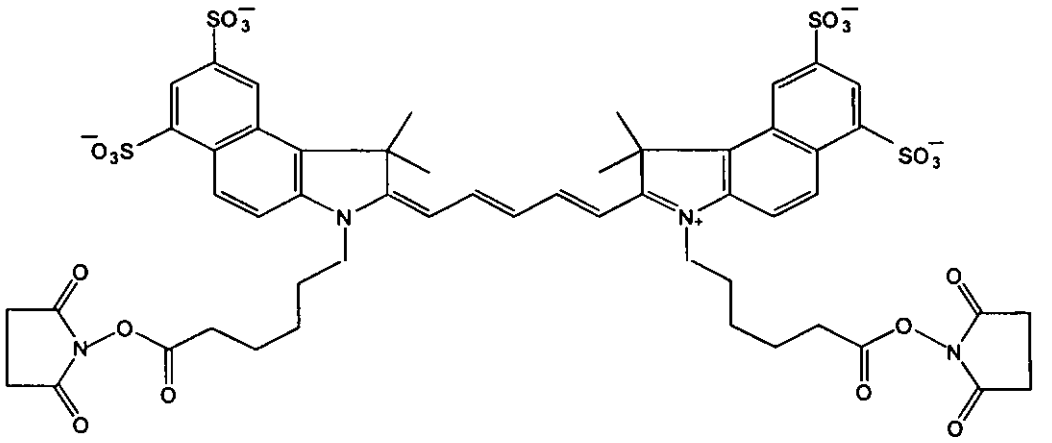

Cy5.5 bisfunctional dye (Cy5.5) is a bisreactive NHS-ester that is intensely fluorescent and highly water soluble, it was supplied in a dried, pre-measured form ready for the labelling of compounds containing free amino groups. Figure 3-7 shows the excitation and emission spectra for Cy 5.5 bisfunctional dye [5].

Figure 3–7 **Cy5.5 Bisfunctional dye excitation and emission spectra**

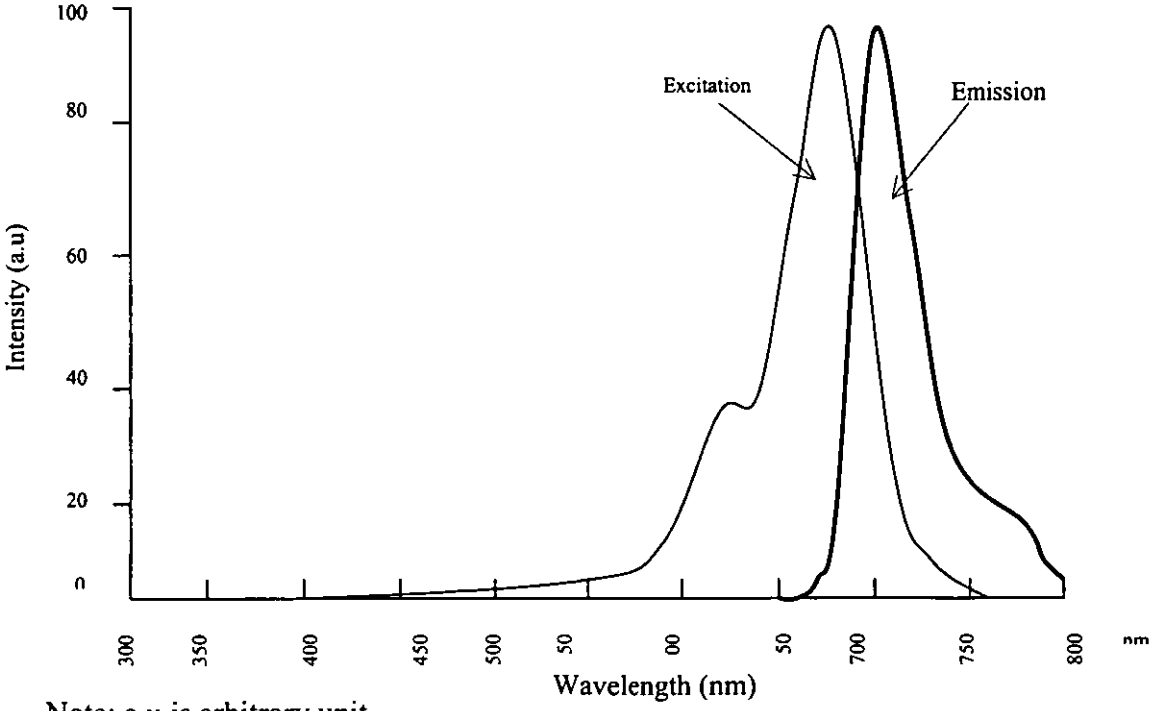

Note: a.u is arbitrary unit.

Characteristics of Cy5.5 Bisfunctional Dye

Formula Weight	1311.58
Absorbance Max	678 nm
Extinction Coefficient	2.5×10^5 $M^{-1}cm^{-1}$
Emission Max	703 nm
Quantum Yield	>0.28 (assumes a dye to antibody ration of 2)

3.5 Preparation of Standard Solutions

Flow injection immunoassay, as with most instrumental methods of analysis is a relative process that is the instrumental signal varies with some physical property of the sample being studied.

In this case, fluorescence emission peaks are collected from a photodetector and quantified using a known concentration of the analyte. A series of standard solutions was used to prepare a working curve known as *a calibration curve* by plotting the measured signal as a function of standard concentration.

Preparation of standard and stock solutions:

3.5.1 Weighing of Pure NF, Cy5 and Cy5.5

A Precisa 405M-200A balance was used to weigh out dried naphthofluorescein and this was dissolved in Tris buffer (pH 9.0) to prepare the analytical stock solution. The concentration of naphthofluorescein can be expressed according to the formula below:

$$C\,(M) = \frac{W}{M \times 1\ (\text{litre})} \qquad (3-1)$$

Where: C – the molar concentration per litre.

W – the weight of naphthofluorescein in gram.

M – the molecular weight of naphthofluorescein.

Naphthofluorescein stock solution was prepared in Tris buffer (pH 9.0) at 1.0×10^{-4} M. Several standard solutions of naphthofluorescein were prepared by diluting the stock solution in Tris buffer (pH 9.0) using a suitable range pipette. The concentrations of

standard solution prepared were 1×10^{-5} M, 1×10^{-6} M, 1×10^{-7} M, 1×10^{-8} M, 1×10^{-9} M, and 1×10^{-10} M.

Also, the dried Cy5 and Cy5.5 dyes for preparing standard solutions were weighed by the Precisa 405M-200A balance and dissolved into PBS buffer (pH 7.4). The dilutions of Cy5 and Cy5.5 dyes in Tris buffer (pH 8.8) were made from these standard solutions.

3.5.2 Calculations from Beer's Law

The confirmation of standard solutions of Cy5 and Cy5.5 dyes can be worked out by an UV/Vis spectrophotometer. Using Beer's law, the concentration of Cy5 and Cy5.5 were calculated from their absorbance when diluted in the assay buffer (PBS/BSA, pH 7.4) or Tris buffer (pH 8.8).

$$A = \varepsilon bc \qquad (3-2)$$

Where: A – absorbance of the solution.

ε - the molar absorptivity ($cm^{-1}\cdot mole^{-1}$).

b – the path length of the sample (cm).

c – the molar concentration of solution [6].

ε for Cy5 and Cy5.5 are 2.5×10^{5} ($cm^{-1}\cdot mole^{-1}$) individually.

The stock solutions of Cy5 were confirmed and diluted as follows:

The Cy5 was reconstituted into PBS/BSA buffer (pH 7.4) and a 1:100 dilution made with Tris buffer (pH 8.8). The absorbance was measured in a standard cuvette and found to be 0.29. According to the formula in 3-2, the concentration of Cy5 was

calculated to be 2.3×10^{-6} M and this was used as the stock solution. Several dilutions of Cy5 were prepared from the stock solution in Tris buffer (pH 8.8) using a suitable range pipette. The concentrations of solution prepared were 2.3×10^{-7} M. 3×10^{-8} M, 2.3×10^{-9} M, 2.3×10^{-10} M, 2.3×10^{-11} M.

100μl Cy5.5 stock solution was transformed to the test bottle and diluted to 4ml with Tris buffer (pH 8.8). The absorbance was measured in a standard cuvette and found to be 0.039. According to formula in 3-2, the concentration of Cy5.5 was calculated to be 6.2×10^{-6} M and this was used as the stock solution. Several dilutions of Cy5.5 were prepared by the stock solution in Tris buffer (pH 8.8) using a suitable range pipette. The concentrations of solution prepared were 6.2×10^{-7} M, 6.2×10^{-8} M, 6.2×10^{-9} M, 6.2×10^{-10} M, 6.2×10^{-11} M.

Preparation of the α-interferon solutions see Chapter 5.

3.6 References

[1] Fowler, K. R., Debugging and testing, Electronic Instrument Design, Oxford University Press, (1996), pp.445.

[2] Sinclair, I., Passive components, Electronics Made Simple, Butterworth-Heinemann, a division of Reed Educational and Professional Publishing Ltd, (1997), pp.16.

[3] Hitachi, Model U2010/U-3010/U-3310 UV/Vis Spectrophotometer, Hitachi Instrument, Co., (1997), pp.2-3, 2-4.

[4] FluoroLink™ Cy5™ Monofunctional Dye5-Pack, Amersham Life Science, Inc., USA, (1997), Cat. No. PA25001.

[5] FluoroLink™ Cy5.5™ Reactive Dye5-Pack, Amersham Biological Detection System, Inc. USA, (1997), Cat. No. PA25500.

[6] Skoog, D. A., Holler, F. J. and Nieman, T. A., An introduction to ultraviolet/visible molecular absorption spectrometry, Principle of Instrumental Analysis, Philadephia, Harcourt Brace, (1998), pp.300–301.

CHAPTER FOUR

INSTRUMENT DEVELOPMENT

4.1 Introduction

The novel fluorescence detection system (NFDS) consists mainly of optical and electronic components each of which have their own specific functions.

The optical system has several functions. Firstly, three separate laser diodes were used as the excitation sources. Each laser diode when selected, excites the fluorophore of the sample in a flow cell or a cuvette. Secondly, the cut-off filter removes unwanted light, e.g. the scattered laser light. Thirdly, a biconvex lens collects and condenses the fluorescence emission of interest.

The electronic system carries out five functions:

(a) Emitted light is collected from the silicon photodiode and is converted into an electrical signal.

(b) A linear amplifier amplifies the input signal from the photodiode in proportion to the radiation of the emission beam.

(c) The distributor delivers the output signal from the linear amplifier to a digital LED display plate, a digital multimeter, or the AD converter, and then to the PC, which displays the results of the fluorescence detection.

(d) The pulse generator and driver generate various pulse speeds, which range between 7 Hz and 1.4 MHz, and directly drive a 2 mW laser diode.

(e) A multiple power supply was needed to supply power to the consuming units, i.e. the linear operational amplifier, the laser pulse generator, two LED digital display plates and the cooling fan.

The optical and electronic systems (i.e. components of the optical bench and various electronic boards including the display unit, various IC chips, resistors and capacitors), were packaged into a portable plastic case. Electronic and optical tests were then carried out on the packaged NFDS.

4.2 Performance of Optical Bench

The optical bench offers a robust, solid and flexible condition for practical applications and due to the ease in which the components can be mounted, reliable and repeatable results can be obtained.

4.2.1 Basic Practical Operations

The components of an instrument for measuring fluorescence are mostly similar to those found in an UV/Vis spectrophotometer. However, the design of an optical layout for fluorescence detection should be in accordance with the following basic principles:

Firstly, fluorescence is propagated from the sample in all directions, but is most conveniently observed at right angles to the excitation beam. At other angles, increased scattering from the solution and the flow cell walls may cause larger errors in the measurement of fluorescence intensity. Secondly, the emitted radiation reaches the photodiode or other photon detector after passing through a short wavelength cut-off or interference filter that isolates the fluorescence for measurement [1].

Since fluorescence detectors are highly sensitive, the selection of materials used to design such a high precision instrument, needs careful consideration. The optical bench should be dimensionally and thermally stable, so its mechanical properties [2] are very important. Stainless steel was selected for the base of the optical bench in this work, which gave good results.

Isolation of the optical bench from vibrations is very important. It has been suggested [3] that a sandwich structure for the base of the optical bench is better than a solid

structure. When the optical components are fitted onto the bench over a long period of time, it is essential not to induce any stresses onto the sensor (photodiode), the filter or the lens. This is because over a period of time the stress components relax and cause the position of the optical components to drift [4]. However, stresses can be minimised by using spring washers under the screw heads. Each step in the construction of the detection system should be very carefully performed to minimise any man-made errors; e.g. the emission beam is not being detected at the focal point of biconvex lens.

External electro-magnetic interference can also be a source of problems; electronic noise can cause the output signal to be unstable, which can affect the measurements. The power cables are well shielded to minimise this problem but it is prudent to keep the photodiode away from potential field sources such as computer monitors or noisy electric motors. It is therefore useful to isolate the photodiode in a metal box, thus minimising interference from other sources. Like most semiconductors, the photodiode detectors are very sensitive to ambient temperature changes. Keeping the temperature of the detector constant over a long working period is necessary to prevent any variation within the range of -2 to 24 ^{0}C. This area is described in Section 4.5.3.

4.2.2 General Considerations for Optical Design

Figure 4-1 shows the scheme of the optical system. An excitation source, which is generated from a laser diode, excites the sample in a flow cell or a standard cuvette. The resulting emission beam from the flow cell or the standard cuvette passes through the short wavelength cut off filter, which then removes any unwanted background.

Also, the emission beam is focused onto the surface of the photodiode by a biconvex lens.

Generally, there are two main aspects in the optical system of the NFDS, i.e. the metal base and the optical components. The metal base consists of the optical bench and the shield. The material selected for the base of the optical bench was a 3.5 mm thick stainless steel sheet which had an adequate strength for the mounting of the lenses, filters, the laser diode and the photodiode. Some holes in the base also helped avoid vibration from the environment. The positions of the laser diode, the photodiode and the lens are adjustable within a certain distance range to allow the optimum position for detection to be achieved. The filter and laser diode can be conveniently replaced if different excitation and emission wavelengths are required.

The optical components include a biconvex lens and a long wavelength cut-off filter, which have been mounted into a matt black painted shield. In fact, the matt black in the shield is sheltered from sunlight and other radiation sources, and isolated from electric interference. Furthermore, small pieces of PVC sheet were used to insulate the laser diode and the photodiode mounting because both the laser diode and the photodiode are positive in operation.

Figure 4 –1 **Schematic of optical bench for detection system**

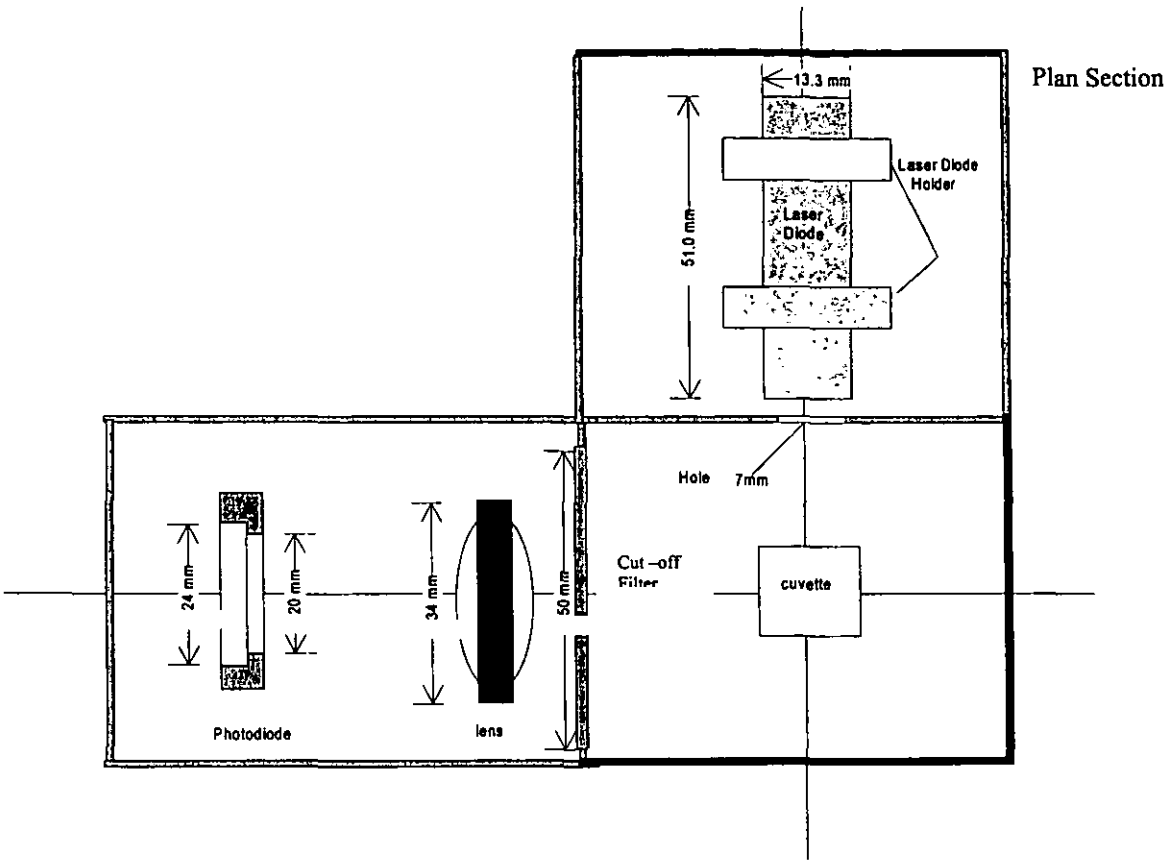

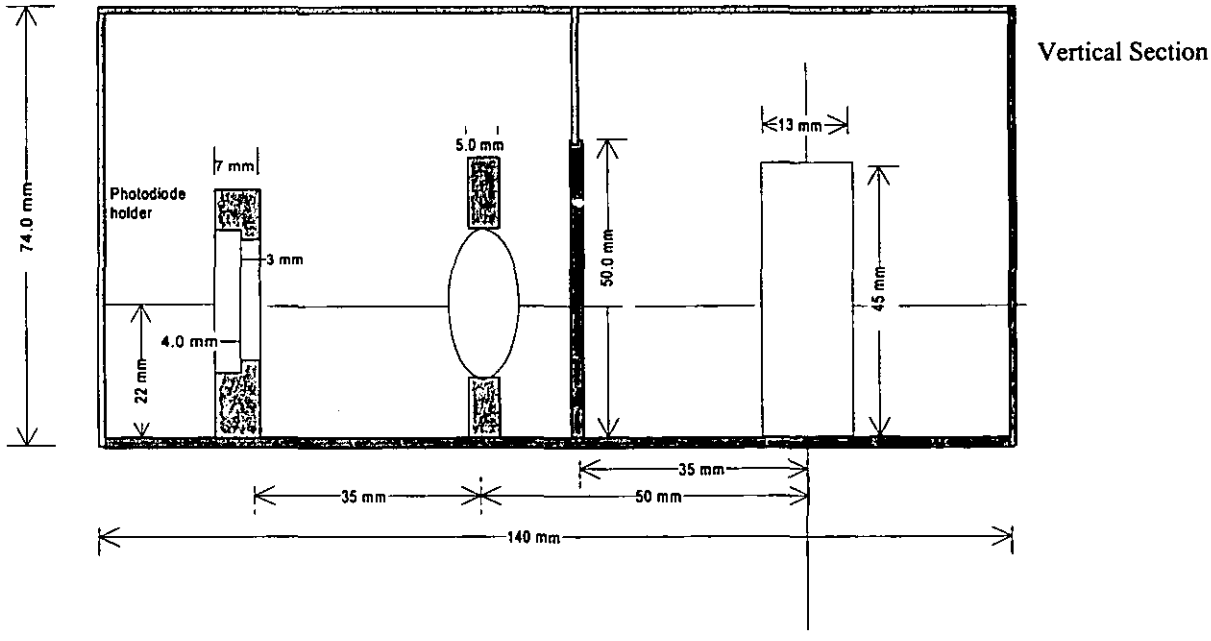

4.2.3 Fluorescence Signal Collection

Fluorescence from a flow cell or a standard cuvette is collected into a condensing emission beam and focused onto the silicon photodiode by a biconvex lens. The optimum distance range between the photodiode position and the lens position was achievable through several practical optical experiments.

Generally, the biconvex lens was positioned onto the optical bench so that it obeyed Newton's lens equation $XX' = f_1 f_2$ [5] and $f_1 = -f_2$ (see Section 2.4.4). The values for f_1= 19 mm and X = 26 mm are known, so the calculated distance between the biconvex lens and the photodiode is 32.9 mm. However, to obtain better fluorescence collection, the distance could be adjusted forwards or backwards by 2.1 mm, because a longitudinal chromatic aberration occurred for long wavelength applications. This is where a single biconvex lens has different focal lengths for different colours: blue light is focused closer to the lens than red light [5-6].

Figure 4 – 2 **Longitudinal chromatic aberration**

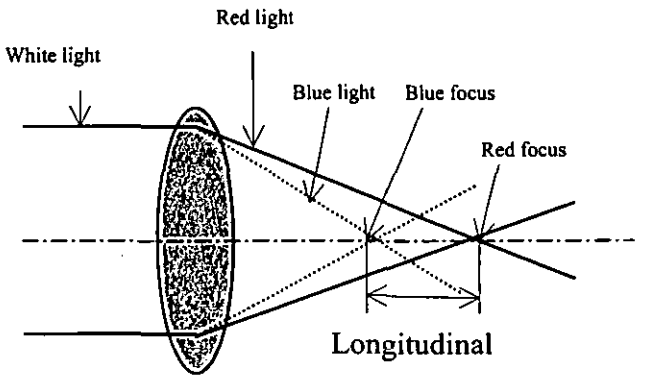

This was a criterion for the silicon photodiode to obtain a higher fluorescence signal from the flow cell or the standard cuvette; e.g. the distance was adjustable, not only for the photodiode mounting but also the biconvex lens. The test results from various dyes are discussed in Chapter 5, as well as a number of optical experiments.

The illuminated area on the surface of the photodiode can be calculated using Equation 4-1.

$$m = \frac{Hl}{Ho} = \frac{s'}{s} \qquad (4\text{-}1)$$

Where: m – the ratio of the image.

Hl – the window size of the standard cuvette or the flow cell.

Ho – the focal point size on to the surface of photodiode.

s' – the emission light side distance.

s – the photodiode side distance.

The illuminated sections on the flow cell or the standard cuvette (object side) had an area of 2.5×10 mm^2 and 10×12 mm^2 respectively. Therefore, the calculated area that was illuminated on the surface of the photodiode for both the flow cell and the standard cuvette were 1.9×7.7 mm^2 and 7.7 ×9.3 mm^2 respectively.

By integrating the two calculations, the magnification through the lens for the flow cell and cuvette was 0.78. Therefore the active area of the photodiode should be at least 9.3×9.3 mm^2 to satisfy the requirement of the detection system. From the resulting calculations a large area 10×10 mm^2 silicon photodiode (*Centronic Inc.*) from RS Limited was used in the design.

4.2.4 Filters for Emission Wavelength Selection

Cut-off filters have a transmittance of near 95% over a portion of the visible spectrum, but then rapidly decrease to zero transmittance over the remainder [6].

Also, the thicker the filter, the more light it will absorb. Coloured glass filters are excellent for fluorescence collection applications.

Cut-off filters remove the scattered light and other unwanted light from the excitation radiation. Cut-off filters are commercially available at a variety of wavelengths. These filters should be suitable for the transmission of emission beam and remove any scattered light. Figures 4–3, 4-4 and 4–5 show the characteristics of the 650 nm, 660 nm and 690 nm cut-off filters determined using a Hitachi U-2010 Spectrophotometer.

Figure 4 – 3 **Spectrum of Optosigma 650 cut-off filter**

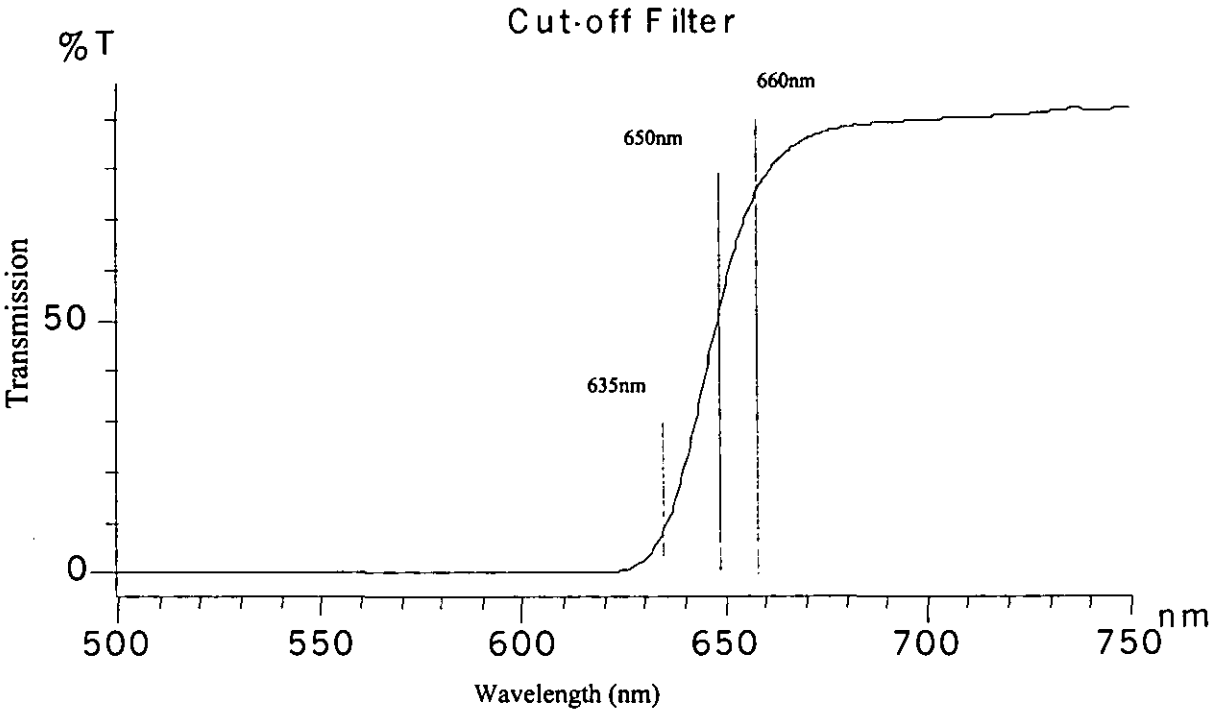

From the spectrum of the Optosigma 650nm cut-off filter, the transmission at 635 nm is 8%. When using a 635 nm 2 mW laser diode as an excitation source, only 8% scattered laser light can pass through the filter. The transmission of the filter at 650 nm is 58% which is less than that specified by the supplier. However, at 660 nm,

which is the maximum emission wavelength of NF, 80% transmission can be achieved.

Figure 4 – 4 **Spectrum of Schott RG-665 cut-off filter**

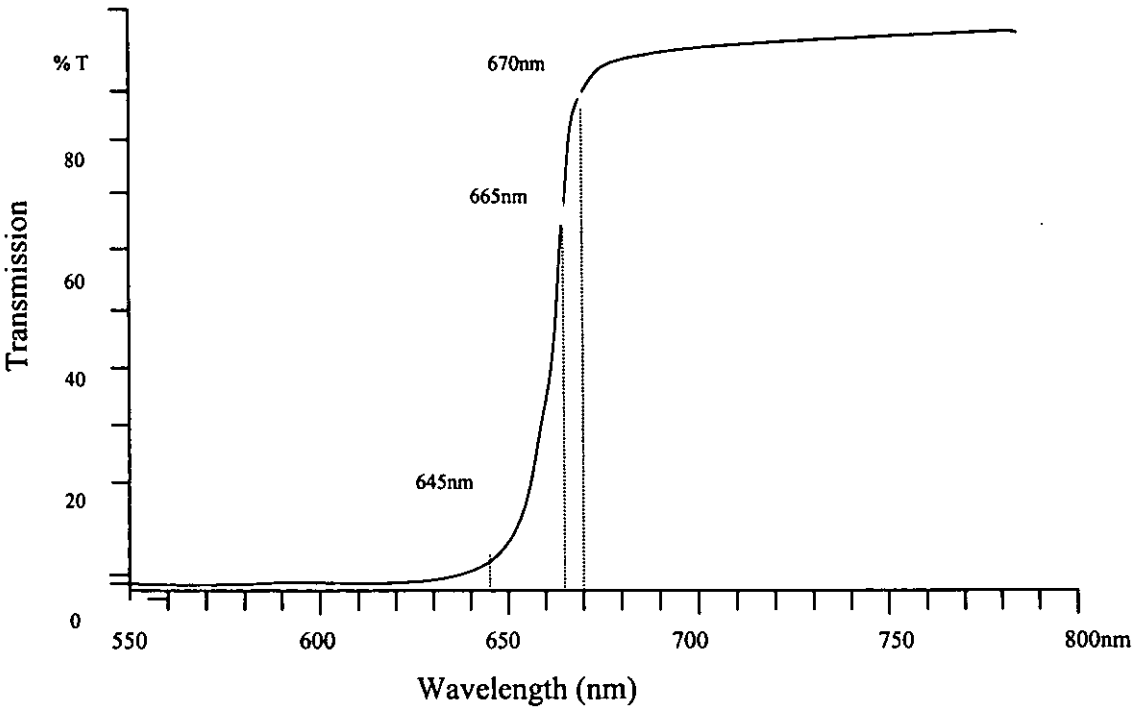

From the spectrum of Schott RG-665 cut-off filter, the transmission at 645 nm is 9%. When using a 645 nm, 2 mW laser diode, only 6% of scattered laser light can pass through the filter. The transmission of the filter at 665 nm was 65% which was less than that specified by the supplier. However, at 670 nm, which is the maximum emission wavelength of Cy5, 89% transmission can be achieved.

Figure 4 – 5 **Spectrum of Schott RG-695 cut-off filter**

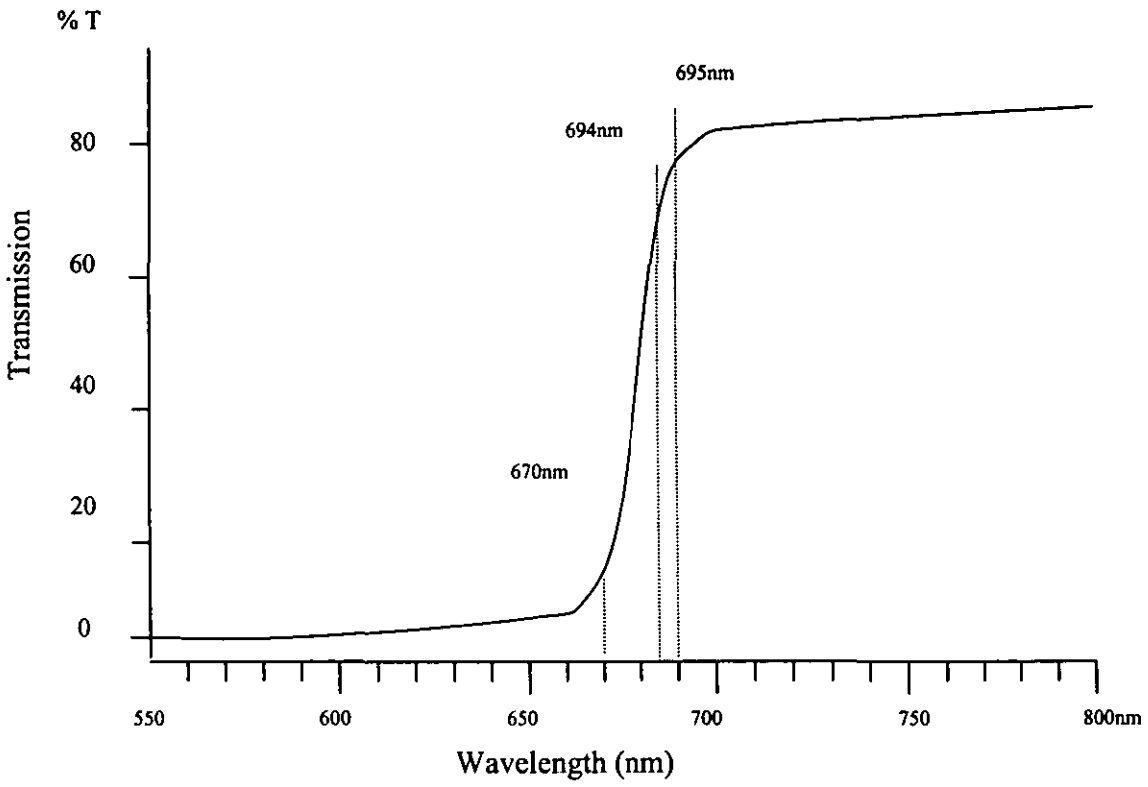

From the spectrum of Schott RG-695 cut-off filter, the transmission at 670 nm is 9%. When using a 670 nm, 2 mW laser diode, only 9% of scattered laser light can pass through the filter. The transmission of the filter at 695nm is 82%, which is higher than that specified by the supplier. However, at 694 nm, which is the maximum emission wavelength of the Cy7, 79% transmission can be achieved.

4.3 Principles of Electronic Circuit Building

The electronic circuits used in the NFDS are generally similar to an analogue instrument or digital instrument, i.e. the estimation of general power consume; the functions of electronics and mechanics; the steps of electronic design; test and confirmation in the procedure. Some are iterative with respect to each other as the following aspects:

1. Define and tentatively achieve targets, e.g. a multiple power supply circuit for the detection system, an operational amplifier circuit for the photodiode, a pulse generation circuit for the laser diode driver, a digital display, and analogue signal to digital converter for output signal processing.

2. Determination of the critical attributes required of the detection system and incorporating these into the specification of the detector. For instance, a linear optoelectronic amplifier can amplify a 50 nA current from the silicon photodiode, and its magnification between the input voltage from the photodiode and the output voltage from the amplifier was proportional to the radiation of emission beam. A pulse generator had several speed options and can also directly drive a laser diode to produce a laser beam.

3. Determination of the critical parameters and requirements. In a multiple power supply unit, there were demands of 2 × +12V, 2 × -12V and 2 × +5V to supply different circuits. The selection of the gain for the linear optoelectronic amplifier depended upon the intensity of the emission beam. Also, the parameters from the pulse generation, which are the laser intensity, the pulse width, the time delay were adjustable if required.

4.3.1 Accomplishment of Electronic System

The main elements of the electronic system are shown in Figure 4-6.

Figure 4-6 **Flow chart of electronic system for a fluorescence detector**

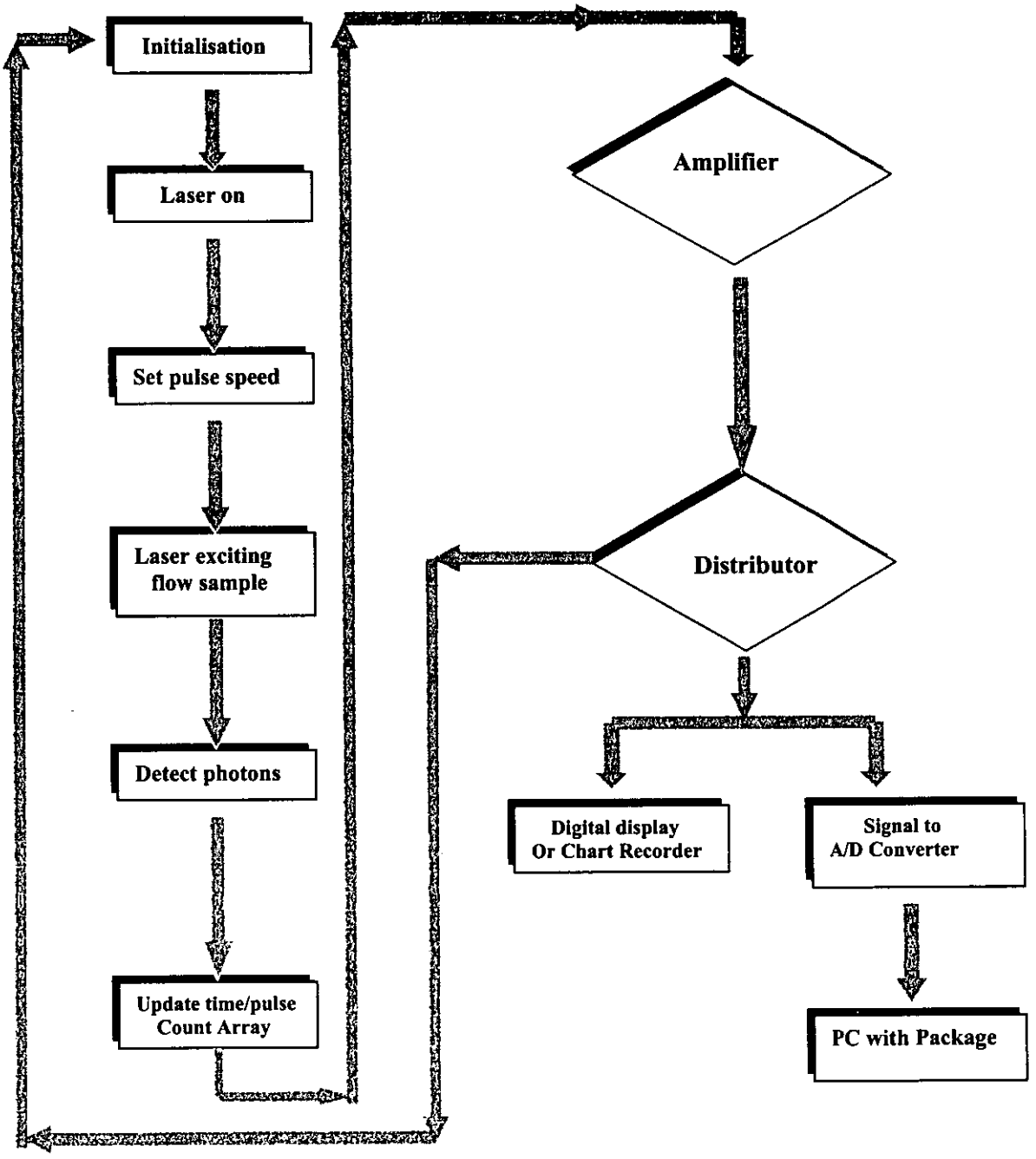

Figure 4-6 illustrates the overall operation of the NFDS. The laser diodes can be replaced depending upon the desired wavelength. A certain pulse speed (5 options on

the control plate) can be selected, depending upon the required sensitivity of the measurement needed. In general, the higher the laser pulse speed, the more sensitive the detection. The excitation beam from the laser diode has a quasi-collimating beam, which passes through the flow cell or the standard cuvette containing the sample mixture. The fluorescent labels for each component are also present in the sample mixture. The resulting emission beam has the same pulse speed as the laser, because the dyes selected for this application have a very short time delay compared to some dyes in other applications [8]. An oscilloscope can count the real pulse speed of the excitation beam, which generates an electrical signal from the photodiode. Actually, the signal from the photodiode is collected through a linear operational amplifier (CA3140, Harris Semiconductor Limited) [9] which is then connected to a high speed MOSFET (Metal Oxide Semiconductor Field-Effect Transistors)-input precision amplifier from which the signal could be amplified by 1 to 1,000 times its original value.

The circuit is shown in Figure 4-11. Also, a low noise circuit concerned with the application of the photodiode has been found [10] which makes it possible to use and improve the ratio of signal to noise. The function of distributor of the circuit is to connect in various ways: an analogue to digital (A/D) converter linked with a PC; and the analogue signal output to a chart recorder; a digital multimeter or the digital display on the control plate of the NFDS. If the output signal from the linear amplifier is off the scale, the energy from laser diode should be decreased by either reducing pulse speed of laser or adjustment of the height of output pulse of laser (see Section 4.3.4).

4.3.2 A Multiple Power Supply

A multiple power supply was designed and built for supplying power to different circuits within the NFDS. The AC to DC conversion stage included a transformer and a rectifier. The filters were composed of capacitors to reduce the voltage ripple by removing the high-frequency components. The regulation stage used several IC regulators, i.e. 7805, 7812, 7912 (see Figure 4 – 7), as a variable resistor to control the voltage across the regulator and flatten the voltage peaks. The regulator also incorporated a voltage reference, which monitors the output DC voltage. This completed the feedback loop within the IC regulator.

Figure 4 - 7 **Circuit of power supply for multiple output**

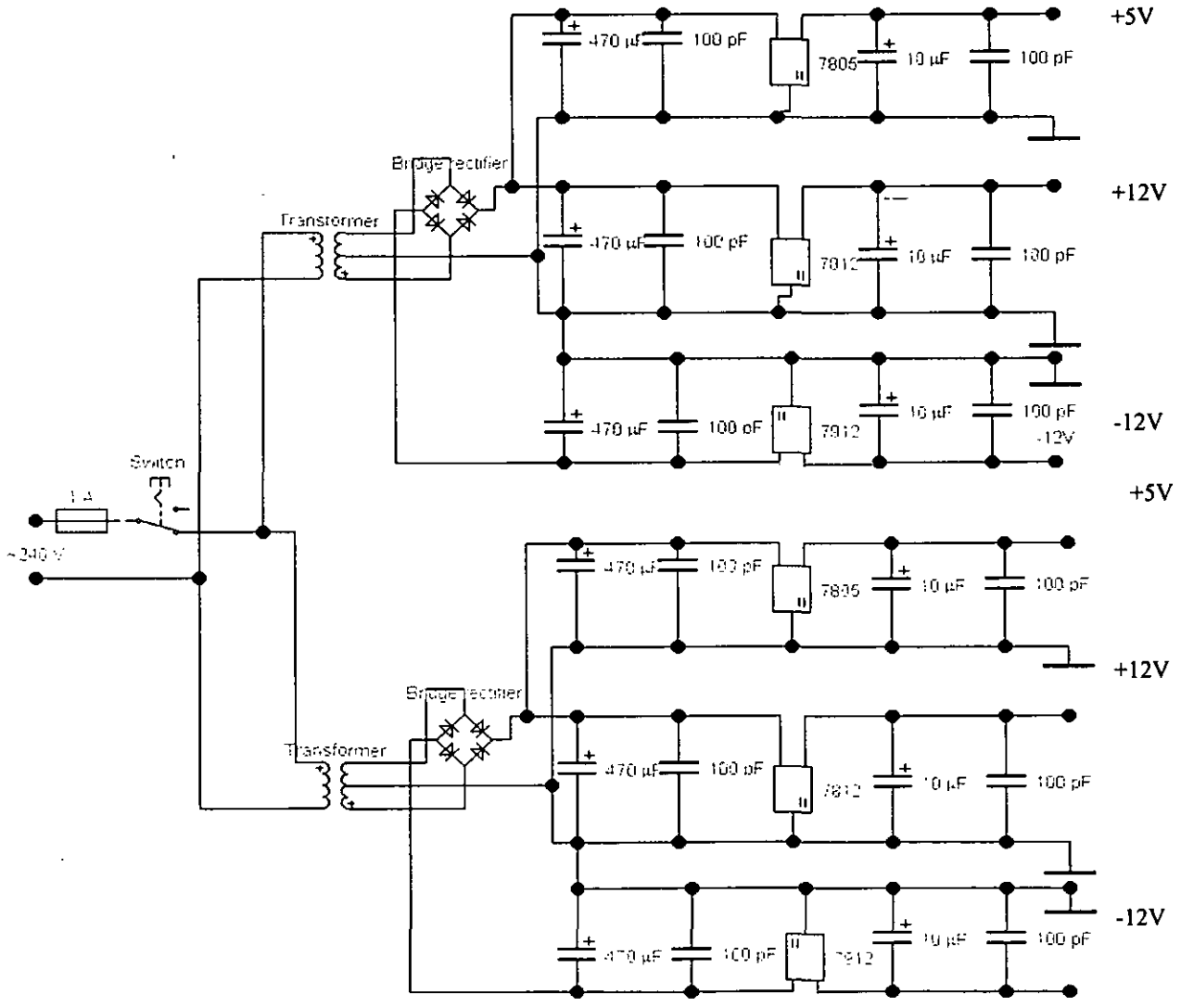

The power supply for multiple output consisted of the following units:

1. One set of +12V, -12V was for the laser pulse generator and driver.
2. One set of +5V was for the IC timer 555 and the laser diode driver.
3. One set of +12V, -12V was for the photodiode driver and the signal amplifier
4. One set of +5V was for two LED digital displays

The power consumption for the detection system was approximately 2 watts. Meanwhile, a heatsink was fitted to the regulator on the printed circuit board (PCB) of the multiple power supply to avoid overheating. Actually, the multiple power supply consists of six single power supplier units. Using individual power supply in the system can be considered as having the following benefits:

1. Less interference from other power sources, in which each divisional power source is response for its electronic circuit as described above.
2. These individual sources give a better constant power for electronic system thus provides a good condition to create a stable output signal.
3. Easily maintaining, e.g. once one set of power unit is failed to work, the replacement of failure unit can be rapidly carried out.

However, a significant disadvantage of this multiple power supply is that six individual power supply units occupy a bigger space in the instrument than using a DC-DC converter for a multiple power supply.

4.3.3 A Laser Pulse Generator

TLC 555 timer supplied from Texas Instruments, USA was used in the NFDS which was one of the most popular and versatile integrated circuits ever produced and

employed for the laser pulse generation. With the charge and discharge action of RC circuit, the IC 555 timer consisted of an astable multivibrator (AMV) which was a free-running circuit and produced a square-wave output signal. Since the values of R_A, R_B and C (see Figure 4-8) affected the frequency of the pulse output in TLC555 timer circuit, several pulse speeds were available. The following diagram shows the astable operation of TLC 555 timer circuit.

The frequency of square-wave output as a pulse generation can be expressed and listed in Table 4-1 by using Equation 4-2 [11].

$$F = \frac{1.44}{(R_A+2R_B)C} \qquad (4\text{-}2)$$

Where: F is the frequency of pulse speed in Hertz.

R_A and R_B are the resistors separatively in Ohm.

C is the capacitor in Farad.

Figure 4-8 **IC 555 timer connection for astable operation**

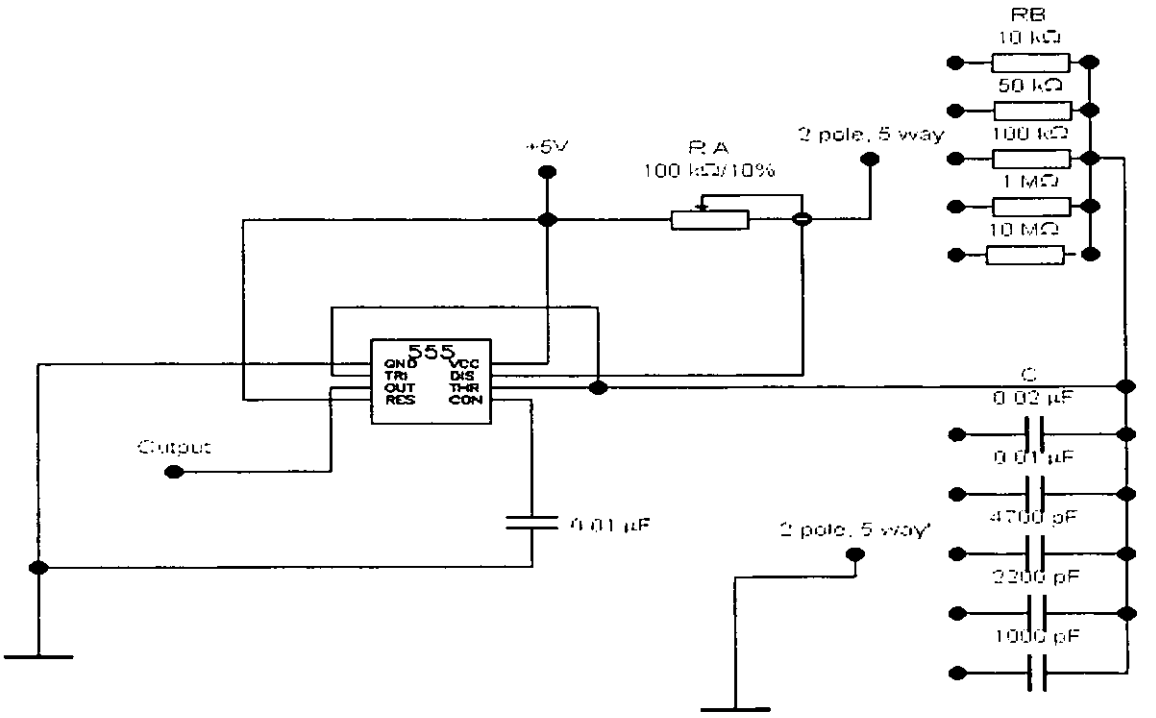

Table 4-1 **Frequency list with a combination of resistors (R_A and R_B) and capacitor C**

Combination of R_A, R_B and C	Frequency (Hz)	Notes
R_B:10MΩ, R_A:100KΩ, C: 0.02μF	7.06 - 7.24	R_A: 100KΩ potentiometer
R_B:1MΩ, R_A:100KΩ, C: 0.01μF	120 - 144	
R_B:100KΩ, R_A:100KΩ, C:4700pF	1,021 - 3,063	
R_B:50KΩ, R_A:100KΩ, C:2200pF	2,619 - 13,091	
R_B:10KΩ, R_A:100KΩ, C:1000pF	6,857 - 14,400	

The TLC555 data sheet indicates its features as same as most of IC555 timer [12], which is Bipolar and C-MOS versions. Compared to a typical IC 555 timer, TLC555 has been improved in its functions, i.e. fast speed which operates at frequencies up to 2 MHz, low power consumption in operating condition, and is even fully compatible with CMOS, TTL, and MOS logic.

In the practical operation of IC555 timer circuit, the output of pulse signal width can be adjusted by the variation of R_A, R_B and C. The following Figure 4-9, Equation 4-3 and Equation 4-4 express the detail.

Figure 4-9 **The output of pulse signal generated by IC555 timer**

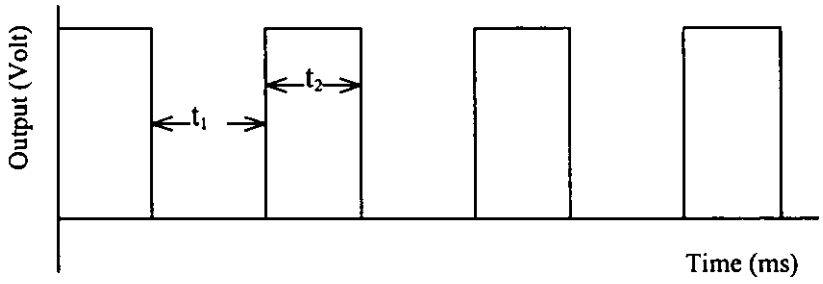

The pulse with of t_1 and t_2 can be written below:

$$t_1 = 0.639\ (R_A+R_B)C \qquad (4\text{-}3)$$

$$t_2 = 0.693\ R_B\,C \qquad (4\text{-}4)$$

The output of pulse varies with the variation of R_A, R_B and C, which made not only many frequency options but also the pulse width. Through this procedure of pulse generation and variation, a laser diode driver modulator (see Section 4.3.4) changed the output energy of laser diode.

4.3.4 A Laser Diode Driver Modulator

In the NFDS the modulator circuit contains four inverting operational amplifiers, which are made up of four low cost IC μ741 chips and a switching transistor 2N3053. The switching transistor 2N3053 turns the laser on and off. The circuit diagram is shown in Figure 4-10.

Figure 4-10 **Electronic circuit of laser diode driver modulation**

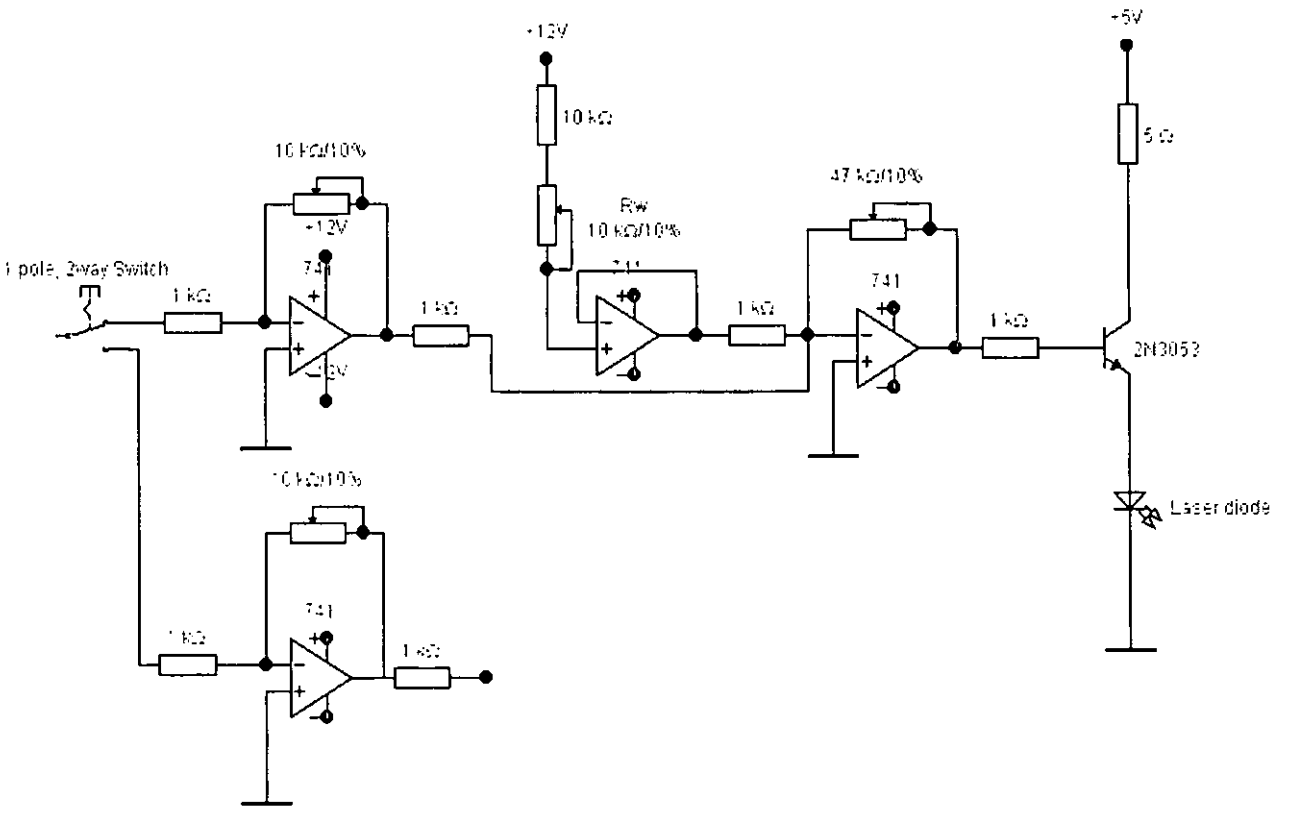

With the IC 555 timer circuit, the adjustable pulse signal was sufficiently amplified to allow the transistor 2N3053 to be in the switching situation within 1 MHz pulse speed, therefore driving the laser diode on and off according to the pulse frequency. The height of output pulse could be adjusted by varying the value of *Rw*, therefore the energy of the laser beam could be controlled in another way. Meanwhile, an oscilloscope was able to monitor the pulse frequency from the IC 555 timer circuit when the switch in the circuit was changed into the monitoring state.

Since the pulse power from IC555 timer was not enough to straightforwardly drive a laser diode, the inverting operational amplifiers made the amplification of pulse signal then the transistor 2N3053 took a switching function to control a laser diode modulator. Over 1 MHz pulse speed, the IC μ741 [13] as inverting operational amplifier could be difficult to meet the requirement of laser pulse format in the NFDS because the gain-bandwidth product (GBP) for IC μ741 is typically 1 MHz. As 2N3053 is a generally proposal bipolar transistor, it is found that this type transistor has a high switching speed, However, leakage currents and offset voltage made the switch less precise.

Providentially, a Junction FET (JFET) acts as a voltage-controlled resistance; the channel resistance between drain and source depends on the gate voltage. The ratio between the off- and on-resistance is high. Therefore the advantages for using a JFET over the bipolar transistor are very low control current (the gate current) and the low offset voltage [14]. If a JFET is used as a switching transistor in the NFDS, it is possible to make the laser diode driver simpler than the current one without any operational amplifier in the circuit.

4.3.5 A Linear Optoelectronic Amplifier

In the linear amplifier circuit, the voltage generated by the photodiode, which was processed in proportional to the emission light intensity (fluorescence). The gain of the linear amplifier was set within a certain range by the gain of the BiMOS operational amplifiers CA3140. Figure 4-11 shows its electronic circuit.

Figure 4-11 **Linear amplifier for a photodiode**

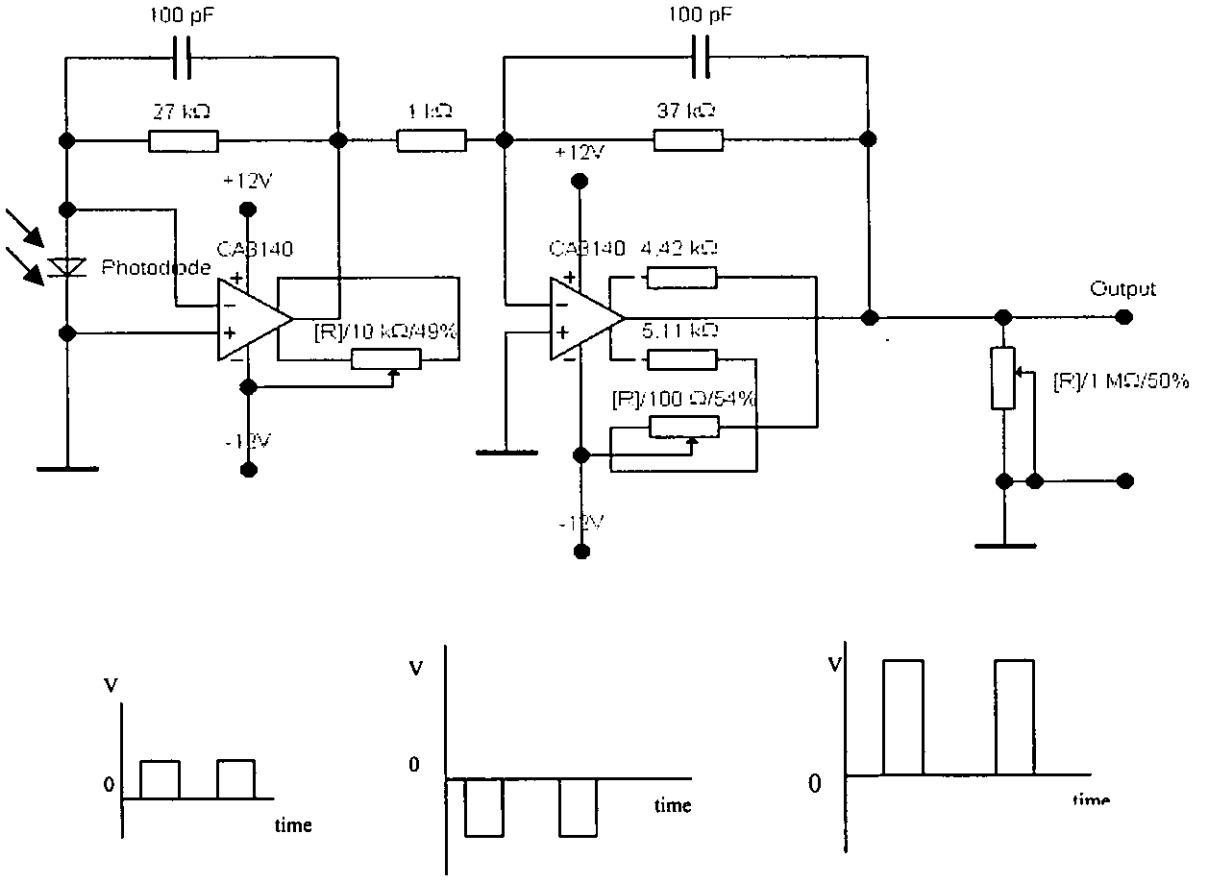

Since the photodiode (RS 303-674) has a large active area of 100 mm^2, 50 ns of the response time (10% to 90%) and a high responsivity of 0.35A/W at 633 nm [15], these characteristics made the NFDS able to enough capture the pulse signal of fluorescence from the sample. Two CA3140 chips were used in the linear amplifier

circuit for amplification of the fluorescence signal through the photodiode. The CA3140 chip has the following features:

1. A very high input impedance: 1.5TΩ (Type)
2. A very low input current: 10pA at ±15V, which is from a source of signal, i.e. a photo-sensor.
3. A low input voltage – can be swung 0.5V below negative supply voltage rail.
4. A high performance speed, i.e. GBP, 4.5 MHz.

In this circuit, two CA3140 chips that were similar to most IC operational amplifiers have a means of compensating for offset voltage [16]. This was done by connecting an external potentiometer 10 KΩ and 100 Ω to designated pins on their package. The two terminals 1 and 5 of CA3140 were labelled offset null. By connecting a 10 KΩ potentiometer in first inverting amplifier, the input offset voltage was roughly nulled. Furthermore, second inverting amplifier consisted of two precise resistors 4.42 KΩ and 5.11 KΩ and a 100 Ω potentiometer, which more precisely provided an offset null than in the first inverting amplifier. This character gave more adjustment range than required [17]. The CA3140 chips have already been used for some precision instrumental amplifiers with a small signal [18].

In the first amplifier, a CA3140 chip was connected to the photodiode and took the role of an inverting amplifier. The generated photocurrent flowed through the input resistor *Ri,* which was fixed in the photodiode and resulted in a voltage that was linearly dependent upon the incident radiation level. The circuit had a linear response and low noise due to the almost complete elimination of leakage current [19]. This also acted as a transimpedance amplifier, which was a *current to voltage converter* in

this application. The voltage gain of the first inverting amplifier could be calculated from Equation 4-5 [20].

$$A = \frac{Rf}{Ri} \qquad (4\text{-}5)$$

Where: *A is* the voltage gain.

Rf is the feed back resistor (Ohm).

Ri is the input resistor (Ohm).

When *Rf* and *Ri* are 27KΩ and 2.8KΩ respectively and the photodiode is in a forward bias, the voltage gain is 9.6. By applying the same procedure to the second CA3140 chip (which is also an inverting amplifier), the voltage gain is 37. Therefore the overall voltage gain was 357. Also, the feed back resistor *Rf* in the second inverting amplifier was changeable, depending upon the gain demanding of the operation. Furthermore, the linear amplification circuit took another function that avoided the output drift by the resistors and two 100 pF feedback capacitors. This allowed the voltage across the capacitors to be restored slowly to zero [21], with the constant time τ, 2.7×10^{-6} s (370KHz), and 3.7×10^{-6} s (270KHz) respectively. When the pulse width was greater than five time constant τ [22], the pulse output signal from this circuit can be detected in as same frequency as laser pulse speed. Therefore, the laser pulse speed the NFDS in the measurement was set around 50KHz, which was the output signal in a pulse format.

Meanwhile, a 1MΩ potentiometer was linked between the output signal and the ground in order to attenuate the output signal.

In Figure 4 –11, two inverting amplifiers were used to amplify small signals ranging from 0.01mV to a few volts, depend upon the output of the photodiode which does not exceed the supply voltages, ±12V. The voltage gains of amplification were set at 9.6 and 37 individually. The first inverting amplifier only made a small gain range and provided a good ratio of signal to noise for second inverting amplification. In the second inverting amplifier there was a slightly higher voltage gain than in first inverting amplifier. However the total voltage gain of this circuit was reached at 357, the significant output signal in volts from the photodiode can be detected by either a PC with data capture package or a digital multimeter (see Section 4.4.1 and 4.5.1). Like most inverting amplifiers [23], the non-inverting inputs in both inverting amplifiers were connected to ground potential, and the input resistors of the circuit are 2.8KΩ (the forward resistance of photodiode) and 1 KΩ respectively. This was generally a much lower value than the input impedance, 1.5TΩ, of CA3140. Such linear operational amplification using CA3140, which was a typical inverting amplifier is not suitable for the amplification of signals from high impedance sources [24].

4.4 Date Capture of Detection System

Data capture is one of most important means for completing chemical analysis. For instance, in this research the output signal was either displayed on a digital multimeter or connected to an ADC, which handled the raw data from the detection system and displayed on a PC.

4.4.1 A Digital Multimeter as Readout

A RACALL-DANA 4009 digital multimeter was used as a readout display through the measurement of NF, Cy5 and Cy7. Most functions at the RACALL-DANA 4009 digital multimeter are same functions as other type multimeters, i.e. resistance measurement, current measurement etc. Of interest is that for this digital multimeter offers better accuracy and higher stability than other types of multimeter. As a result it can simply measure the output signal in voltage from the linear operational amplifier circuit in this research.

In fact, the RACALL-DANA 4009 digital multimeter consists of an integrating AD converter, i.e. *a dual-slope integrating* AD converter, which is widely used in DC current and voltage measurement [25]. This had the effect that the input signal from the linear amplifier was integrated during conversion in the digital multimeter, the digital output is proportional to the mean value of the input signal. The principle of dual-slope integrator can be described in the following Figure 4-12.

Figure 4 – 12 **Dual Slope Conversion Cycle**

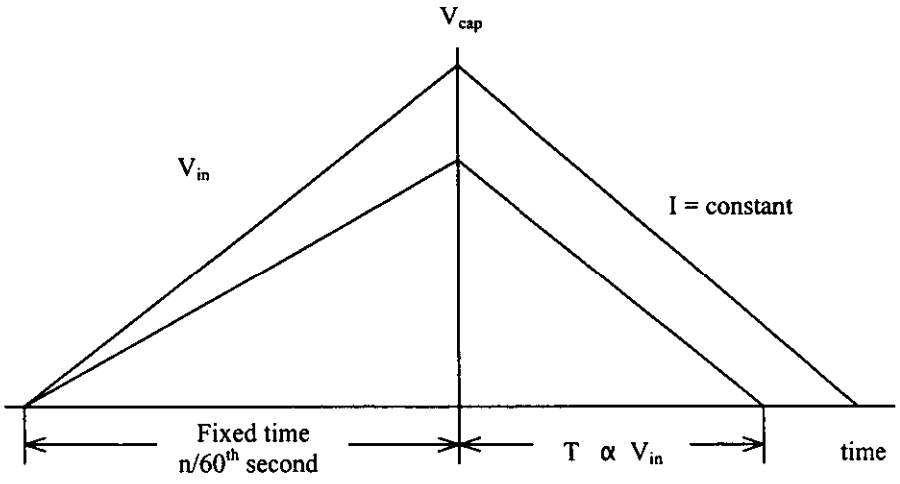

Note: V_{in} is the input signal in voltage; V_{cap} is the integrator output voltage; T is the integration time which is proportional to input voltage V_{in}; I is the discharge current for the integrator in mA.

Firstly, a current proportional to the input level charges a capacitor for a fixed time interval (RC); secondly, the capacitor is discharged by a constant current until the voltage reaches zero again. The time (T) to discharge the capacitor is proportional to the input level and is used to enable a counter driven from a clock running at a fixed frequency. The final count is proportional to the input level, i.e. the digital output in the RACALL-DANA 4009 digital multimeter. Therefore dual-slope integration provides very good accuracy without putting extreme requirements on the components' stability [26 – 27].

For the practical measurement for selected dyes, NF, Cy5 and Cy7 using the NFDS, the signal applied to the RACALL-DANA 4009 digital multimeter was about 50 KHz in constant pulse format. However because of the integrating nature of the APC in the digital multimeter, the readout showed very good stability and good accuracy.

4.4.2 An ADC and Distribution Board

Analogue-to-digital conversion (ADC) transforms an input signal from the continuous analogue domain in the detector, to the discrete digital domain. The *FlowTEK* (Global FIA Inc., USA) took the role of the ADC and displayed the results of flow injection immunoassay on the PC screen. This was done by using the NFDS and the main procedures are described in Figure 4-13.

Figure 4-13 **General test configuration of ADC for a fluorescence detection**

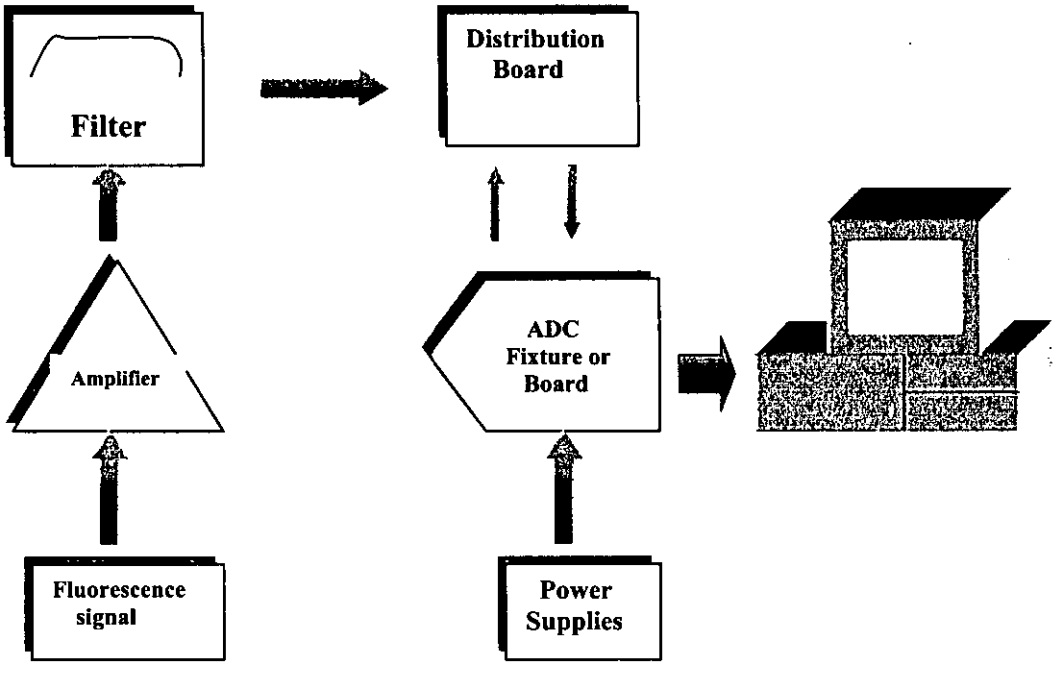

The linear optoelectronic amplifier amplified the fluorescence signal and most of the electronic noise was filtered through a capacitor. A distribution board interfaced the input signal (which magnified the voltage gain by 1, 20 and 100) to the ADC board. The PC supplied power to the ADC. The FlowTEK, had a 10 bit ADC and performed the conversion process, and its software was run through the DOS system on the PC. The sampling speed of the ADC could be reached to 125KHz and also depended upon the set-up time of FlowTEK software. The FlowTEK analyser control software was

produced by MINTEK, and was capable of providing the flow-based analyser with microprocessor control and data acquisition capabilities. The main functions were:

1. Three analogue input ports and three digital input ports

2. *Set-up* allowed the package to be configured so that it met the requirements, i.e. time drive period (1 – 999 second) in which a peak area was integrated was fitted for flow injection and displayed in the screen

3. *Method* provided the definition of the devices and a description of the device control methods. The devices in an experimental set-up were defined as those components which required the digital or serial control, (e.g. pumps, valves, auto sampler, etc.).

4. *Calibration* provided various options in performing regression on the acquired data or entered data and reported in concentration units.

5. *History* provided a means of viewing data acquired by the package.

6. *File* gave certain file choices and the manipulation utilities including a means of switching to DOS.

The peak area generated by the flow injection reading from the NFDS and the FlowTEK analyser software was integrated and displayed on the screen.

4.5 Optima of Detection System

Although the optical system and the electronic circuits were established and used for fluorescence measurements, there are still many areas that need to be improved and refined before it can be used in practical applications. For instance, overcoming the noise, which was showed as baseline drift within the time period, was important in order to increase the sensitivity of detection.

4.5.1 Heating Dispersion and Elimination

The heat transfer was taken into account in the instrument because all the electronics generated heat. In most equipment, the cooling design is as important as the electronic design [28]. The energy loss between the input and output of an electronic device manifested itself as thermal energy dissipation, or heat. Heat consisted of two deleterious effects on the electronics of the NFDS. It reduced reliability by inducing thermal stress on the components, which eventually lead to failure and it altered the circuits operation in temperature-sensitive devices.

Furthermore, some fluorescent compounds are sensitive to the ambient temperature, for example, a variation of 16% was seen in the fluorescence intensity between 20 ^{0}C and 40 ^{0}C when B-2 Welf-F(ab)$_2$-Bodipy dye was excited at 696 nm. The results are shown in Table 4-2 and Figure 4-14.

Table 4-2 **Fluorescence intensity of B-2 Welf-F(ab)$_2$-Bodipy dye in Tris buffer (pH 9.0) with ambient temperature using LS 50 uminescence spectrofluorometer**

Sample No.	Ambient Temperature (^{0}C)	Fluorescence Intensity (a.u)	Note
1	20	696.4	The flow cell holder had a liquid cooling system specially made for decreasing ambient temperature variation
2	25	669.5	
3	30	649.3	
4	35	628.3	
5	40	592.7	

Note: a.u is arbitrary unit.

Figure 4-14 **Fluorescence intensity variation of B-2 Welf-F(ab)$_2$-Bodipy dye in Tris buffer (pH 9.0) with ambient temperature using LS 50 Luminescence spectrofluorometer**

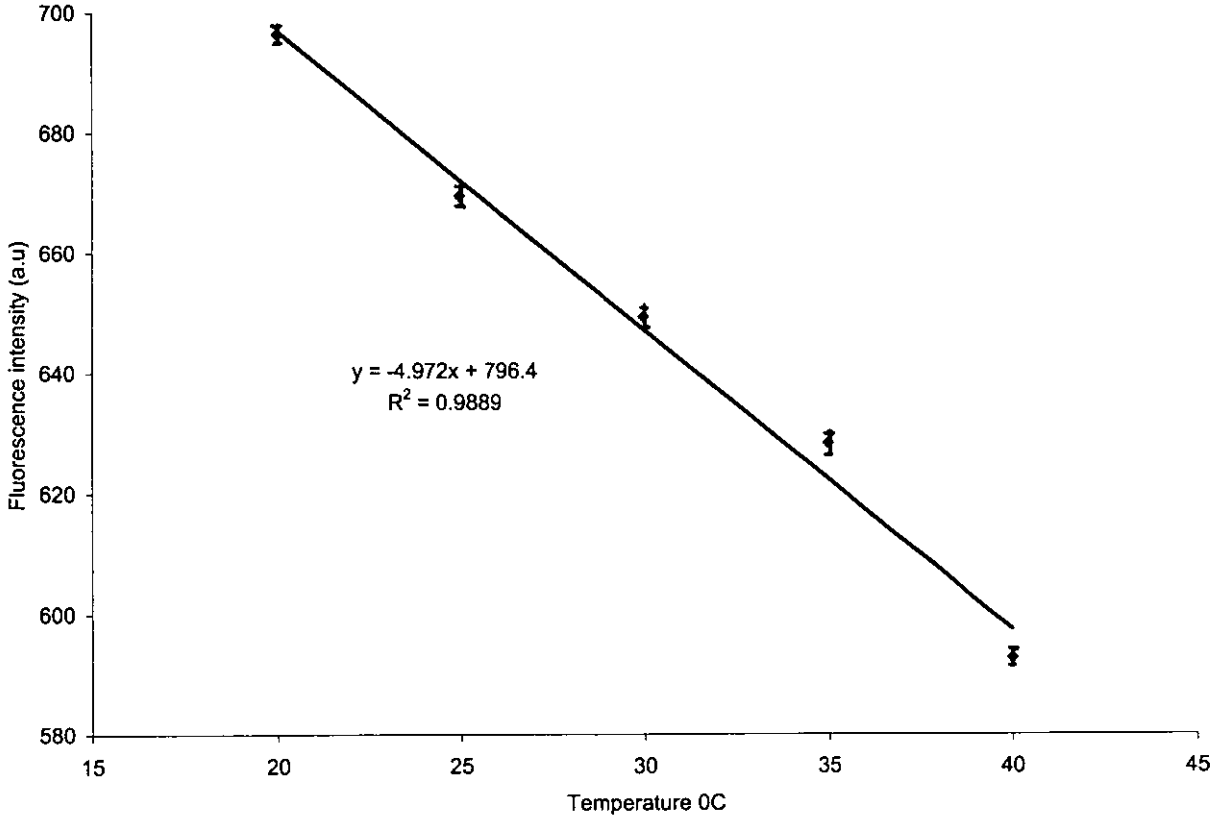

Note: a.u is arbitrary unit.

Therefore, there were two aspects to be considered when cooling. Firstly the mechanisms of thermal energy transfer occurred from the power supply. To reduce such heat, a number of heat sinks were fitted onto the regulator in the power supply printed circuit board (PCB). One miniature-cooling fan (Papst Plc.) was installed on the rear plate of the instrument box. Secondly, the flow/cuvette holder had a liquid cooling system specially made for decreasing the ambient temperature variation when required. The following figure shows the feature of the sample holder.

Figure 4-15 **Feature of cuvette or flow cell holder**

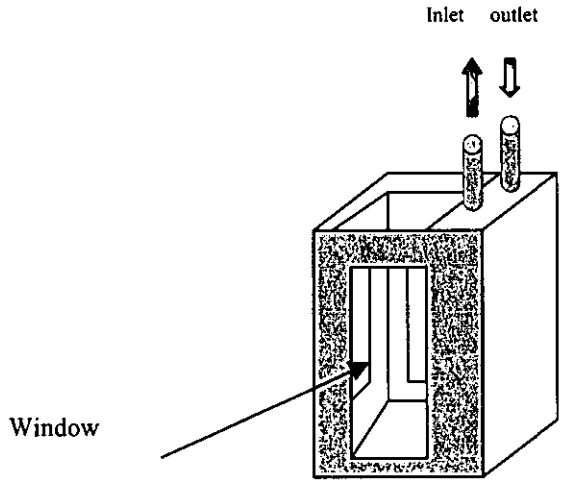

4.5.2 Minimising Drift of Output Signal and Systemic Noise

The detector responds to the input signal and produces a voltage change ΔV. ΔV is a function of several quantities as shown below:

$$\Delta V = \Delta V\,(b, f, \lambda, P, A_d) \qquad (4\text{-}6)$$

Where b is the applied electrical gain, f is the frequency of modulation, λ is the wavelength of the incident radiation, P is irradiance (power per unit area, i.e. Wcm^{-2}) and A_d is the detector area [29], i.e. photodiode in this research.

Therefore, the output signal voltage of the NFDS relies on these factors. Obviously, each procedure generated not only the desired output signal but also the noise. If the noise in the system is a significant proportion of the expected signal it will influence the measurement, which will decrease the sensitivity of the detection system.

4.5.3 Output Drift with Ambient Temperature

The drifting of the output signal regularly occurred in the preliminary testing. This is because the photodiode is a semiconductor, and is sensitive to changes in the operational temperature of the NFDS. Also, heat transfer arose from the power supply. Therefore increasing the operating temperature of the photodiode resulted in two distinct changes in operating characteristics. The first change was a shift in the quantum efficiency (QE), due to changes in the radiation absorbability of the device. QE values decreased in the UV region and increased in the infrared-red (IR). Figure 4-16 illustrates the QE shift.

Figure 4-16. **Temperature dependence of QE.**

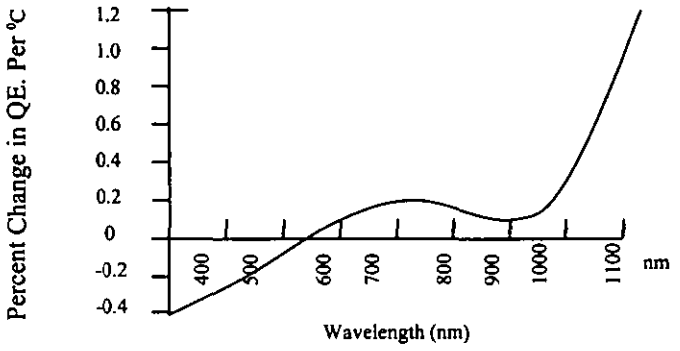

The percentage change in QE varied between 0.02 and 0.2 for the particular wavelength region, 600 nm to 900 nm, and did not seriously affect this detection compared to other wavelength regions.

However, the second change was caused by an exponential increase in the thermally excited electron-hole pairs resulting in the dark current increasing in magnitude. Figure 4-17 shows the dark current when the ambient temperature increases.

Figure 4-17 **Dark current versus ambient temperature**

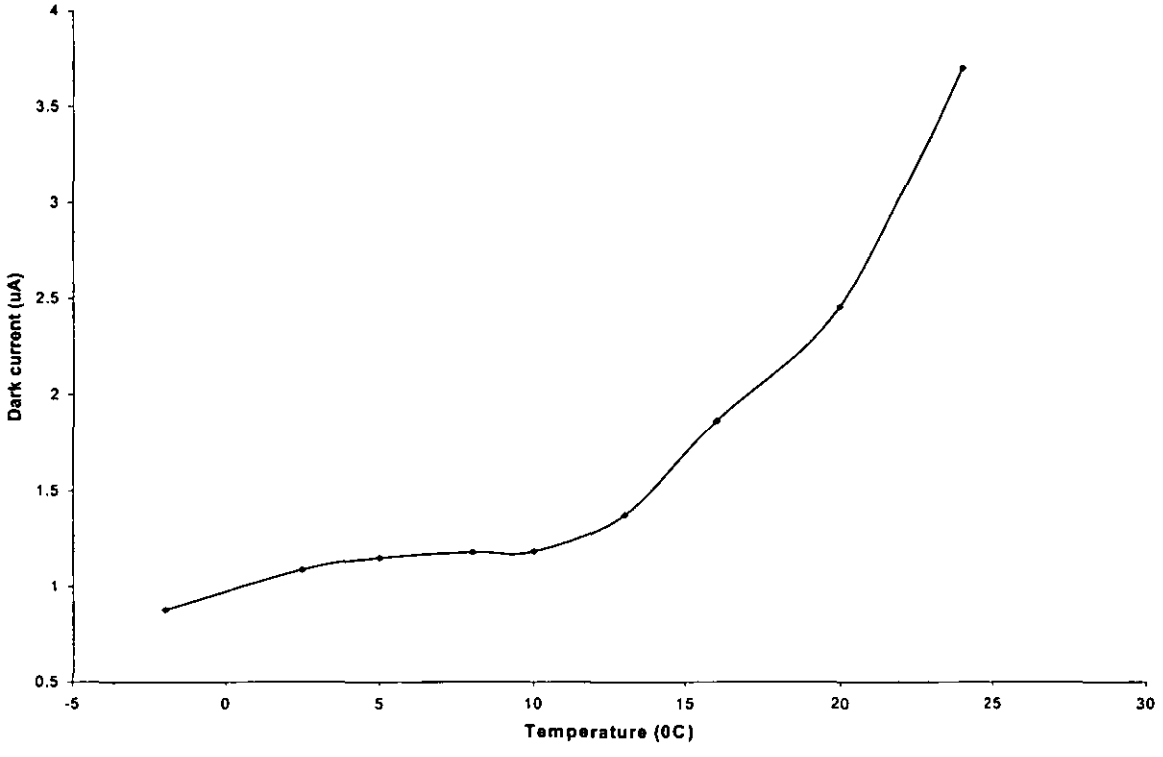

Table 4-3 **Variation of dark current of photodiode with operating temperature**

Sample No.	Dark current (μA)	Operating Temperature (^{0}C)	Note
1	0.8795	-2	Photodiode type: RS303-674
2	1.0885	3	
3	1.1507	5	
4	1.1814	8	
5	1.1838	10	
6	1.3768	13	
7	1.8649	16	
8	2.4619	20	
9	3.7059	24	

Note: μA is microamp.

When the operating temperature was between -2 ^{0}C and 24 ^{0}C, the change of dark current ranged from 0.88 μA to 3.71 μA. For low fluorescence signal detection, it was obviously taken into account to keep minimum change of dark current from ambient temperature. In the construction of the detection system, the photodiode was mounted and inserted into the metal holding block that was made from aluminium. This feature is illustrated in Figure 4-18.

Figure 4-18 **Feature of photodiode mounts**

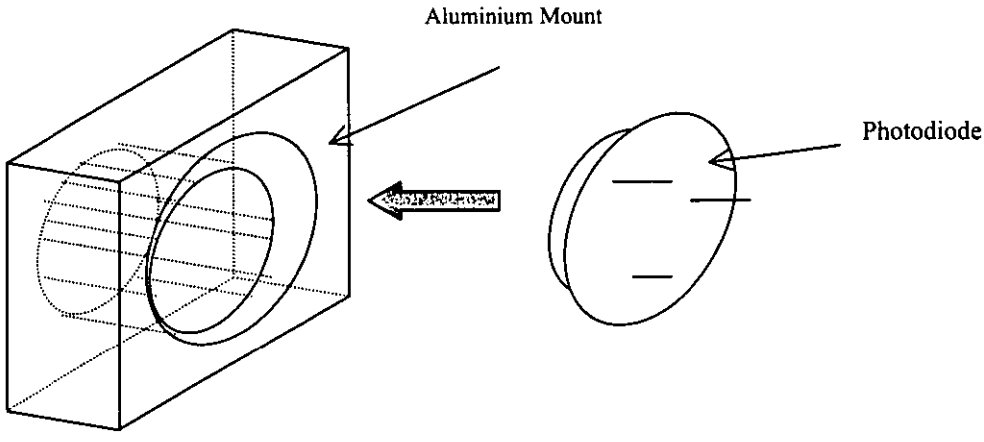

Since the surface of the photodiode was metal, the aluminium mount obviously increased the area of heating transfer thus preventing the operational temperature

from increasing. After mounting the aluminium block, the variation of the temperature was kept to a minimum, which gave a high level of sensitivity for detection.

4.5.4 Reducing the Systemic Noise

Each electronic component can be modelled as an ideal device with a noise voltage and noise current referenced to its input. Noise or errors accumulate through the root sum square of the individual components [30].

$$V_{total} = (V_1^2 + V_2^2 + \ldots + Vn^2)^{1/2} \qquad (4\text{-}7)$$

Where:

V_{total} is total noise (V); $V_1^2 + V_2^2 + \ldots + Vn^2$ are the individual noise components.

Three main factors were considered to eliminate the noise generation, and these were the cable connection, the linear optoelectronic amplification and the laser pulse generation.

4.5.4.1 Cable Connection with Interference

There were different power sources in the NFDS, i.e. the main power AC 240 voltage 50 Hz, and the multiple power supply, DC, +12 volts, -12 volts 5 volts. The cable connection for these sources was isolated and kept at a certain distance (20 – 30 mm) from each other. The cables in the NFDS were properly connected for reducing the interference from the power sources.

4.5.4.2 Linear Optoelectronic Amplifier with Interference

Although the CA3140 chip generated a low noise level in the circuit, the interference was still found irregularly when electronic components were mounted on the PCB. This phenomenon made it particularly difficult to detect low fluorescence signal. Therefore, it was critical to improve the sensitivity of the detection system by decreasing the noise from the CA3140 chips. Two metal baffles made from a thin aluminium sheet were used to cover the amplifier circuit on the PCB thus protecting the system from environmental effects. By using this procedure, satisfactory results were obtained from the experiments in Chapter 5.

4.5.4.3 Laser Pulse Generation to Reduce the Noise

As *Johnson or Nyquist* noise exists in many optoelectronic detection system, and to restrict the amount of noise from a source it is often 'chopped' and the amplifier in the detector is switched on and off at the same chopping frequency. This technique also was a narrow-band electrical filter centred on the chopping frequency that reduces the effective bandwidth. In the NFDS the laser pulse generated a regular pulse, the emission beam also produced a regular pulse signal, which was similar to a 'chopping' frequency and could contribute to reducing the noise from the sample background (see Section 2.3.3). Although, the linear optoelectronic amplifier did not use a 'chopping' frequency, the noise was still reduced compared to using a constant source for excitation. However, a lock-in amplifier, which has a 'chopping' frequency can be easily improved in future work and details are given in Chapter 6.

4.6 Reference:

[1] Skoog, A. D., Holler, F. J. and Nieman, T. A., Molecular luminescence spectrometry, Principles of Instrumental Analysis, Philadelphia, Harcourt Brace, (1998), pp.364-365.

[2] Hicks, T. R. and Atherton, P. D., Material Properties, The Nano Positioning Book, Queensgate Instruments Ltd., (1997), pp.43-48.

[3] Newport Limited, Why honeycomb structure deflect less than solid structure, Vibration Control, Newport Corporation Catalogue, USA, (1997), pp.6 – 8.

[4] Hicks, T. R. and Atherton, P. D., Material properties, The Nano Positioning Book, Queensgate Instruments Ltd., (1997), pp.67.

[5] Hecht, E., Geometrical optics, Optics, (3rd edition), Addison-Wesley Longman, Inc., USA, (1998), pp.162-165.

[6] Meyer-Arendt, J. R., Aberrations, Introduction to Classical and Modern Optics, (4^{th} edition), Prentice-Hall Inc., (1995), pp.98 – 99.

[7] Skoog, A. D., Holler, F. J., and Nieman, T. A., Wavelength selectors, Principles of Instrumental Analysis, Saunders College Publishing, USA, (1998), pp156-157.

[8] Birch, D. J. S. and Hungerford, G., Instrumentation red/near-infrared fluorescence, Fluorescence Spectroscopy, Volume 4, Plenum Press, New York, USA, (1994), pp.380-383.

[9] Harris Corporation CA3140, CA3140A 4.5MHz, BiMOS Operational amplifier with MOSFET, (1996), pp.3-85, pp.3-94.

[10] Hyyppa, K. and Ericson, K. Low-noise photodiode-amplifier circuit, IEEE Journal of Solid-State Circuits, (1994), Vol. 29, No.3, pp.363 –364.

[11] Carr, J. J. IC and Digital timer circuits, Designer's Handbook of Instrumentation and Control Circuits, Academic Press Inc., (1991), pp.531-533,

[12] RS Data Sheet, IC timers 555 and 556, RS components Ltd., UK, (1997), pp.1-3.

[13] Malcolme-Lawes, D. J., The Elements of analog signal handling, Microcomputers and Laboratory Instrumentation, Plenum Press, (1988), pp.34 – 35.

[14] Regtien, P. P. L., Electronic switches, Instrumentation Electronics, Prentice Hall, (1992), pp246 – 248.

[15] RS Data Sheet, IC timers 555 and 556, RS components Ltd., UK, (1997), pp.16.

[16] Floyd, T. L., Operational amplifiers, Electronics Fundamentals, Prentice Hall, (1998), pp.842 – pp.843.

[17] Harris Corporation CA3140, CA3140A, BiMOS Operational Amplifier with MOSFET, (1996), pp.3-79.

[18] Lu, S. and Chei, D., Design of analogue circuit, Technologies of Electronic Design, China Science and Technology Press, (1997), pp.461-462.

[19] Centronic Limited A Primer on Photodiode Technology, (1998), www.centronic.com/

[20] Flody, T. L., Operational amplifier, Devices and Application, Prentice Hall, (1988), pp.837-838.

[21] Malcolme-Lawes, D. J., Analogue signal handling, Microcomputers and Laboratory Instrumentation, Plenum Press, (1988), pp.55 – 56.

[22] Flody, T. L., Pulse response of reactive circuits, Electronics Fundamentals, Prentice Hall, (1998), pp.586 – pp.590.

[23] Malcolme-Lawes, D. J., Analogue signal handling, Microcomputers and Laboratory Instrumentation, Plenum Press, (1988), pp.38 – 39

[24] Wobschall, D., Operational amplifiers, Circuit Design for Electronic Instrumentation, McGraw-Hill Book Company, (1987), pp.16.

[25] Horowitz, P. and Hill, W., Digital meets analogue, The Art of Electronics, Cambridge University Press, (1980), pp.418.

[26] Malcolme-Lawes, D. J., Digital signal handling, Microcomputers and Laboratory Instrumentation, Plenum Press, (1988), pp.91 – 92.

[27] Regtien, P. P. L., Digital-to-analogue and analogue-to-digital conversion, Instrumentation Electronics, Prentice Hall, (1992), pp314 – 316.

[28] Flower, K. R., Cooling, Electronic Instrument Design: Architecting for the Life Cycle, Oxford University Press, (1996), pp.365.

[29] Smith, S. D., Detector, Optoelectronic Devices, Prentice Hall, (1995), pp285.

[30] Flower, K. R., Cooling, Circuit design, Electronic Instrument Design: Architecting for the Life Cycle, Oxford University Press, (1996), pp.251-252.

CHAPTER FIVE

PRACTICAL INVESTIGATION

5.1 Introduction

Immunoassays are currently one of the most widely used biochemical methods. Applications include clinical analysis, drug monitoring and pesticides monitoring in drinking water.

Flow injection immunoassay, a variation of immunoassays, consists of flow injection analysis (FIA) and immunoassays. FIA is a method, which involves injecting a sample directly into an unsegmented flow stream. There are five main components, i.e. a propelling unit, an injection system, a length of tubing, a flow cell and a detector. Immunoassay is a powerful means of determining a broad spectrum of substances of interest in biochemistry, using the specific characteristics of antibody (Ab) and antigens (Ag). Using a labelled antibody (Ab*) or a labelled antigen (Ag*) in a given solution, it is possible to determine an unknown amount of antigen or antibody. There are two main formats of immunoassays, competitive assays and non-competitive assays. A further subgroup includes heterogeneous and homogeneous based assays. A heterogeneous assay requires a separation step of free from bound, and a homogeneous assay does not require a separation step.

Practical investigations were carried out using the NFDS. These included determining the limit of detection of the NFDS using NF in 0.50M Tris buffer (pH 8.8), containing 2.5% (w/v) CHAPS, excited by a 635 nm laser diode. Cy5 in 0.50 M Tris buffer (pH 8.8), excited by a 645 nm laser diode. Cy5.5 in 0.5M Tris buffer (pH 8.8), excited by a 670 nm laser diode. A comparison with a commercial instrument, the Hitachi F4500 was undertaken to measure the detection limit of Cy5 in 0.50M Tris buffer (pH 8.8). The development of an assay for the α-interferon was carried out using the NFDS.

5.2 Flow Injection Immunoassays

Flow injection techniques coupled to immunoassays can be termed as flow injection immunoassay, which has many advances in their recent applications [1 - 4] for the development of analytical protocols.

5.2.1 Principle of Flow Injection

The term 'flow injection analysis' (FIA), was first used by Ruzika and Hansen in 1975 [5], which described the use of sample injection directly into an unsegmented flowing stream for rapid continuous – flow analysis. FIA is now widely used and well characterised; its simple basis, relatively inexpensive equipment and ease of result generation that are excellent in view of the rapidity, accuracy and precision with which they are obtained. The critical features of FIA can be described as:

1. Unsegmented flow;
2. Direct injection;
3. Controlled partial dispersion;
4. Reproducible operational timing.

The fundamental scheme of an FIA system is in Figure 5-1

Figure 5-1. **Schematic diagram of a single line FIA manifold**

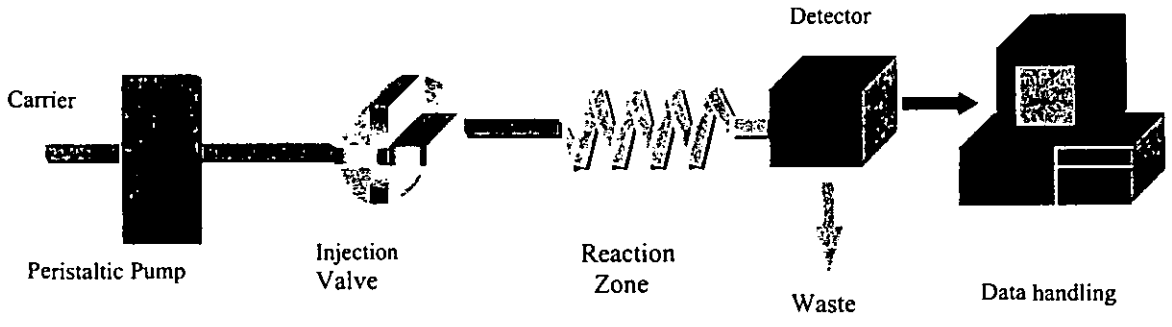

Usually, a FIA system consists of four components:

a. A *propelling unit* which produces the flow of one or several solutions, either containing a dissolved reagent or merely acting as carriers. This function can be performed in various ways, for example by a pump, a gas-pressure system or even gravitation.

b. An *injection system* which allows the reproducible insertion or introduction of an accurately measured sample volume into the flow without stopping it.

c. A *length of tubing,* along which the transport operation takes place, this is referred to as the reactor. Dispersion of the sample plug into the carrier or reagent takes place as the plug passes along the tube, also there may be chemical reactions occurring.

d. A *flow cell,* accommodated in a detector (e.g. photometer, fluorimeter, colorimeter) which transduces some property of the analyte into a continuous signal to a recorder or a PC with data handling package.

The flow emerging from the sensing system usually goes to waste, although it is sometimes recirculated through the peristaltic pump to achieve greater constancy of flow rate. The signal obtained from FIA techniques is transient. A typical FIA peak is shown in Figure 5-2.

Figure 5-2 **A typical FIA peak**

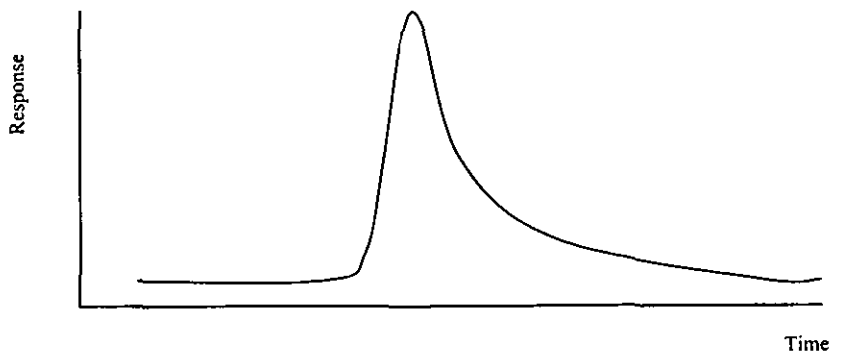

The parameters of the peak shape are affected by;

a. The flow rate of the carrier;

b. The volume injected along with the length and bore of the sample;

c. The length and bore of the manifold;

d. The viscosity of the sample and carrier;

e. The detector and recording system time constant.

5.2.2 Fundamental of Flow Injection Analysis

In FIA, immediately after injection through the sampling valve, a sample zone is formed in the flow injection apparatus which has a rectangular concentration profile. As it moves through the tubing, band broadening or *dispersion* takes place, if the sample *dispersion* is due to convection, the flow profile is characterised by a parabolic head and tail. This type of flow is called *laminar flow*, and is characteristic of most flow injection systems. If this were the only mass transport process operating, the peak would have an infinitely long tail, as the velocity at the walls of the tubing is zero. Two additional mass transport processes are operating though; molecular diffusion in the longitudinal direction (parallel to the direction of flow) and molecular diffusion in the radial direction (perpendicular to the direction of flow). The longitudinal diffusion is small compared with the dispersion due to the flow velocity and can be ignored under the conditions of most flow injection experiments. Radial diffusion moves sample molecules to and from the tubing walls, where the radial flow velocity profile is zero towards the centre of the tube, where the mass flow velocity is at a maximum. The net result of radial diffusion is that a peak with a finite peak width is obtained. Radial diffusion becomes more important as the residence time of the sample increases, at long residence times, primarily the radial diffusion process

controls the dispersion product process and the peak shape assumes a symmetrical *Gaussian* shape.

Dispersion ***D*** is defined by the equation

$$D = C_0/C \qquad (5\text{-}1)$$

Where: C_0 is the analyte concentration of the injected sample.

C is the peak concentration at the detector.

Dispersion is readily measured by injecting a dye solution of known concentration C_0 and then measuring the absorbance in the flow cell. After calibration, C is calculated from Beer's law. *Dispersion* is influenced by the three interrelated and controllable variables: sample volume, tube length, and pumping rate [6].

5.2.3 Principle of Immunoassays

Since the principle of immunoassays were first expounded by Rosalyn Yallow and Solomon Berson in 1959 [7], the technique has provided a powerful means of determining a broad spectrum of substances of interest, and has helped biochemists to understand many physiological, pathological and pharmacological processes. Immunoassays are based on a reaction between a target analyte and a specific antibody (Ab) they are widely used in biochemistry and play a key role in the laboratory. Their use for both qualitative and quantitative analysis has proved to be one of the most productive technological contributions to medicine, fundamental life science and even environmental monitoring, because of the combination of specificity, versatility, practicability and sensitivity.

Immunoassays derive their unique and specific characteristics from two important properties of *antibodies* [8], firstly an unparalleled specificity for the substance to which they bind and secondly the strength of the bond once formed. Examples of other substances with specific binding properties (i.e. molecular recognition) include enzymes, lectin, transport proteins and cell surface receptors. However, the most commonly used binding proteins presently used in immunoassays are antibodies, both monoclonal and polyclonal which bind specifically to a target molecule, known as an antigen.

Antigens are substances which are foreign to the animal in which they have been introduced, once introduced they will cause the animal to produce an immune response resulting in the production of antibodies, termed an antigenic response. Small molecules like peptides and drugs do not themselves initiate antibody production, but can be made to do so by coupling them to macromolecule carriers (i.e. proteins or synthetic peptides) before injecting them into the animal. These small molecules are known as haptens.

The principles of immunoassays are quite simple and are based largely on the reversible non-covalent interaction between an antigen (and hapten) with its specific binding partner, e.g. antibodies.

$$\mathbf{Ag + Ab \rightleftarrows Ag\text{-}Ab} \qquad (5\text{-}2)$$

Ab = antibody.

Ag = antigen.

Ag-Ab = antibody-antigen complex.

In most formats this binding can not be detected directly since there are no easily measured changes in the properties of either the Ag or Ab. Immunoassays overcome this

limitation by incorporating a label with some measurable property (e.g. fluorescence, radioactivity) through which the reaction can be followed.

If the label is covalently attached to the antigen such that it does not block the antigen region recognised by antibody, the presence of the label will not significantly perturb the binding of labelled antigen (Ag*) to antibody. Therefore in the situation in which a mixture of labelled (Ag*) and unlabelled (Ag) antigen react with antibody, competition for the antibody binding site occurs:

$$Ag + Ag^* + Ab \rightleftarrows Ag\text{-}Ab + Ag^*\text{-}Ab \qquad (5\text{-}3)$$

Where: Ag* = labelled antigen

By using a labelled antigen (Ag*), it is possible to determine an unknown amount of antigen in a given solution. The above reaction, known as a competitive binding reaction or competitive immunoassay is normally allowed to attain equilibrium, where the binding sites of the antibody are saturated with Ag* and Ag in proportion to their relative concentration in the assay solution. The antibody bound and unbound forms of the antigen are separated and the amount of signal generated by the label in the bound fraction plotted as a function of unlabelled antigen concentration. The concentration of Ag in an unknown sample may thus be determined from a competitive binding reaction with known amounts of labelled antigen and antibody, the antigen content subsequently being determined from a calibration curve.

Conversely, it is also possible to label the antibody rather than the antigen.

$$Ag + Ab^* \rightleftarrows Ag\text{-}Ab^* + Ab^* \qquad (5\text{-}4)$$

Where: Ab* = labelled antibody

Therefore, immunoassays may be classified as:

- Antibody capture assays.
- Antigen capture assays.
- Double antibody sandwich assays.

Based on the methodology employed. These include:

- Antibody excess.
- Antigen excess.

} Non-competitive

- Antibody competition.
- Antigen competition.

The competition assays use a limited amount of reagent.

5.2.3.1 Competitive Immunoassays

Competitive assays are based on competition between a labelled standard (antigen or antibody) and the analyte in the sample for the binding partner as shown in Figure 5-3. In order to facilitate this competition, a limited amount of reagent is used, i.e. coating antibody or antigen. If the concentration of coating antibody is too high then all antigen, labelled and unlabelled will be bound at equilibrium and variation in antigen in the sample is not detected.

Figure 5-3 **Competitive immunoassay (reagent-limited)**

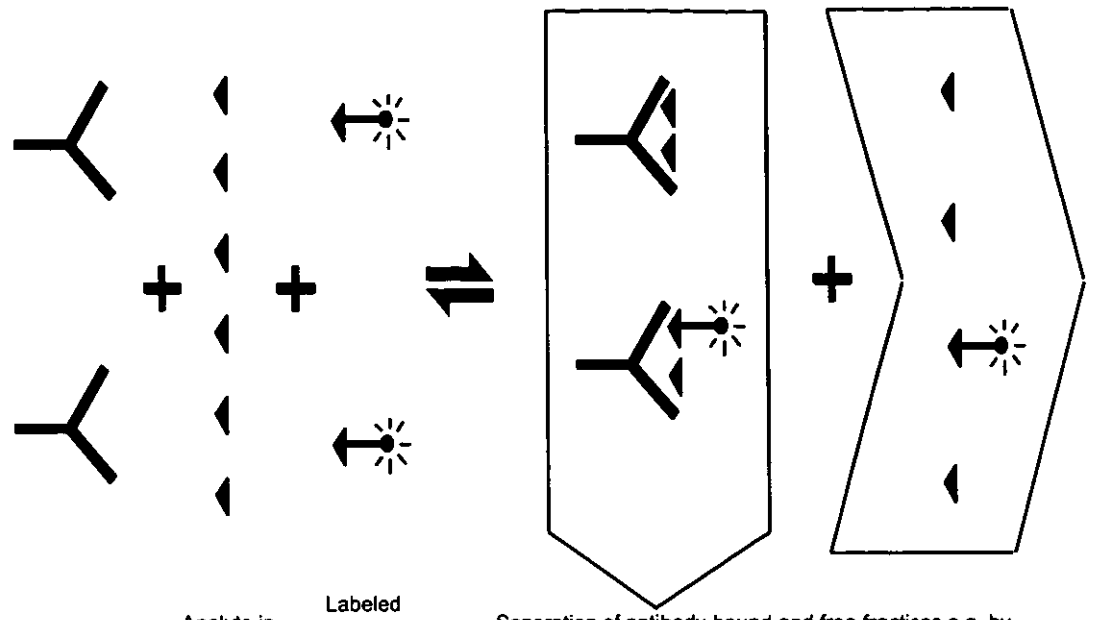

Figure 5-4 **Antibody Excess Immunometric Assay.**

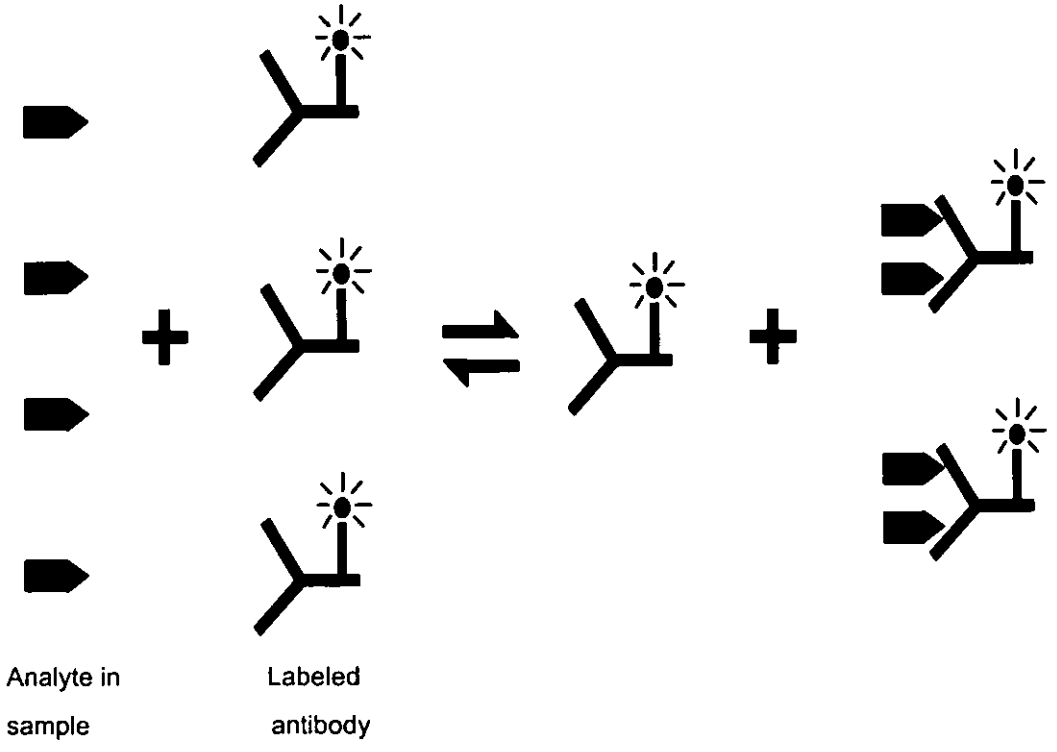

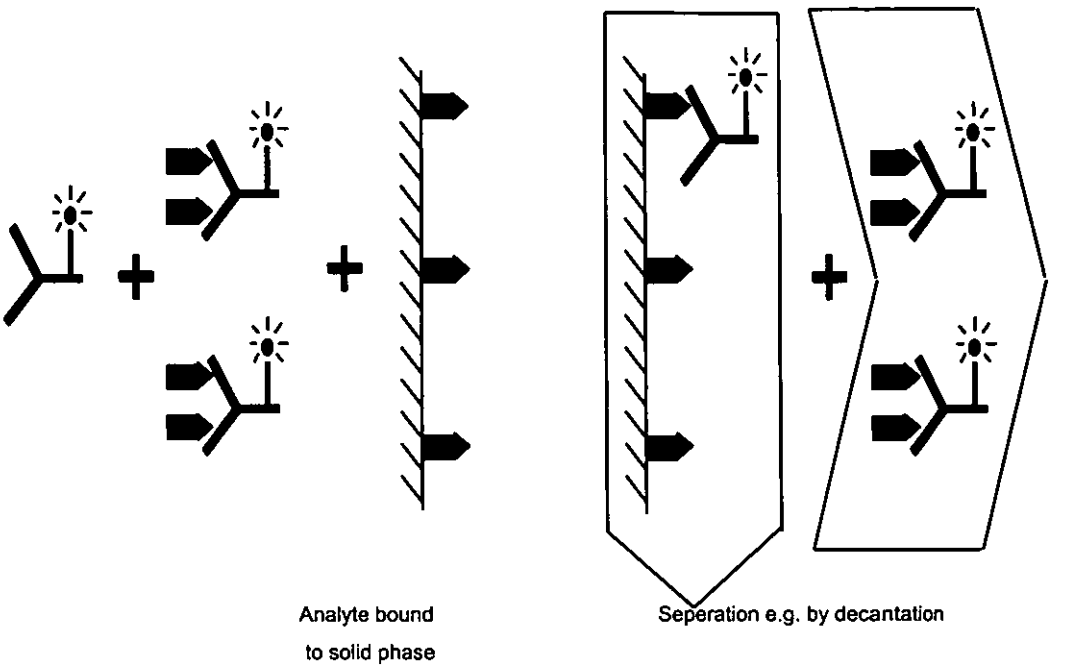

With competitive assays there is an inverse relationship between the concentration of analyte in the sample and the resulting label signal as shown in shown in Figure 5-5.

Figure 5-5 **Competitive assay response plot**

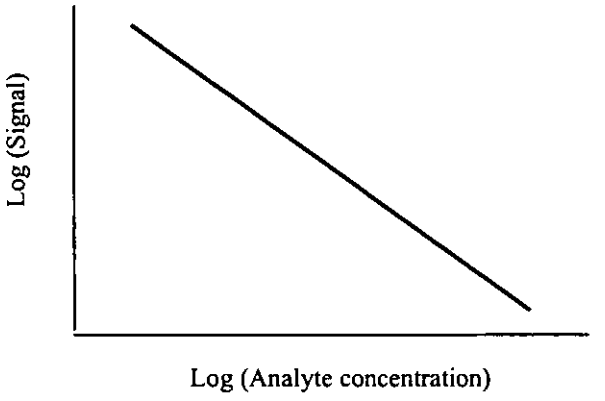

5.2.3.2 Non-competitive Immunoassays

Non-competitive or immunometric assays are the most commonly employed format, they use excess of coating reagent so that all analyte is bound at equilibrium. The presence of analyte is then quantified using a secondary labelled antibody and in these assays the concentration of analyte is directly proportional to the label signal observed, as shown in Figure 5 - 6.

Figure 5-6 **Non-competitive assay response plot**

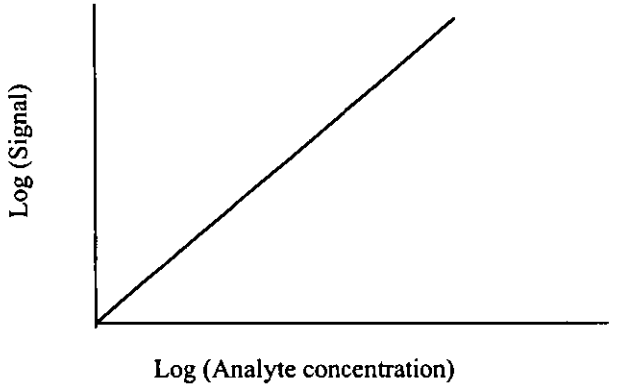

Immunoassays can also be considered on the basis of whether a separation step is necessary to remove antibody-bound from unbound materials.

5.2.3.3 Heterogeneous Immunoassay

Heterogeneous Immunoassay requires a step in the procedure to separate free from antibody bound antigen, although the separation step may be time-consuming and labour-intensive, it removes interfering substances from the sample before measurement takes place. Many separation techniques have been applied in this area, of these column separation has been used in this research [9].

There are many referenced approaches to immunoassay including the traditional radioimmunoassay; immunometric assay with a radioactive label (IRMA); enzyme

immunoassay, such as immunoassay with an enzyme label (IEMA); enzyme-linked immunosorbent assay (ELISA); fluorescence immunoassay, such as particle concentration fluorescence immunoassay (PCFLIA) and flow injection immunoassays (FIIA) [10-11]; and time-resolved fluoroimmunoassay. These techniques have been well reviewed in Daniel W. Chan's Immunoassay Handbook [12].

In practice, there are problems associated with fluorescence measurements. Firstly, endogenous fluorophores, i.e. bilirubin and proteins, can increase the non-specific background fluorescence and reduce the sensitivity of fluorescence immunoassay. Secondly, light scattering by high concentrations of protein, lipid, and other particles in serum will reduce the fluorescence signal. Finally, quenching due to the non-specific binding of albumin and the interaction with other specific quenching species may change the quantum yield of the fluorescence. A number of steps can be taken to minimise the interference in the biological sample, such as sample pre-treatment, washing and separation of other interference, and careful selection of a filter.

An important function of heterogeneous fluoroimmunoassay is the removal of endogenous fluorescent compounds and interfering substances from sample prior to the detection step. In fact, the basis of heterogeneous fluoroimmunoassay can be described that after the antigen/hapten-antibody reaction has occurred, the antibody bound and unbound fractions are separated on some form of solid-phase reactor incorporated into the flow injection analysis manifold. The bound fraction is eluted from the reactor using a change of conditions (pH, ionic strength, etc.) and the reversal of this change regenerates the reactor prior to the injection of the next sample. Heterogeneous fluoroimmunoassay can take many forms, involving off-line, on-line and on reactor incubation, a range of possible fluorescent labels etc. It is convenient to

create the flexibility of the flow injection approach that can readily accommodate these numerous variants, usually by means of a simple and robust flow manifold.

Furthermore, an automated heterogeneous immunoassay offers many advantages; they are more sensitive, especially for large proteins, less prone to interference, and extremely flexible to the point of choosing the detection principle and solid phase. Methods have been reported using automated flow injection instrument coupled the high sensitive fluorescence detector [13 – 14].

5.2.3.4 Homogeneous Immunoassays

Homogeneous immunoassays do not require a separation step of the free analyte from the antibody bound fraction of the analyte. Separation of the components of the immunoassay is not required because the assay employs a label whose properties are altered in the bound and unbound states. These assays generally have shorter incubation times, are simpler to perform due to elimination of the physical separation of bound from unbound antigen and as a direct consequence of this are easier to automate than heterogeneous assays. Either the EIA or the fluorescence immunoassay format is frequently used [15 - 16].

There are a number of approaches to homogeneous immunoassay including enzyme immunoassay system (EIA) that is in contrast to heterogeneous EIA. Enzyme-multiplied immunoassay technique (EMIT), which are used primarily for small molecules, i.e. drugs, the antigen is labelled with an enzyme. Fluorescence immunoassay including fluorescence polarisation immunoassay (FPIA), substrate labelled fluoroimmunoassay (SLFIA) [17].

5.3 Preliminary Tests

Several fluorophores have been measured for preliminarily testing when the NFDS was established and constructed in the laboratory.

In order to test the NFDS, naphthofluorescein (NF) was chosen as a fluorescence dye model and a 635 nm, laser diode with the output power 2 mW was selected as an excitation source. The absorbance maximum for NF is 595 nm which is not compatible with the laser source used. However on addition of certain compounds, i.e. CHAPS and hydroxy propyl β-cyclodextrin, the absorbance maximum for NF can be red shifted in wavelength. Furthermore, the shift of absorbance maximum is varied with the type of the compounds and the pH value. The following experiments show the response of NF in Tris buffer (pH 9.0) with CHAPS and hydroxy propyl β-cyclodextrin. The output from the NFDS was measured in millivolts using a digital multimeter (RACALL-DANA 4009). The output for NF solutions with and without CHAPS and hydroxy propyl β-cyclodextrin (HPB.Cyd) are shown in Table 5-1 and Figure 5-7.

Table 5-1 **Responses of NF in Tris buffer (pH 9.0) with HPB.Cyd, with and without CHAPS using the NFDS with the RACALL-DANA 4009 multimeter**

Conc. (M)	Resp1 (Volt)	Resp2 (Volt)	Resp3 (Volt)	Log10Conc. (M)	Ln10 Resp1 (Volt)	Ln10 Resp2 (Volt)	Ln Resp3 (Volt)
Blank	0.000	0.000	0.000				
9.25×10^{-9}	0.005	0.017	0.023	-8.03386	-5.29832	-4.07454	-3.77226
1.85×10^{-8}	0.010	0.044	0.032	-7.73283	-4.60517	-3.12357	-3.44202
4.63×10^{-8}	0.036	0.103	0.082	-7.33489	-3.32424	-2.27303	-2.50104
9.25×10^{-8}	0.048	0.132	0.106	-7.03386	-3.03655	-2.02495	-2.24432
1.85×10^{-7}	0.134	0.276	0.312	-6.73283	-2.00992	-1.28735	-1.16475
4.63×10^{-7}	0.208	0.660	0.755	-6.33489	-1.57022	-0.41552	-0.28104
9.25×10^{-7}	0.568	1.371	1.449	-6.03386	-0.56563	0.31554	0.370874
1.85×10^{-6}	1.048	3.132	2.622	-5.73283	0.04688	1.141672	0.963937

Note: Conc. – the concentration of NF, Resp1 – the response in Tris buffer pH 9.0, Resp2 – the response in Tris buffer pH 9.0 + HPB.Cyd, Resp3 – the response in Tris buffer pH 9.0 + CHAPS. The speed of laser pulse in the NFDS was set around 50KHz.

Figure 5-7 **Calibration curves for NF using the NFDS**

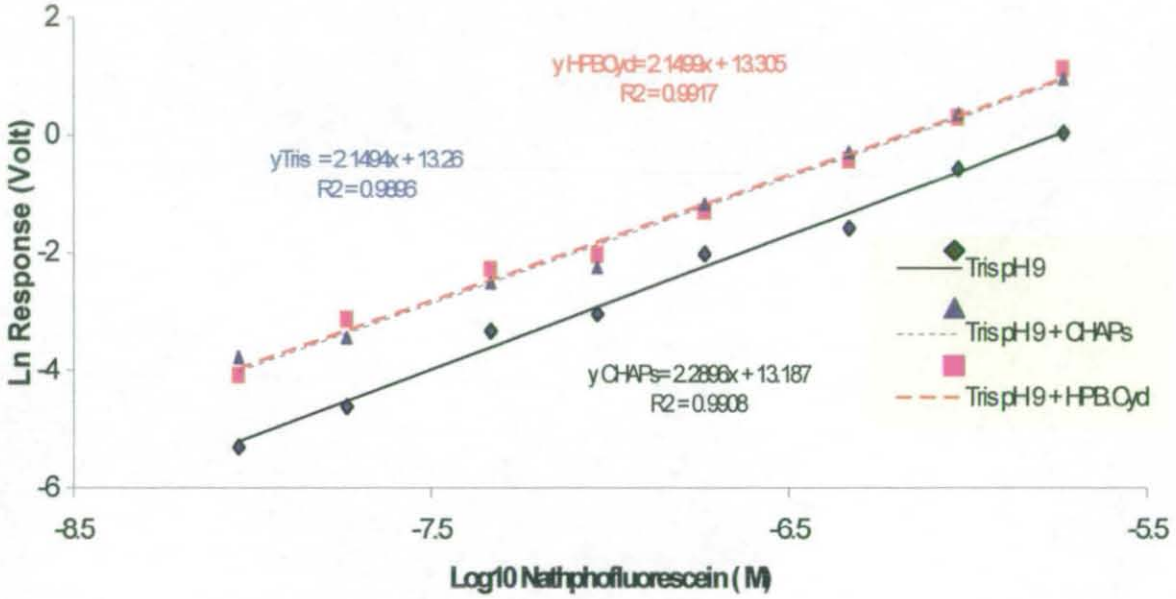

Using Tris buffer pH 9.0, the fluorescence intensity of NF was enhanced with CHAPS compared to NF without CHAPS, and slightly lower than hydroxy propyl β-cyclodextrin.

The following assay method was used for the determination of NF using a Perkin Elmer LS50 luminescence spectrofluorimeter (LS50) and the NFDS. 100 µl of NFMP (naphthofluorescein monophosphate) (50 µg/ml) was added to 20 µl of alkaline phosphatase (10 µg/ml) and the volume made up to 2.0 ml with 0.05M Tris buffer (pH 9.0) containing 2.0% (w/v) CHAPS. The mixture was then incubated at 22°C for 20 mins. The fluorescence spectrum of the hydrolysis product NF was measured using a LS50 over the range 650 – 840 nm with the excitation monochromator set at 635 nm

(i.e. the excitation maxima of NF in the presence of CHAPS). The above procedure was repeated with the inclusion of varying amounts of theophylline over its therapeutic range (0-18 μg/ml) in the incubation mixture. The inhibition of alkaline phosphatase activity by theophylline is shown in Figure 5-8.

Figure 5-8 **Inhibition of alkaline phosphatase by increasing concentration of theophylline 20 minute incubation at 22 ^{0}C**

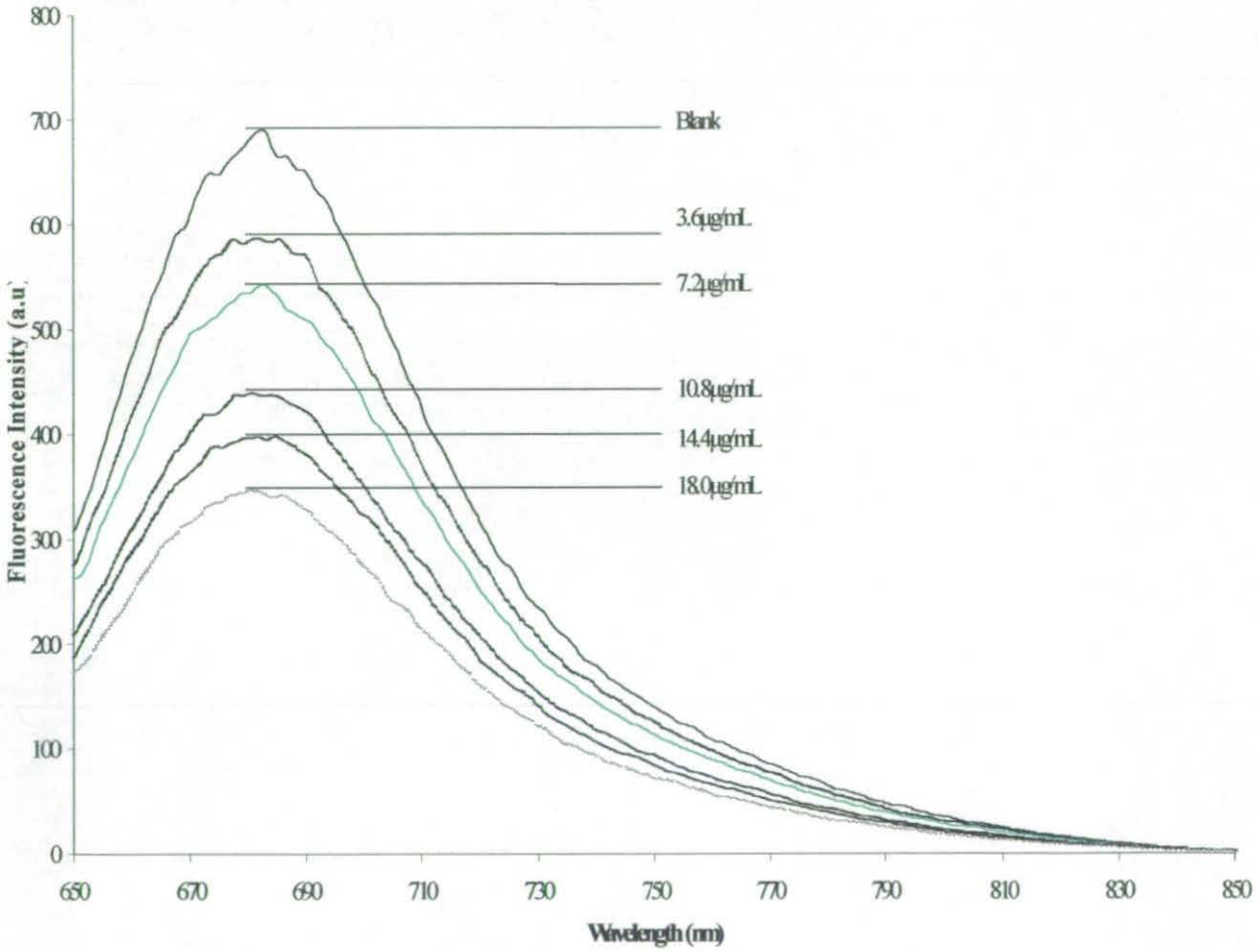

Note: a.u is arbitrary unit.

Figure 5-8 shows the trend that a decrease of fluorescence intensity occurs with an increase in the concentration of theophylline over a 20-minute incubation at 22^{0}C. The above results of assay were in Table 5-2 and replotted as a calibration curve in Figure 5-9.

Table 5- 2 **Response of theophylline inhibition assay using the Perkin Elmer LS50 luminescence spectrofluorimeter**

Sample No.	Theophylline ($ugml^{-1}$)	Fluorescence intensity (a.u)
1	0.0	692.0
2	20	587.7
3	40	543.5
4	60	439.7
5	80	397.6
6	100	346.8

Note: The data of fluorescence intensity are mean values; a.u is arbitrary unit.

Figure 5-9 **Calibration curve for theophylline inhibition assay using the Perkin Elmer LS50 luminescence spectrofluorimeter**

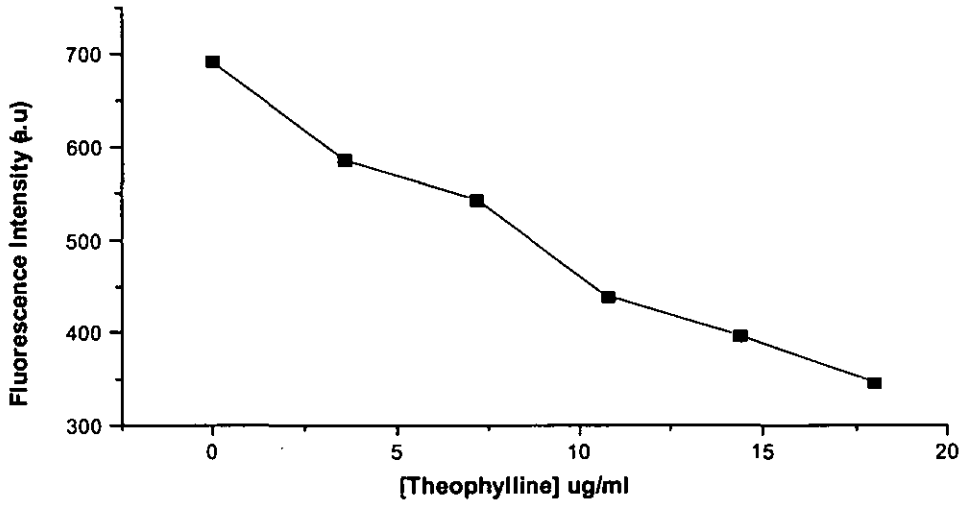

The above assay was then repeated using the NFDS. The results are in Table 5-3 and shown in Figure 5-10.

Table 5- 3 **Response of theophylline inhibition assay using the NFDS**

Sample No.	Theophylline ($ugml^{-1}$)	Response (Volt)
1	0.0	0.708
2	20	0.690
3	40	0.668
4	60	0.603
5	80	0.446
6	100	0.370

Note: The data of fluorescence response are mean values. The speed of laser pulse in the NFDS was set around 50KHz.

Figure 5-10**Calibration curve for theophylline inhibition assay using the NFDS**

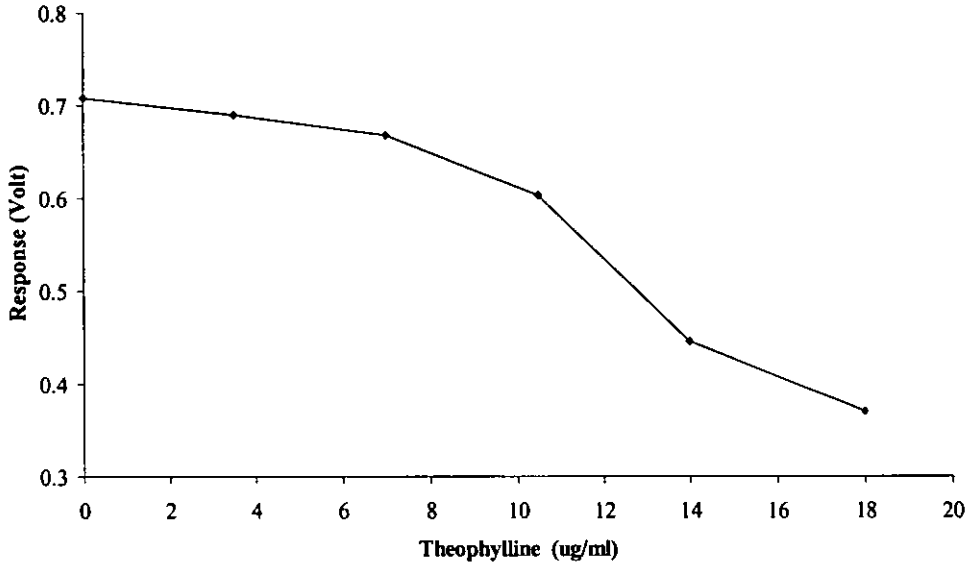

Figure 5-9, Figure 5-10, Table 5-2 and Table 5-3 demonstrate a comparative assay model based on the inhibition of alkaline phosphatase by a drug (theophylline) using NF, and different detection systems.

These two figures also indicate the difference of fluorescence response using the same assay but different detection systems. The variation of fluorescence intensity between 2.5 μgml^{-1} and 10 μgml^{-1} is about 35% using a LS50 and is about 15% using the NFDS. The difference can be explained in that the LS50 is a commercial instrument, which has been fully optimised and the NFDS was preliminarily established without any optimisation. However, the NFDS was optimised to carry out further experiments using the selected dyes (see Section 5.4 and Section 5.5).

5.4 Comparative Tests

The reliability and acceptability of chemical analysis measurements depends upon rigorous completion of all requirements stipulated in a well-defined protocol; the protocol should describe procedures, sample preparation and storage and analytical measurement, calculation and comparison.

In order to compare the NFDS with the commercial detectors, Cy5 monofunctional dye (Cy5) was prepared at concentrations between 2.3×10^{-8}M and 2.3×10^{-12}M using Tris buffer (pH 8.8). These Cy5 dilutions were firstly measured with the Hitachi F-4500 fluorescence spectrophotometer. The blank sample used in the experiment was Tris buffer (pH 8.8). The following spectral profile of Cy5 in Tris buffer (pH 8.8) between 640 nm and 700 nm shows the detection limit using the Hitachi F-4500 fluorescence spectrophotometer.

Figure 5-11 **Response of Cy5 in Tris buffer (pH 8.8) using the Hitachi F-4500 fluorescence spectrophotometer**

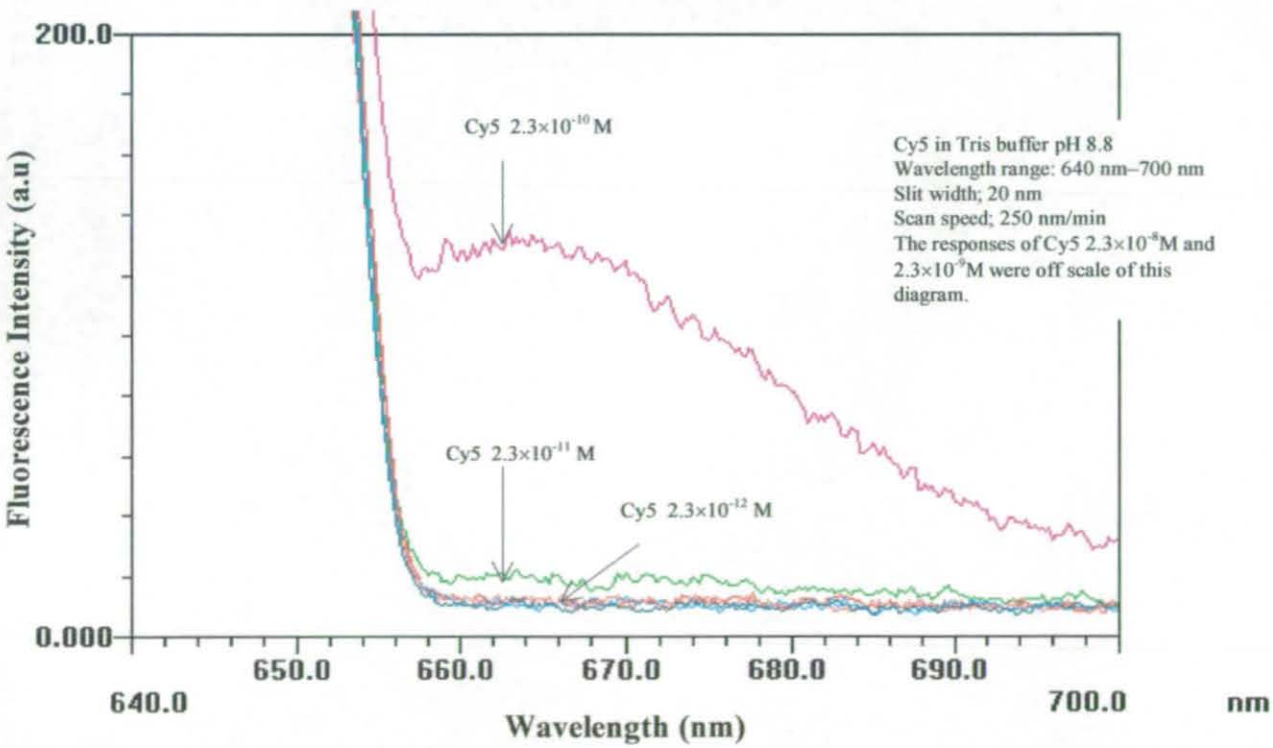

Note: a.u is arbitrary unit.

When Cy5 was excited with a 645 nm laser diode, the emission wavelength was found to be around 670 nm as described in Chapter 3. However, when the Xenon lamp in the Hitachi F-4500 fluorescence spectrophotometer was used to excite low concentrations of Cy5 in Tris buffer (pH 8.8) at 645 nm, the emission spectra was found have a peak at 662.6 nm. Table 5-4 lists the data of Cy5 in Tris buffer (pH 8.8) using a 100 µl volume flow cell and the Hitachi F-4500 fluorescence spectrophotometer.

Table 5-4 **Response of various concentration of Cy5 in Tris buffer (pH 8.8) using the Hitachi F-4500 fluorescence spectrophotometer**

Titles	Intensity (a.u) @662.6 nm	Actual Intensity (a.u) @662.6 nm	Log 10 Cy5 [M]	Log 10 Actual Intensity(a.u)
Deionised Water	14.02			
Tris Buffer pH:8.8	8.767			
Cy5 2.3×10^{-12} M	11.07	2.303	-11.6364	0.362294
Cy5 2.3×10^{-11} M	11.95	3.183	-10.6364	0.502837
Cy5 2.3×10^{-10} M	18.30	9.533	-9.63639	0.97923
Cy5 2.3×10^{-9} M	128.1	119.3	-8.63639	2.07664
Cy5 2.3×10^{-8} M	2269	2260.3	-7.63639	3.54166

Note: a.u is arbitrary unit; the speed of laser pulse in the NFDS was set around 50KHz;

Figure 5-12 **Calibration curve of Cy5 response in Tris buffer (pH 8.8) using the Hitachi F-4500 fluorescence spectrophotometer**

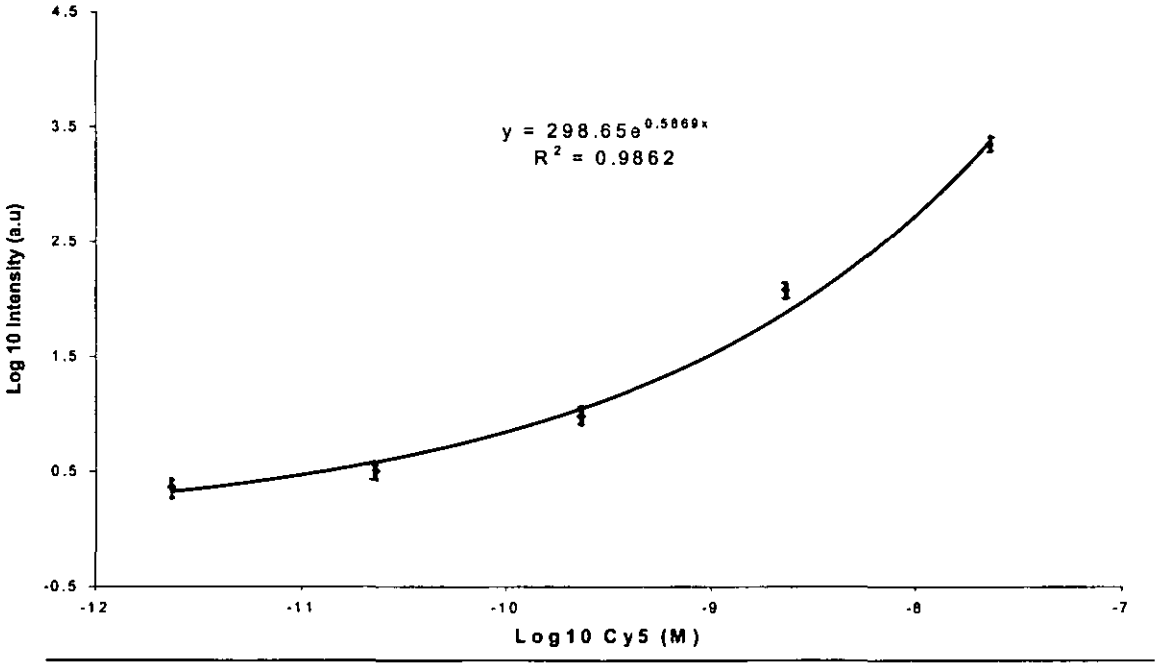

In Table 5-4, the detection limit for Cy5 in Tris buffer (pH 8.8) using the Hitachi F4500 fluorescence spectrophotometer was 2.31×10^{-10} M according to the ratio of signal-to-noise 2. The curve in Figure 5-11 also shows the trend of flattening below the concentration of Cy5 2.3×10^{-10} M, and it is not linear because the (R^2) between 2.3×10^{-12} M and 2.3×10^{-8} M was 0.9862. These two factors were worse than expected for routine analysis. These results expressed the Hitachi F-4500 fluorescence spectrophotometer was not suitable to detect low concentration of Cy5, i.e. below 2.3×10^{-10} M.

Using same dilutions of Cy5 in Tris buffer (pH 8.8), results were obtained for the NFDS, the data is shown in Table 5-5.

Table 5-5 **Response of various concentrations of Cy5 in Tris buffer (pH 8.8) using the NFDS**

Title	Response (mV)	Actual Response (mV)	Log10 Cy5 [M]	Log10 Actual Response (mV)
Tris Buffer pH:8.8	0.0			
Cy5 2.31×10^{-12} M	2.5	2.5	-11.6364	0.3979
Cy5 2.31×10^{-11} M	8.5	8.5	-10.6364	0.9294
Cy5 2.31×10^{-10} M	28	28	-9.63639	1.4472
Cy5 2.31×10^{-9} M	363	363	-8.63639	2.5599
Cy5 2.31×10^{-8} M	2326.3	2326.3	-7.63639	3.3667

Note: mV is millivolt; the speed of laser pulse in the NFDS was set around 50KHz.

The NFDS was connected to a RACALL-DANA 4009 digital multimeter from where readings were taken, the NFDS contained a 100 µl volume flow cell, a 665 nm cut off filter and a 645 nm laser diode with the output power 2 mW.

Since the zero reading in the multimeter was able to adjust through the detection system, the background of Tris buffer (pH 8.8) was minimised to zero. After the

completion of measurement of Cy5 with Tris buffer (pH 8.8), the reading from the multimeter was still between 0.000 and 0.001 mV.

Figure 5-13 shows the linearity of Cy5 with Tris buffer (pH 8.8) using the NFDS.

Figure 5-13 **Calibration curve of response for Cy5 in Tris buffer(pH8.8) using the NFDS**

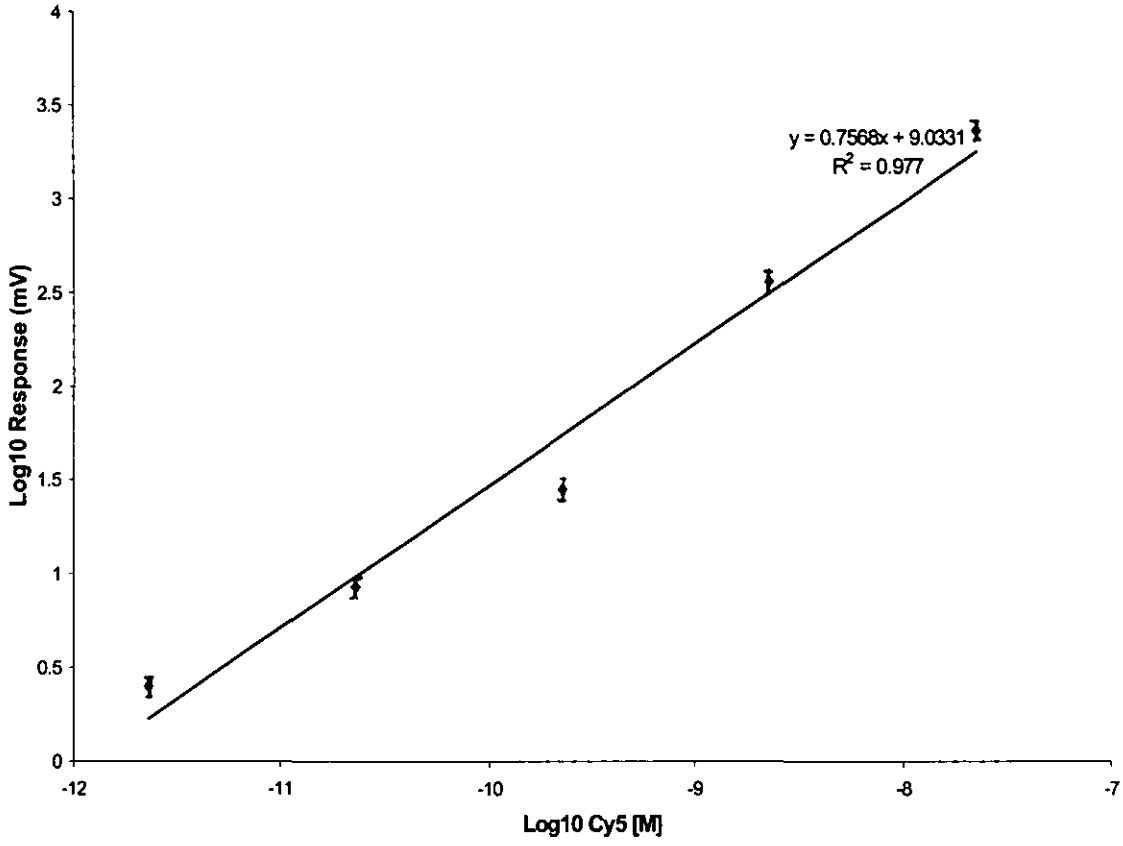

As a general rule, reliable signal detection becomes impossible when the signal-to-noise ratio becomes less than 3. From the data presented in Table 5-5 the detection limit for Cy5 in Tris buffer (pH 8.8) using the NFDS was found to be between 2.3×10^{-12} M and 2.3×10^{-11} M. The linearity (R^2) of Cy5 within the concentration range 2.3×10^{-12} M and 2.3×10^{-8} M was 0.977 which along with the sensitivity level compares favourably with the Hitachi F4500 fluorescence spectrophotometer.

5.5 Detection Limit of Novel Fluorescence Detection System

Further experiments were carried out to investigate the measurement of naphthofluorescein (NF) in Tris buffer (pH 8.8) and 2.5% (w/V) CHAPS, and Cy5.5 bisfunctional dye (Cy5.5) in Tris buffer (pH 8.8).

5.5.1 Nathphofluorescein Dye (NF)

Various dilutions of NF were prepared and measured using the NFDS with the RACALL-DANA 4009 digital multimeter, a 100 µl volume flow cell, a cut off filter of 650 nm and a 635 nm laser diode with the output power 2 mW. Table 5-6 shows the data collected and Figure 5-13 indicates the responses of various concentrations of naphthofluorescein using the NFDS.

Table 5-6 **Response of various concentrations of NF in Tris buffer (pH 8.8) using the NFDS**

Title	Response (mV)	Actual Response (mV)	Log10 NF [M]	Log10 Actual Response [mV]
Tris Buffer pH:8.8	-0.3			
NF 1.0×10^{-10} M	1.8	2.1	-10	0.32222
NF 1.0×10^{-9} M	6.5	6.8	-9	0.83251
NF 1.0×10^{-8} M	30.3	30.6	-8	1.48572
NF 1.0×10^{-7} M	169.7	170	-7	2.23045
NF 1.0×10^{-6} M	13336.	1333.9	-6	3.12512

Note: mV is millivolt; the speed of laser pulse in the NFDS was set around 50KHz.

During the measurement of NF in Tris buffer (pH 8.8) and 2.5% CHAPS, the NFDS was not modified. The reading from the RACALL-DANA 4009 digital multimeter was not able to adjust to a zero reading. However, the various range of background for Tris buffer (pH 8.8) was still within ±0.3.

Figure 5-14 **Calibration curve of NF response using the NFDS**

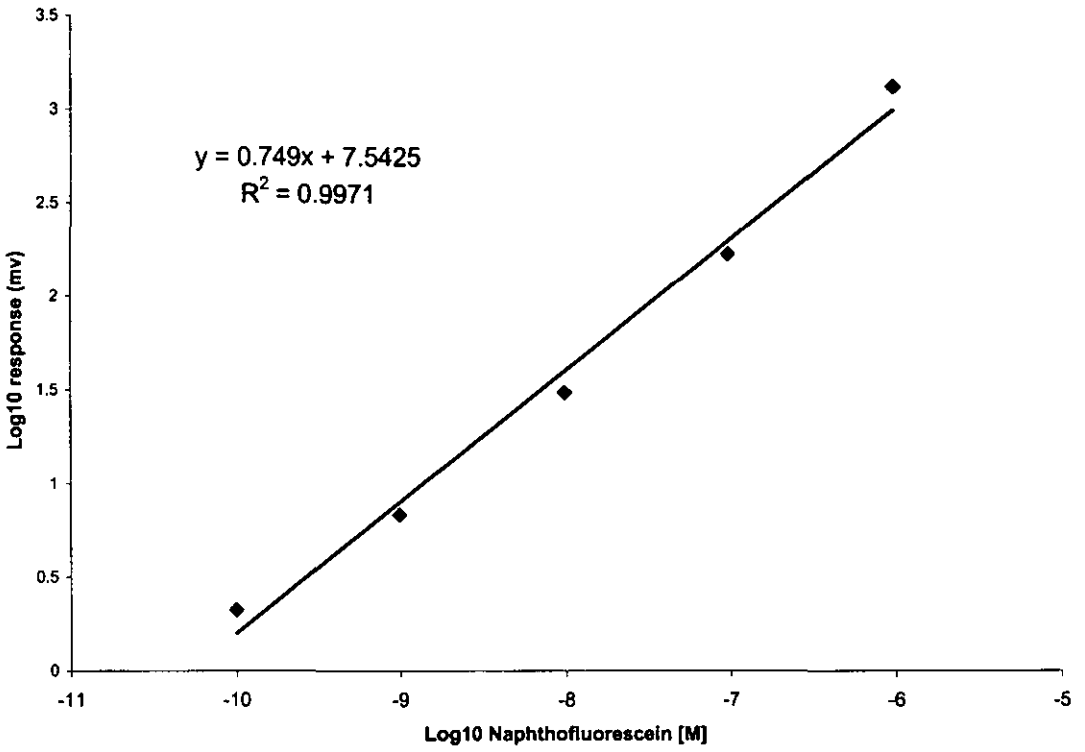

Figure 5-14 indicates the detection limit for NF in Tris·buffer (pH 8.8) and 2.5% CHAPS using the NFDS was between 1.0×10^{-10} M and 1.0×10^{-9} M. The linearity (R^2) of NF with Tris buffer (pH 8.8) and 2.5% CHAPS between the concentration range 1.0×10^{-10} M to 1.0×10^{-6} M was 0.9971.

5.5.2 Cy5 Monofunctional Dye (Cy5)

Various dilutions Cy5 in Tris buffer (pH 8.8) was carried out with the Global DAQ box and the FlowTEK data capture software (detailed in Chapter 4) using the NFD. The results were monitored on a PC.

Table 5-8 lists the data from the FlowTEK software and Figure 5-15 shows the linearity of the results for Cy5 in Tris buffer (pH 8.8).

Table 5-8 **Response of various concentrations of Cy5 in Tris buffer (pH 8.8) using the NFDS with the FlowTEK software**

Title	Response Area (a.u)	Actual Response Area (a.u)	Log10 Cy5 [M]	Log10 Actual Response [a.u]
Tris Buffer pH 8.8	0.1638			
Cy5 2.3×10^{-12} M	0.1906	0.0268	-11.6364	-1.57187
Cy5 2.3×10^{-11} M	0.4231	0.2593	-10.6364	-0.5862
Cy5 2.3×10^{-10} M	1.994	1.8302	-9.63639	0.262499
Cy5 2.3×10^{-9} M	17.3671	17.2033	-8.63639	1.235612
Cy5 2.3×10^{-8} M	122.9224	122.7586	-7.63639	2.089052

Note: a.u is arbitrary unit; the speed of laser pulse in the NFDS was set around 50KHz;

Figure 5-16 **Calibration curve of Cy5 in Tris buffer (pH 8.8) using the NFDS with the FlowTEK software**

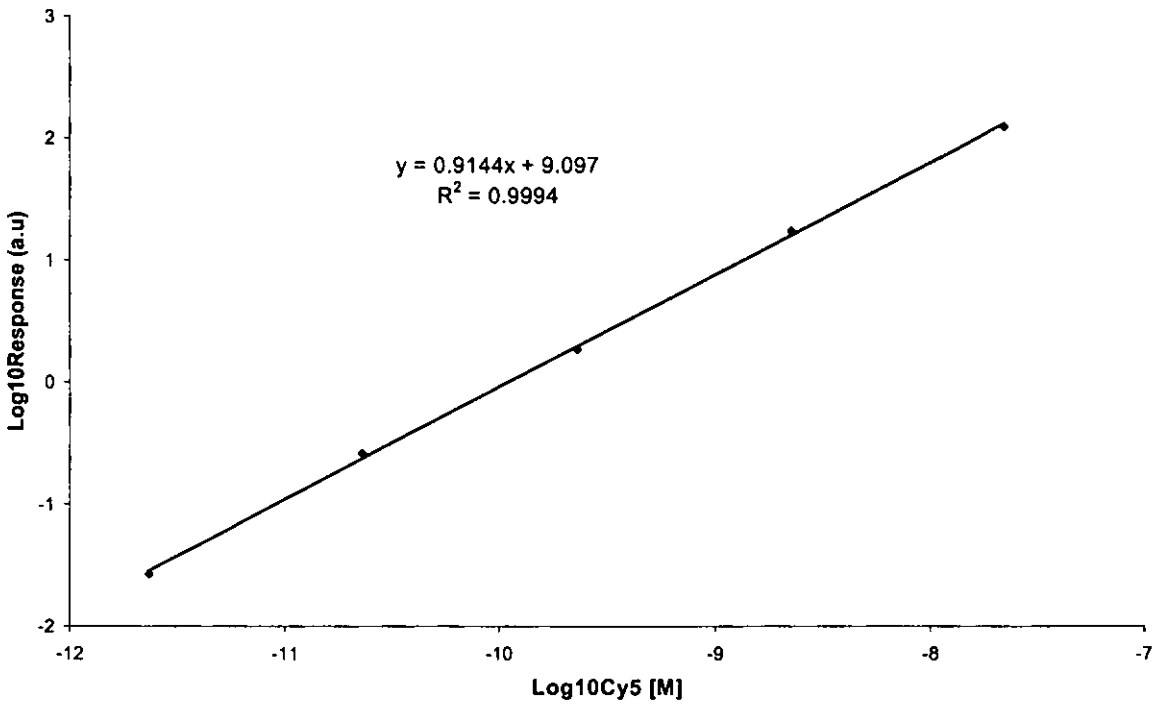

Figure 5-16 also indicates the detection limit for Cy5 in Tris buffer (pH 8.8) was 2.3×10^{-11} M, when using the NFDS with the Global DAQ box and the FlowTEK data capture software. The linearity (R^2) of Cy5 in Tris buffer (pH 8.8) between the concentration range 2.3×10^{-12} and 2.3×10^{-8} M was 0.9994. Since the ratio of signal to noise from the Global pre-amplifier was quite small when detecting low concentration

of Cy5 using the NFDS. The detection limit of Cy5 with Tris buffer (pH 8.8) using the NFDS with the Global DAQ box and the FlowTEK data capture software was lower than using the RACALL-DANA 4009 digital multimeter. However, the linearity using the FlowTEK data capture software was better than using the RACALL-DANA 4009 Digital Multimeter.

5.5.3 Cy5.5 Bisfunctional Dye (Cy5.5)

Another experiment of Cy5.5 in Tris buffer (pH 8.8) were prepared for testing detection limit using the NFDS including the RACALL-DANA 4009 digital multimeter as a reading, a 100 µl volume flow cell, a cut off filter of 695 nm and a 670 nm, 2 mW laser diode. Table 5-7 lists the data and Figure 5-15 shows the linearity of Cy5.5 measurement.

Table 5-7 **Response of various concentrations of Cy5.5 in Tris buffer(pH 8.8) using the NFDS**

Title	Response (mV)	Actual Response (mV)	Log10 Cy5.5 [M]	Log10 Actual Response [mV]
Tris Buffer pH:8.8	-0.2			
Cy5.5 6.2×10^{-13} M	0.10	0.12	-12.2048	-0.92080
Cy5.5 6.2×10^{-12} M	2.0	2.2	-11.2048	0.342423
Cy5.5 6.2×10^{-11} M	8.6	8.8	-10.2048	0.944483
Cy5.5 6.2×10^{-10} M	43.3	43.5	-9.20482	1.638489
Cy5.5 6.2×10^{-9} M	339.7	339.9	-8.20482	2.531351
Cy5.5 6.2×10^{-8} M	3058.8	3059	-7.20482	3.485579

Note: mV was millivolt; the speed of laser pulse in the NFDS was set around 50KHz.

Figure 5-15 **Calibration curve of response for Cy5.5 in Tris buffer (pH 8.8) using a NFDS**

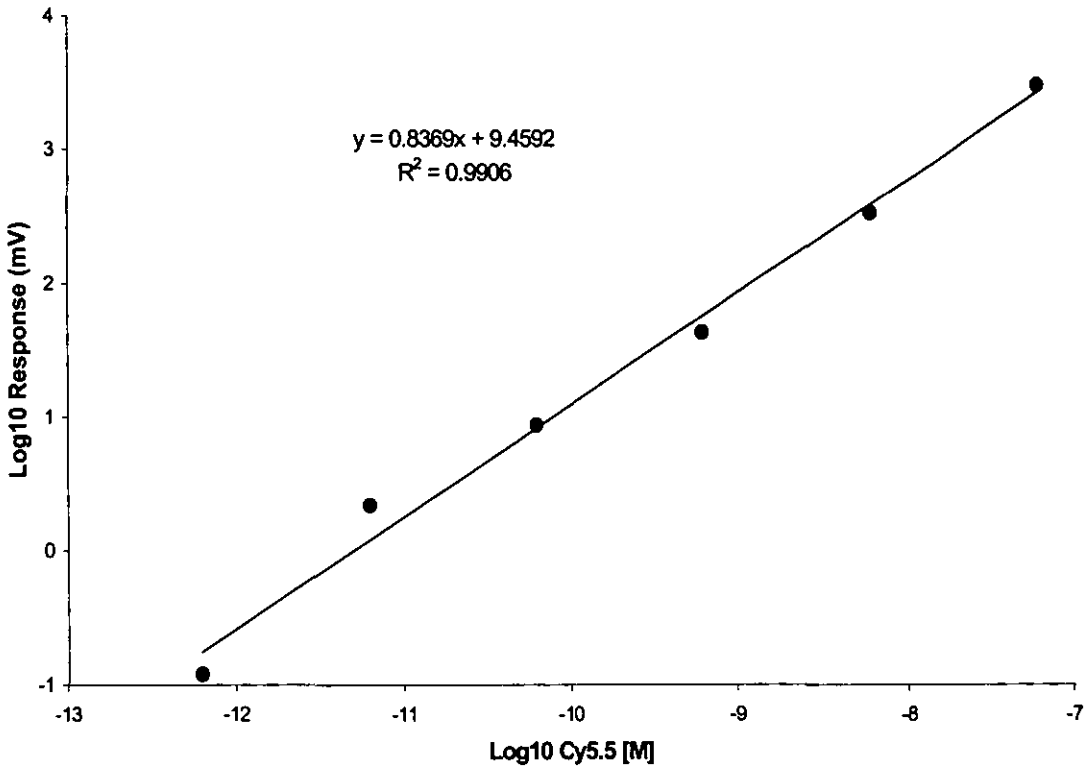

Figure 5-15 indicates the detection limit for Cy5.5 in Tris buffer (pH 8.8) using the NFDS was between 6.2×10^{-12}M and 6.2×10^{-11}M. The linearity (R^2) of Cy5.5 in Tris buffer (pH 8.8) between the concentration range 6.2×10^{-13}M and 6.2×10^{-7}M was 0.9906.

5.6 Practical Application for Flow Injection Immunoassay

A competitive spectrofluorimetric flow injection immunoassay (FIIA) for determination of the α-interferon based on a pre-incubation of the anti-α-interferon bovine antibody with the α-interferon and the α-interferon-Cy5 was developed using the NFDS with the FlowTEK data capture software.

The absorbance spectrum for the α-interferon in PBS buffer (pH 7.4) using the Hitachi U-2010UV-Vis spectrophotometer showed in Figure 5-16.

Figure 5-17 **Absorbance spectrum for α-interferon in PBS buffer (pH 7.4) using the Hitachi U-2010UV-Vis spectrophotometer**

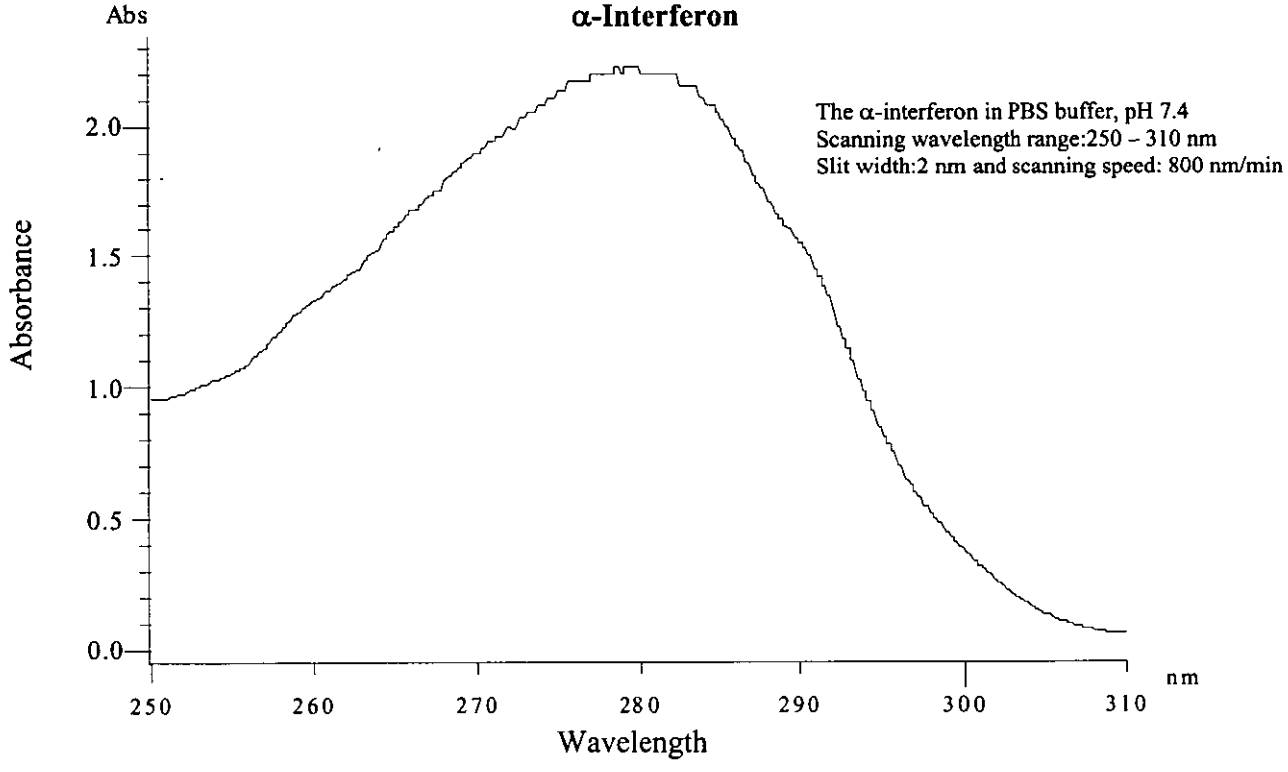

From Figure 5-17, the maximum absorbance of the α-interferon in PBS (pH 7.4) was 2.1 at 280 nm, far away from the excitation wavelength @ 649 nm and the emission wavelength @ 670 nm of Cy5. This did not cause interference when using Cy5 as labelling in a practical detection.

5.6.1 A Flow Injection Immunoassay (FIIA)

The α-Interferon stock material (3.39 $mgml^{-1}$) was diluted to 1.9 μgml^{-1}, 3.8 μgml^{-1}, 19 μgml^{-1}, 38 μgml^{-1}, 76 μgml^{-1} and 380 μgml^{-1} using Tris buffer (pH 8.8).

The α-interferon (41.5 $mgml^{-1}$) antibody (Ab) was diluted to 0.1 $mgml^{-1}$ using Tris buffer (pH 8.8).

The α-Interferon conjugated Cy5 was prepared at 0.032 $mgml^{-1}$, which was provided by one member of the research group.

Prior to measurement, a pre-incubation of the reactants was carried out as follows:

1. Transfer 475 µl of Tris buffer (pH 8.8) into the 3 ml volume standard test bottle.
2. Add 300 µl of 0.1$mgml^{-1}$ Ab.
3. Add 150 µl of conjugated solution (1:10 dilution in Tris buffer pH 8.8).
4. Add 25 µl of the α-Interferon standard solution.
5. Incubate at room temperature for 3 minutes.

The total volume of the test tube was 950 µl. Therefore when using the above α-interferon stock solutions the concentration of the α-Interferon in the test bottle can be worked out as below:

0.05 μgml^{-1}, 0.1 $\mu g\ ml^{-1}$, 0. 5 $\mu g\ ml^{-1}$, 1.0 $\mu g\ ml^{-1}$, 2.0 $\mu g\ ml^{-1}$and 10$\mu g\ ml^{-1}$.

The blank sample was 25 µl Tris buffer (pH 8.8) instead of the addition of the α-interferon stock solution, which the concentration of the α-interferon in the sample can be written as 0.00 μgml^{-1}, The adjustable column was packed with 140 µl POROS protein A beads (20 µm). A flow system for the determination of the α-Interferon is shown in Figure 5-18.

Figure 5-18 **Schematic of the generalised flow injection immunoassay configuration**

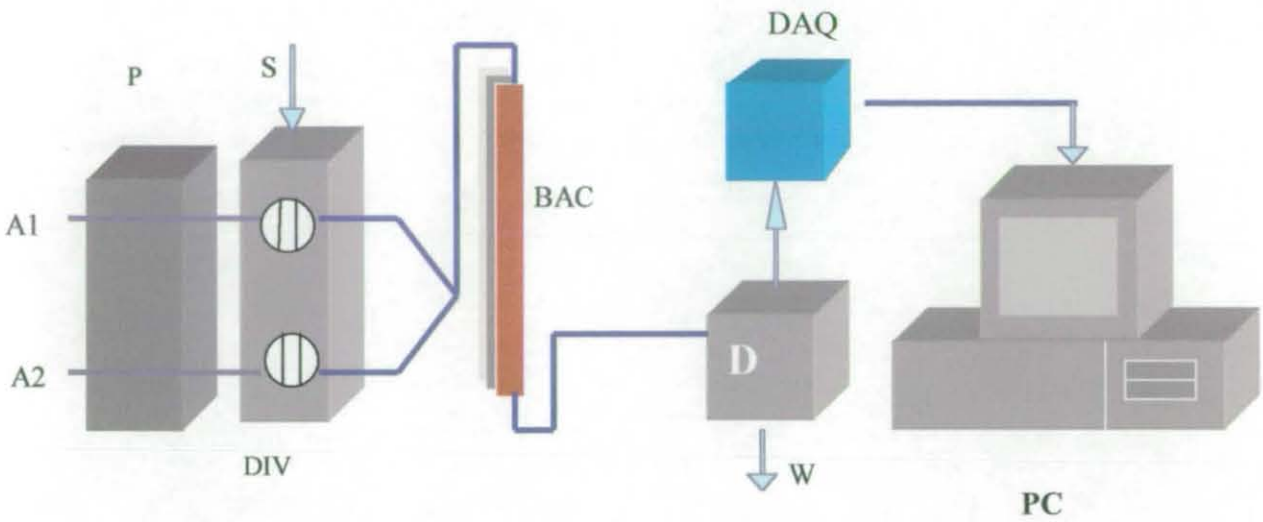

Notes: S, denotes sample; A1, Tris carrier buffer (pH: 8.8); A2, Citric acid elution buffer (pH: 2.5); P, peristaltic pump; DIV, dual injection valve; BAC, POROS protein A beads (20 microns) adjustable column; D, detector; W, waste; DAQ, FlowTEK DAQ interface card; PC, Personal computer with the FlowTEK data capture package.

The operational procedures can be described as follows:

The buffers (Tris and Citric acid) were introduced into the FI system by a peristaltic pump at a defined flow rate (1.30 $mlmin^{-1}$). When the dual valve was set to select carrier buffer, 50 µl incubated sample was introduced into the system through the 105 mm length injection loop. After 120 second the dual valve was switched to allow the elution buffer to flow to the column which eluted the captured antibody fraction to the detector. At the same time the FlowTEK software was switched on to capture the fluorescence signal of the elution peak, it took 30 seconds for completion of data capture. Figure 5-19 shows a typical profile for the α-interferon sample using the NFDS and the FlowTEK data capture software.

Fig. 5-19 **The Binding and elution profile of α-interferon through POROS protein A beads adjustable column using the NFDS and the FlowTEK data capture software**

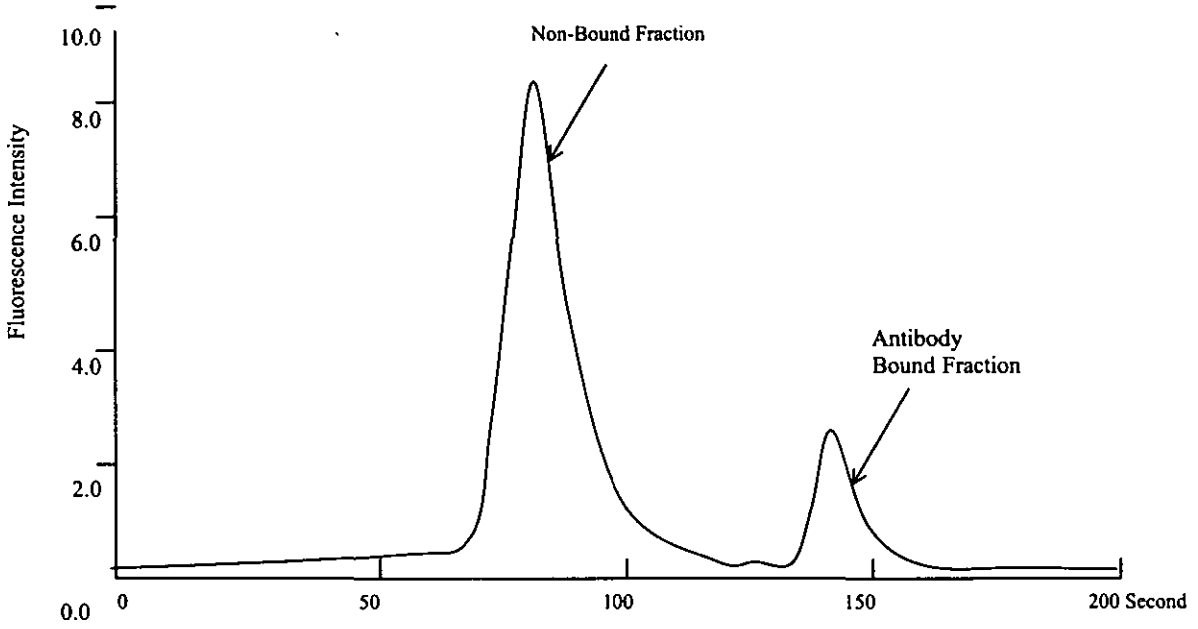

The procedure described was repeated with 0.00 μgml^{-1}, 0.05 μgml^{-1}, 0.10 μgml^{-1}, 0.50 μgml^{-1}, 1.0 μgml^{-1}, 2.0 μgml^{-1}, and 10.0 μgml^{-1} of the α-interferon samples. The results were collected using the FlowTEK data capture software. Table 5-9 lists the data, mean value, CV and CV%, and Figure 5-19 shows a calibration curve for the α-interferon generated from this data.

Table 5-9 **Variation of response for various α-interferon samples in flow injection system using the NFDS with the FlowTEK**

Title	B_0 0.00μgml^{-1}	B_1 0.05μgml^{-1}	B_2 0.1μgml^{-1}	B_3 0.5μgml^{-1}	B_4 1.0μgml^{-1}	B_5 5.0μgml^{-1}	B_6 10.0μgml^{-1}
Response (a.u)	3.0172	3.0062	2.9576	2.7787	2.0255	1.5908	1.161
	3.2268	2.9852	3.0016	2.6604	2.1505	1.4243	1.1139
	3.1066	2.9714	2.7401	2.7309	2.2388	1.4814	0.923
SUM	9.3506	8.9628	8.6993	8.1700	6.4148	4.4965	3.1979
MEAN	3.116867	2.9876	2.899767	2.723333	2.138267	1.498833	1.065967
B/B_0%	100.00	95.85267	93.03467	87.37407	68.60308	48.08782	34.19994
STD DEV	0.105176	0.017524	0.140015	0.059512	0.107175	0.084608	0.126033
CV	0.033744	0.005865	0.048285	0.021853	0.050122	0.056449	0.118233
CV%	3.37443	0.586548	4.828478	2.185259	5.012234	5.64492	11.82331

Note: a.u is arbitrary units; the speed of laser pulse in the NFDS was set around 50KHz.

Figure 5-20 **Flow injection immunoassay for the α-interferon using the NFDS and the FlowTEK data capture software**

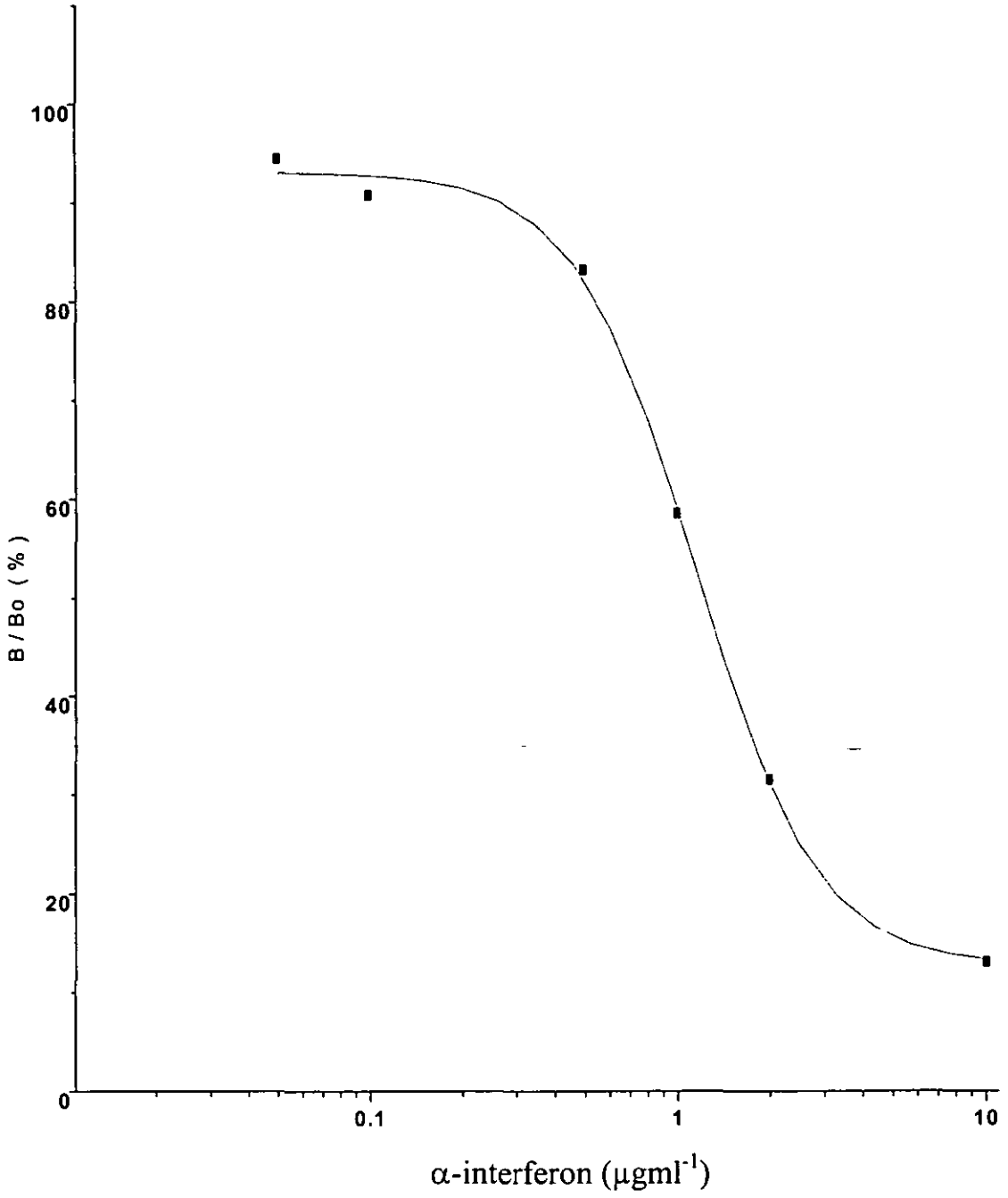

Fig 5-20 shows the characteristic sigmoidal shape normally associated with a competitive binding assay. The working range of the assay in this case was approximately 0.5 μg ml^{-1} to 10 μg ml^{-1}. Due to the inaccuracy of the data collection

package, lower concentrations of α-interferon sample could not be detected but this was more a consequence of the data handling software and not the limits of the detector. Both Figure 5-20 and Table 5-9 show that it was possible to develop a model immunoassay for α-interferon using the system described above, despite one or two drawbacks provided a working assay.

In order to validate the FI system with the FlowTEK data capture software, 50 μl Tris buffer was measured the data for these experiments were collected in Table 5-10.

Table 5-10 **Variation of responses for Tris buffer injection in flow injection system using the NFDS with the FlowTEK**

Sample No.	Response area (a.u)	Note	
1	0.6952		
2	0.7701		
3	0.6842	SUM	9.0653
4	0.8014	MEAN	0.755442
5	0.8359		
6	0.8585	STDVEA	0.073174
7	0.7976		
8	0.7830	CV	0.096863
9	0.6634		
10	0.7600	CV%	9.686295
11	0.7953		
12	0.6207		

Note: a.u is arbitrary units; the speed of laser pulse in the NFDS was set around 50KHz.

Prior to the FlowTEK data capture, the analogue signal from the detector was pre-amplified in the DAQ board. The pre-amplifier in the DAQ board not only magnified the signal from the detector but also increased the noise. The CV% for 50 μl of Tris buffer (pH 8.8) was 9.7%, somewhat larger than the values subsequently found for the α-interferon injections. Further modification of the DAQ for this application will be discussed in Chapter 6.

Several experiments have confirmed that the CV's in the majority of cases using the FlowTEK were larger than expected but this was due to instability of pre-amplifier for small signal in DAQ board and not the detection system. An improved assay could be performed if an alternative DAQ card and data collection system, which provides more accurate integration peak area, is used. The further modification of data handling software and the DAQ for the novel detection system will be discussed in Chapter 6.

5.7 References

[1] Lim, Tae-Kyu, Nakamura, N. and Matsunaga, T., Flow immunoassay using a cation exchange column and fluorescence-labelled antibody for detection of allergen, Analytica Chimica Acta, (1997), Vol.345, pp.29-34.

[2] Liao, N. L., Rapid determination of atrazine in environmental samples using automated flow injection immunoassay, Abstract of Papers of The American Chemical Society, (1996), Vol.211, No. Pt.1, pp.10.

[3] Kronkvist, K., Lovgren, U., Svenson, J., Edholm L. E. and Johanson, G Competitive flow injection enzyme immunoassay for steroids using a post-column reaction technique, Journal of Immunological Methods, (1997), Vol.200, No.1-2, pp.145- 153.

[4] Bjarnason, B., Bousios, N., Eremin, S. and Johansson, G., Flow injection enzyme immunoassay of atrazine herbicide in water, Analytica Chimica Acta, (1997), Vol.347, No.1-2, pp.111-120.

[5] Valcarcel, M. and Luque de Castro, M. D., Introduction to flow-injection analysis, Flow-Injection Analysis: Principle and Application, Ellis Horwood, (1987), pp.39-40.

[6] Skoog, D. A., Holler, F. J. and Nieman, T. A., Flow–injection analysis, Instrumental Analysis, Philadelphia;London: Harcourt Brace, (5th Edition), (1998), pp.836.

[7] Berson, S. A. and Yalow, R. S., Journal of Clinical Investigation, (1959), Vol. 38, pp.1996.

[8] Davies, C., Principles, The Immunoassay Handbook, The MaCmillan Press Ltd., Edited by David W., (1994), pp.3-6.

[9] Wild, D. and Davies, C., Components, The Immunoassay Handbook, Edited by David W., The Macmillan Press Ltd., (1994), pp.58-59.

[10] Evans, M., Palmer, D. A., Miller, J. N. and French, M. T., Flow injection fluorescence immunoassay for serum phenytoin using perfusion chromatography, Analytical Proceedings Including Analytical Communications, (1994), Vol. 31, pp.7-8.

[11] Miller, J. N., Evans, M., French, M. T. and Palmer, D. A., Injection based heterogeneous fluorescence immunoassays, Applied Fluorescence in Chemistry, Biology and Medicine, Springer-Verlag, Berlin, (Rettig, W. edited 1999), pp.510-515.

[12] Chen, D. W., General Principle of Immunoassay, Immunoassay: A Practical Guide, Edited by Chen, D. W., Academic Press, (1987), pp.13-16.

[13] Palmer, D. A., Evans, M., Miller, J. N. and French, M .T., Rapid fluorescence flow injection immunoassay using a novel perfusion material, Analyst, (1994), Vol.119, pp.943.

[14] Afeyan, N. B., Gordon, N. F. and Regnier, F. E., Automated real-time immunoassay of biomolecules, Nature, (1992), Vol.358, pp.603-604.

[15] Scharpé, S. L., Cooreman, W. M., Blomme, W. J. and Laekman, G. M., Quantitative enzyme immunoassay: current status, Clinical Chemistry, (1976), Vol.22, No.6, pp.733 – 738.

[16] Hage, D. S., Immunoassays, Analytical Chemistry, (1995), Vol. 67, No.12, pp.455R - 4462R.

[17] Wild, D. and Davies, C., Components, The Immunoassay Handbook, Edited by Wild, D., The MaCmillan Press Ltd., (1994), pp.78-80.

CHAPTER SIX

CONCLUSIONS AND FUTURE WORK

6.1 Introduction

The development of the NFDS successfully met the initial research proposal through a series of practical experiments. Future improvements will still be required to develop and update the technology.

Several investigations were used to evaluate the NFDS. Firstly, the detection limit was estimated according to the principle of signal to noise, in which several selected dyes, i.e. naphthofluorescein (NF), Cy5 monofunctional dye (Cy5) and Cy5.5 bisfuncational dye (Cy5.5) were tested using the NFDS with the FlowTEK data capture software. Secondly, comparative tests were carried out with the NFDS and the RACALL-DANA 4009 digital multimeter and the Hitachi F-4500 fluorescence spectrophotometer using various concentrations of Cy5 solutions. Thirdly, a practical flow injection immunoassay was developed for the α-interferon over the range 0.5 μgml^{-1} – 10 μgml^{-1}, using the NFDS with the FlowTEK data capture software. Finally, the benefits and drawbacks were summarised, which highlighted the low cost and the high sensitivity of the NFDS. However, there were some limitations, i.e. inability to use the device at wavelengths below 600 nm, and inefficient data capture software.

The NFDS has three main applications. The first important application involves its use as a detector in a flow injection coupled immunoassay, which offers a simplified system of automation. Another use is as a portable instrument with field applications. Finally the NFDS can be used as a stand alone long wavelength fluorescence detector providing very sensitive measurements.

Two improvements of the NFDS which can be carried out to improve portability include the use of superluminescent light emitting diodes (SLEDs) as excitation sources instead of laser diodes. SLEDs can extend the wavelength region of the NFDS to 400 nm – 630 nm and also reduce the cost of the NFDS. Another important improvement would introduce superior electronics and more efficient data capture. A lock-in amplifier can be used instead of the linear optoelectronic amplifier, a microprocessor can synchronise the entire operational system, and the LabVIEW 5.0 data handling software can capture the analogue signal and handle raw data instead of the FlowTEK software.

6.2 Evaluation of Novel Fluorescence Detection System

The NFDS with the RACALL-DANA 4009 digital multimeter and the FlowTEK data capture software has been used for the investigation of selected dyes, e.g. NF, Cy5 and Cy5.5. The α-interferon sample was selected as a model to develop the flow injection immunoassay using the NFDS with the FlowTEK data capture software.

6.2.1 Detection Limit of Novel Fluorescence Detection System

The detection limit is a measure of the smallest signal that can be detected in a single readout, in which the analytical concentration giving a signal equal to the blank signal, Y_B, plus two standard deviations of the blank, S_B; [1]

$$Y - Y_B = 2 S_B \qquad (6\text{-}1)$$

Also, The detection limit is sometimes quoted as two or three times the signal-to-noise ratio [2]. In this research, the detection limits for several selected dyes; i.e. NF, Cy5 and Cy5.5 were introduced as three times the signal-to-noise ratio to evaluate the NFDS.

The detection limit for NF with 2.5% (w/V) CHAPS in Tris buffer (pH 8.8) was 1.0×10^{-10} M when using the NFDS with the RACALL-DANA 4009 digital multimeter.

The detection limit for Cy5 in Tris buffer (pH 8.8) was 2.3×10^{-12} M when using the NFDS with the RACALL-DANA 4009 digital multimeter.

The detection limit for Cy5.5 in Tris buffer (pH 8.8) was 1.0×10^{-12} M when using the NFDS with the RACALL-DANA 4009 digital multimeter.

6.2.2 Comparative Tests

Against existing commercial research fluorescence detector in the laboratory, a comparative test was processed using the NFDS with the RACALL-DANA 4009 digital multimeter and the Hitachi F-4500 fluorescence spectrophotometer.

With the same concentration range of Cy5 in Tris buffer (pH 8.8), the detection limit for Cy5 using the Hitachi F-4500 fluorescence spectrophotometer it was 2.3×10^{-10} M and using the NFDS with the RACALL-DANA 4009 digital multimeter it was 2.3×10^{-12} M.

Obviously, the detection limit for same solutions of Cy5 in Tris buffer (pH 8.8) using the NFDS with the RACALL-DANA 4009 digital multimeter seemed better than using the Hitachi F-4500 fluorescence spectrophotometer.

Again, using the same NFDS but different data capture formats, the detection limit for same concentrations of Cy5 in Tris buffer (pH 8.8) using the FlowTEK data capture software was 2.31×10^{-11} M, was slightly lower than using the RACALL-DANA 4009 digital multimeter.

6.2.3 Practical Flow Injection Immunoassay

The α-interferon as a model was selected for practical investigation in a flow injection immunoassay using the NFDS with the FlowTEK data capture software. A calibration curve was obtained from experiments within the α-interferon concentration range 0.05 μgml^{-1} to 10 μgml^{-1}. The working range of the assay was approximately 0.5 μgml^{-1} to 10 μgml^{-1} due to the inaccuracy of the data capture software and analogue to digital signal conversion. Additionally, the CV's in this case were larger than expected because of poor background in the pre-amplifier of the data acquisition (DAQ) board and the FlowTEK software.

However, these experiments have confirmed that the NFDS is highly suitable for flow injection immunoassay. Improved response can be achieved if a better DAQ with data capture software is associated with the detection system (See section 6.3.2).

6.2.4 Advantages of the Novel Fluorescence Detection System

The advantages of using the NFDS can be summarised as following aspects:

1. Since using small size laser diodes as sources, the spectral range from excitation beam is narrower than using a lamp, therefore, the exciting beam is efficient without a monchromator compared with a regular research grade instrument. In addition, the output beam from a laser diode can be flexibly controlled by the laser pulse generator, with the pulse speed can be adjustable from several Hz to kHz. The detection for sample measurement can easily be optimised by means of laser pulse adjustment.

2. As the detector itself is portable and robust, this provides the possibility for field monitoring without the aid of a laboratory, e.g. in therapeutic drug assay and pesticide monitoring through immunoassays. If rechargeable batteries are used in the NFDS, the detection can be achieved in any conditions even without a mains power supply.

3. In the NFDS, a cut-off filter can easily be fitted into the optical system, which eliminates the undesirable background radiation and defines the emission wavelength band. There are many commercially available and reliable cut-off filters. Furthermore, a biconvex lens, which might be replaced by an achromatic lens, was used to condense the emission beam from the sample in a cuvette or flow cell to the surface of the photodiode.

4. In the electronic system, two CA3140 IC chips were adopted in the linear optoelectronic amplifier. This provided low noise and a stable output signal thus making it possible to detect low fluorescence in the NFDS. The use of two metal shield baffles in the PCB mounting overcame the thermal drift, which might be otherwise a problem in the detector. Additionally, the signal output was distributed in not only the digital display and the chart recorder but also the connection of ADC to a PC with an appropriate data capture package, i.e. the Global ADC box and the FlowTEK data capture software.

6.2.5 Drawbacks of the Novel Fluorescence Detection System

Despite the high sensitivity of detection using the NFDS, many disadvantages can also be outlined.

1. Initially the NFDS was designed for long wavelength (>600 nm) fluorescence detection. For some flow injection immunoassay, it is a possible to use shorter wavelengths (450 nm to 600 nm) fluorescent dyes. Currently the NFDS can not be used in the shorter wavelength ranges, i.e. for Cy2, Cy3 etc. Further improvements are discussed in Section 6.4.1.

2. Although the NFDS gave good detection limits for selected long wavelength dyes, the linear optoelectronic amplifier circuit did not possess a 'chopping' function, which can cut off the undesired background signal and increase the sensitivity for low concentration detection. Also, the optoelectronic linear amplifier has not been synchronised with the laser pulse generator that provides the adjustable laser pulse. The laser pulse generator can use a crystal oscillator, which provides a more accurate pulse frequency than an IC 555 timer.

3. In a practical flow injection immunoassay, the results of α-interferon demonstrated the CV% was 4.8 and the detection limit was only 0.5 $\mu g ml^{-1}$ in Figure 5-19 due to the inaccurate FlowTEK data capture software and the Globe DAQ card. Furthermore the results of the blank sample confirmed the drawbacks of this data capture package, that a 50 μl Tris buffer (pH 8.8) was injected into the flow system instead of the α-interferon sample. The operational procedure was the same as the

sample injection. The results were obtained from the FlowTEK data capture software in a PC. The CV% of the experiment was 4.2, which is unacceptable for routine analysis. Therefore the Global DAQ box and FlowTEK data capture software should be replaced by a better DAQ card and a better data handling package when detecting very small fluorescence signal.

6.3 Application Scope of Novel Fluorescence Detection System

The NFDS developed in the laboratory can be applied in following aspects:

6.3.1 Flow Injection Coupled Immunoassays

Preliminary studies, several practical investigations of detection limits and immunoassay suggested that the NFDS can be applied in not only directly measuring fluorophores but also high throughput screening application including therapeutic drugs and pesticide monitoring.

6.3.2 A Portable Instrument

In all practical experiments, the results already expressed that the NFDS is suited for field application without laboratory base even an analyst can carry it to non-laboratory without any special care. For example, when only the peak intensity on the selected fluorescence bands is needed, the results can be obtained from the NFDS.

6.3.4 Fluorescence Wavelength Region Between 600 nm to 900 nm

As described in Chapter One, there has in recent years, been a major expansion in the area of molecular fluorescence in long-wavelength. Advances in solid state devices for developing novel instruments and data handling packages, and the syntheses of new fluorescent labels and probe molecules, i.e. Cy5, Cy5.5 and Cy7 dyes, have combined to produce a wide range of new applications. Advantages of long wavelength fluorescence methods in biological and environmental chemistry include their exceptional sensitivity, the ease with which different samples decreased interference from the fluorescence phenomena due to the sample, in which is the basis of other techniques. Nevertheless,

this portable NFDS provides the efficient means to utilise the long wavelength fluorescence application where it is immunoassay or directly detecting the fluorescence signal from the sample.

Since the current supply restriction of laser diode as excitation sources and the initial proposal of project, this portable NFDS can be used in detecting wavelength region for fluorescence signal detection is between 600 – 900 nm. Its further applications in the other wavelength region have been described in detail in Section 6.4.

6.4 Future Work for Improvement

There is still future work required to improve the behavior of optical and electronic system in the NFDS, although the sensitivity and stability of detection system met the requirement of the research proposal. With the fast development of current technology in solid state devices, there is high possibility that the NFDS can be improved to be more robust, versatile, cheaper and easier to operate.

6.4.1 Superluminescent Light Emitting Diodes (SLEDs) as Excitation Sources

A laser diode as the light source has been introduced to spectrometers for many years, i.e. near infrared laser diode for long wavelength fluorescence detection, in which some simple but sensitive fluorescence spectrometers have been successfully studied [3]. Despite their considerable advantages, namely, considering their unique characteristics, their compact size, high spatial and narrow spectral tuning range (a few nanometers), there are a number of reasons, including the high costs of those devices compared with other light sources, which have as yet limited their appeal.

The possibility of using SLEDs instead of laser diodes is of particular interest. Alexander etc. have discussed the construction of a fluorimeter based on SLEDs, for the determination of chlorophylls *a* and *b* [4]. In addition, the spectrum range for excitation source can be extended to the region of wavelength between 400 nm and 630 nm which fills the gap of spectrum using the near infrared laser diodes. These relatively inexpensive SLEDs are potentially suitable as the light sources for fluorescence spectrometers because they can provide the output of power between microwatts to milliwatts of continuous-wave (CW) or several kHz pulsed light.

Recent advances on gallium nitride have made it possible to develop SLEDs for shorter wavelength regions, i.e. the blue region at 450 nm. Because many fluorescent compounds absorb light in the blue, green regions, these SLEDs with their advantages (i.e. wide spectral bandwidth, high intensity, low cost) were particularly suited for the development of a novel, compact, inexpensive, and highly sensitive fluorescence spectrophotometers. A large number of commercially available labels have been reported to be suitable for using SLEDs, such as Cyanine dyes, Cy2 @ 489 nm, FluorX @ 494 nm, Cy3 @ 550 nm and Cy3 @ 581 nm [5]. Generally, the output power of SLED is higher than regular light emitting diodes (LEDs) and the spectral bandwidth is narrower than those LEDs. The electronic behaviour of laser diodes, i.e. the output power, the spectral bandwidth etc, is superior to SLED, but the costing of SLED compared to laser diodes is only one tenth or even less.

These SLEDs can easily be installed in the optical system instead of the laser diodes and easily be connected to the laser pulsed driver in current NFDS. The radiant beam from SLEDs can be collimated by a set of lenses. Therefore both blue, green and red (470 nm, 565 nm and 660 nm) spectral region SLEDs have been demonstrated as inexpensive light sources.

Future study for selected fluorescent dyes will be under investigation using these SLEDs.

6.4.2 Improvement of Electronic Behaviour and Data Capture

Fast development of electronic technology enables the instrument to be improved using the latest solid state components. Although the function of electronic system in the NFDS was reached, there are still demands for future improvement, i.e. a lock-in amplifier instead of the linear optoelectronic amplifier, a microprocessor to control entire operational system and the LabVIEW 5.0 data handling software to capture analogue signal and handle raw data from the NFDS.

6.4.2.1 A Chopper Amplifier and Lock-in Amplifier

As described in Chapter Four, the laser beam was modulated in pulse light output by means of the laser pulse driver from several Hz to MHz. To restrict the noise from the source is often 'chopped' and the detector's amplifier is switched on and off at the same frequency. Although the laser beam from the laser pulse generator was 'chopped' in a regular pulse and excites the sample thus the emission beam also produces a regular pulse signal, which is similar to laser pulse 'chopping' frequency. When detecting low fluorescence signal in the sample, a high gain of optoelectronic linear amplifier has to be used, of course, the noise and baseline drift will be also increased. However, the chopper amplifier has its unique characteristics: eliminating the inherent thermal drift and the DC offset baseline in high gain amplifier. Because it makes use of a relatively narrow-band AC-coupled amplifier in which the advantages of feedback can optimised. Chopper amplifier is partially suitable for high gain of amplifier and high frequency of input signal.

In current optoelectronic linear amplifier, it has no 'chopping' function yet in which it can be switched on and off in same frequency of laser pulse. A simple way can be created out with which has both a 'chopping' function and synchronisation with the laser pulse driver: the laser pulse generator can be connected with not only the laser diode driver but also with the optoelectronic linear amplifier that has the same frequency. The electronic system possesses lock-in amplifier and synchronisation in which the bandwidth is very narrow. The signal-to-noise ratio shall be improved through this procedure. Figure 6-2 shows the synchronisation schematic of the electronic system in the NFDS.

Figure 6-2 **Schematic of synchronisation to laser pulse generation and optoelectronic amplification**

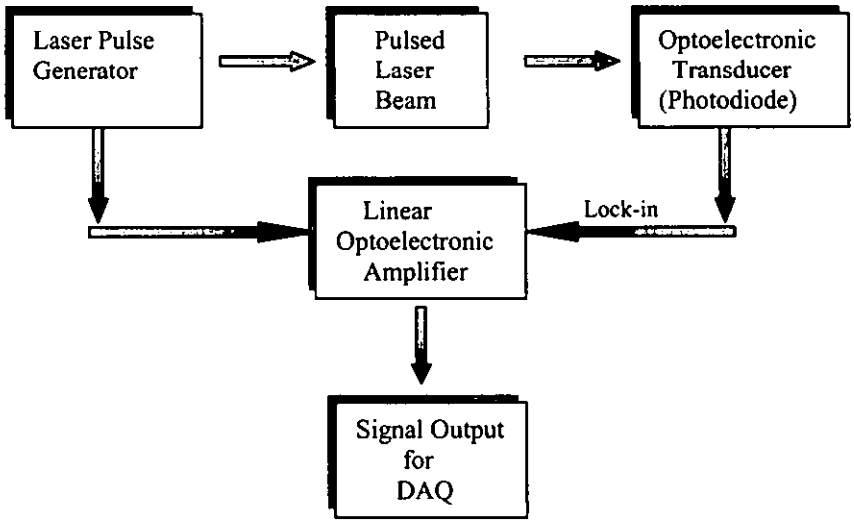

Since the lifetime of fluorescence in this application is less than 10^{-9} second, the delay time of response can be negligible when the radiant beam excites the sample.

Through this simple procedure, the sensitivity and reliability expected shall be improved on the current status when using the NFDS.

6.4.2.2 A Microprocessor

Microprocessors have been introducing to analytical instruments for many years, which are simple but versatile in a signal integrated circuit (IC) package. Their cost is low enough that even when accessory units such as memory are added, therefore they are practical in the instrument of modest size. Actually, a microprocessor often serves as an arithmetic and logic component, called the central processing unit (CPU), of a digital microcomputer. It also be found widespread use in controlling the operation of such diverse items as analytical instrument. Several publications [6-7] have well described to use microprocessors or microcomputers for analytical instruments.

Some fluorescence spectrometers have been successfully constructed with the microprocessor to incorporate a laser diode fluorimeter [8]. With the diversity of the microprocessors, the variety of ways of connecting the microprocessor to the NFDS through various support ICs (hardware), and the programming variation (software), there is high possibility to control the electronic system with the keyboard. Figure 6-3 demonstrates the principle of NFDS incorporating a microprocessor.

Figure 6-3 **General block diagram of the electronic module coupled microprocessor in the NFDS**

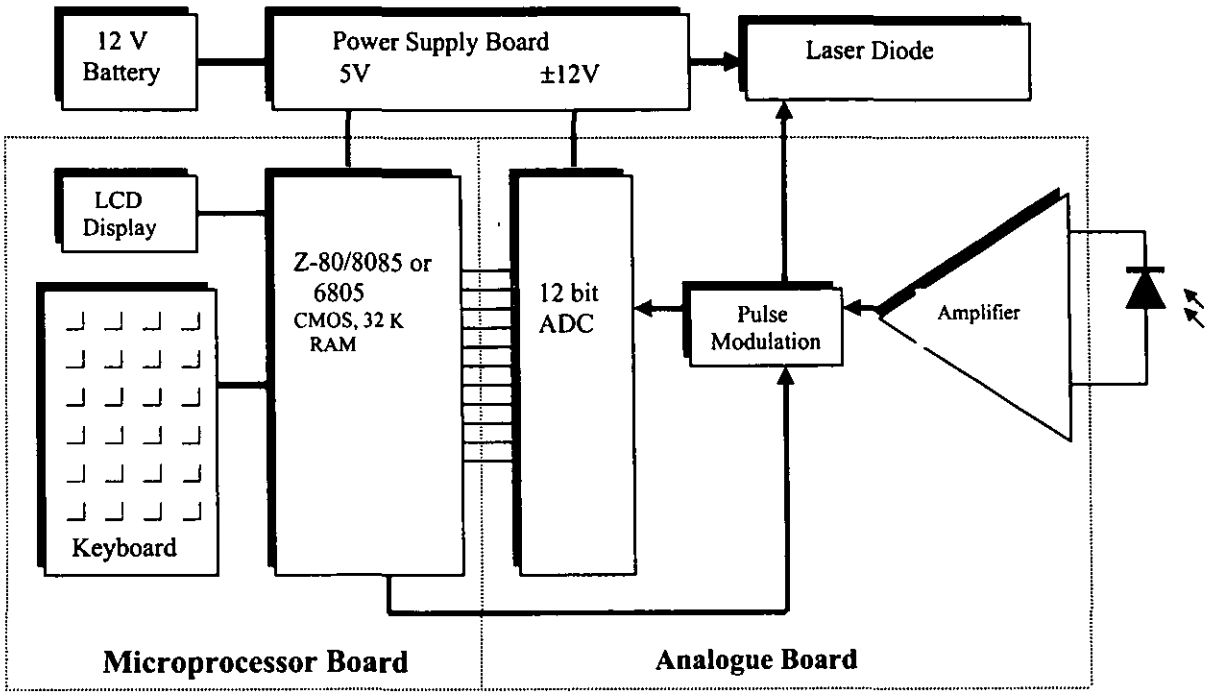

With a microprocessor in the NFDS, it is possible to combine other circuit components that provide a memory storage, timing, input, output function even connect to a PC with an appropriate data capture software, i.e. RS232 connection.

The effect of utilising a microprocessor in the NFDS is:

1. Partial or complete automation of fluorescence measurement becomes possible and leads to more rapid data acquisition. Additionally, the automation frequently will provide better control over experimental variables than a human operator can achieve; more precise and accurate data will be the result.

2. To interface a computer with the NFDS is to take advantage of a computer's tremendous computational and data handling capabilities. These capabilities make possible the routine use of techniques in which some commercially available software can be installed in a PC.

Obviously, the NFDS can be updated by a microprocessor, which will provide a more powerful measurement tool and easier to operate.

6.4.2.3 A NI DAQ Card with LabVIEW 5.0 Software

As described in Chapter Five, the CV% and the detection limit of the α-interferon testing in flow injection immunoassay were poor due to the inaccurate data capture software and the Global ADC box. It is seemingly important to select an appropriate DAQ and data handling package otherwise poor results will still be obtained although the NFDS has a high sensitivity to capture fluorescence signal for detecting NF, Cy5 and Cy5.5.

A NI (National Instrument) DAQ card coupled LabVIEW 5.0 software is one of many approaches to capture the analogue signal from a instrument and handle raw data to display on the screen of a PC. Actually, the LabVIEW is a development environment based on the graphical programming language G, which also has built-in libraries for using software standards [9]. The spectrum programme to capture fluorescence signal in the NFDS that is one of functions in the LabVIEW 5.0 software was successfully developed in this laboratory.

A PC-LPM-16PnP interface card can be selected as a DAQ, in which the board contains a 12-bit, successive-approximation, self-calibrating ADC with 16 analogue inputs, 8 lines of TTL-compatible digital input, and 8 lines of digital output. The sampling speed of this ADC can be reached to 5MHz [10].

The PC-LPM-16PnP DAQ card coupled the LabVIEW 5.0 data capture software performs following functions:

1. Capture the analogue signal (Voltage) from the NFDS into the NI DAQ card and display in Voltage-to-Time on the screen of a PC.

2. Readout the peak areas in chart recorder and real time and count the number of peaks occurred from flow injection immunoassay or other fluorescence analysis.

3. Set up the threshold option prior to detection in which can minimise the background of operation.

4. Set up the data logging, storage and data reading in the spreadsheet.

The further practical investigation using the NFDS with the NI DAQ card and the LabVIEW 5.0 data capture software is being used to study naphthofluorescein phosphates enzyme immunoassay utilising flow injection analysis.

6.5 References:

[1] Miller, J. C. and Miller, J. N., Errors in instrumental analysis; regression and correlation, Statistics for Analytical Chemistry, Ellis Horwood Ltd., (1992), pp.114-115.

[2] The Wellcome Foundation Beckenham Analytical method validation, Statistics for Industry, (1994), pp. 3.8.

[3] Casay, G. A., Shealy, D. B. and Patonay, G., Near-Infrared fluorescence probes, topics in fluorescence spectroscopy, Vol. 4: Probe Design and Chemical Sensing, Lakowicz Plenum Press, New York, USA, (1994 edited by Joseph R.), pp.185-194.

[4] Alexander, T. A., Gao, Guan-Hong and Tran, Chieu D., Development of a novel fluorimenter based on superluminescent light-emitting diodes and acousto-optic tunable filter and its application in the determination of chlorophylls a and b, Applied Spectroscopy, (1997), Vol. 51, pp.1603-1606.

[5] Cyanine Dyes, Amersham Life Science, Inc., USA, (1998), http://www.amersham.com.

[6] Malcome-Lawes, D. J., System design and case study, Microcomputers and Laboratory Instrumentation, Plenum Press, (1988), pp.225 – 237.

[7] Wobschall, D., Introduction to microprocessor, Circuit Design for Electronic Instrumentation, McGraw-Hill Book Company, (1987), pp.311 – 337.

[8] Mazzinghi, P., Laser diode fluorimeter for field measurement of the F685/F730 chlorophyll fluorescence ratio, Review of Scientific Instrumentation, (1996), Vol. 67, No.10, pp.3737-3744.

[9] LabVIEW, Part No. 350100C, National Instrumental Co., USA, (1998), http://www.natinst.com/LabVIEW.

[10] PC-LPM-16/PnP User manual, National Instrument Co. USA (Nov. 1996 Edition). Part No. 320278C-01.